

INTERNATIONAL ACADEMIC STUDIES IN SCIENCE AND MATHEMATICS

June 2024

EDITORS

PROF. DR. ALPASLAN DAYANGAÇ

PROF. DR. GÜNAY ÖZTÜRK

Genel Yayın Yönetmeni / Editor in Chief • C. Cansın Selin Temana

Kapak & İç Tasarım / Cover & Interior Design • Serüven Yayınevi

Birinci Basım / First Edition • © Haziran 2024

ISBN • 978-625-6319-28-8

© copyright

Bu kitabın yayın hakkı Serüven Yayınevi'ne aittir.

Kaynak gösterilmeden alıntı yapılamaz, izin almadan hiçbir yolla çoğaltılamaz.

The right to publish this book belongs to Serüven Publishing. Citation can not be shown without the source, reproduced in any way without permission.

Serüven Yayınevi / Serüven Publishing

Türkiye Adres / Turkey Address: Kızılay Mah. Fevzi Çakmak 1. Sokak

Ümit Apt No: 22/A Çankaya/ANKARA

Telefon / Phone: 05437675765

web: www.serüvenyayınevi.com

e-mail: serüvenyayınevi@gmail.com

Baskı & Cilt / Printing & Volume

Sertifika / Certificate No: 47083

INTERNATIONAL ACADEMIC STUDIES IN SCIENCE AND MATHEMATICS

June 2024

Editors

PROF. DR. ALPASLAN DAYANGAÇ

PROF. DR. GÜNAY ÖZTÜRK

Contents

Chapter 1

DARK MATTER IN COSMOLOGY

E. Nihal ERCAN.....1

Chapter 2

QUANTITATIVE ANALYSIS OF MARKET VALUE PREDICTORS IN TURKISH SÜPER LIG: A PCA AND REGRESSION APPROACH

Mohammed ADEM, Mehmet Ali CENGİZ..... 15

Chapter 3

CONDURITOLS: PIONEERING SYNTHETIC MARVELS WITH PROFOUND BIOLOGICAL SIGNIFICANCE

Sedat Sadi İNCİ, Hülya ÇELİK29

Chapter 4

HISTORY OF ASTRONOMY

E. Nihal ERCAN.....47

Chapter 5

A STUDY ON TZITZEICA HYPERSURFACES IN EUCLIDEAN 4-SPACE \mathbb{E}^4

Emrah TUNÇ, Bengü BAYRAM.....67

Chapter 6

ON QUATERNIONS AND THEIR MATRICE REPRESENTATIONS WITH COMPLEX MATRICES*

Ali ATASOY83

Chapter 7

**PRODUCTION FACTORS AFFECTING NANOPARTICLE SIZE AND THE
EFFECT OF SIZE ON THERMOPHYSICAL PROPERTIES**

Hakan ŞAHAL 103

Chapter 8

**ON THE CONTINUITY WITH RESPECT TO DENOMINATOR OF RATIO
NUMERICAL RADIUS AND RATIO CRAWFORD NUMBER FUNCTIONS**

Ümmügülsün ÇAĞLAYAN, Pembe İpek AL 121



Chapter 1

DARK MATTER IN COSMOLOGY

E. Nihal Ercan¹

¹ Prof. Dr., Boğaziçi University, Physics Department

Introduction

Cosmology is a fascinating field of science that includes many mysteries and exciting concepts to be explored. Dark matter, which has puzzled scientists for decades, is an example. The fact that dark matter cannot be directly observed using telescopes or other astronomical instruments has also increased the curiosity about it considerably. We can only infer dark matter's presence and its gravitational effects on visible matter. Dark matter reveals much valuable information in understanding the universe's large-scale structure and determining how galaxies and clusters of galaxies are formed. Many attempts have been made to find out the exact nature of dark matter and find evidence about it. Although none of these efforts provide satisfactory information on our understanding of dark matter, they continue to take scientists' attention because they completely changed our understanding of the universe and provide insight into its fundamental structure.

History

The history of dark matter can be traced back to 1884 when Lord Kelvin mentioned that some of the stars may be dark and hence cannot be seen in estimating the number of stars around the Sun [1]. Theories about dark matter started to emerge in the 1930s when Swiss astronomer Knut Lundmark noticed that there should be more mass in the universe compared to our observations [2]. Then, another Swiss astronomer, Fritz Zwicky, who is a Swiss astronomer, supports Lundmark's hypothesis. During observations of the Coma cluster, Zwicky detected strange gravitational interactions between the galaxies in the Coma cluster, which the observed mass of that cluster could not explain. Therefore, he theorised that there must be an unseen force exerting gravitational pull on visible matter, which is caused by an invisible matter with a significant amount of mass that can affect galaxies [3]. Nevertheless, until the 1970s and 1980s, when new observations were made about evidence of dark matter, his findings were not considered sufficient enough to achieve consensus on the existence of such an invisible matter with mass among scientists.

In the 1970s, when astronomer Vera Rubin and her colleagues were studying the rotation curves of spiral galaxies, they discovered key evidence supporting the dark matter theory. They observed that the stars were moving too fast in the outer regions of galaxies, and the mass of the visible matter in that cluster couldn't create enough centrifugal force to hold the stars together in the galaxies [4]. So, they concluded that an additional mass (dark matter) must be responsible for holding the stars of galaxies together by creating enough centrifugal force.

The dark matter theory continued to be supported by observations in the 1980s. X-ray observations about galaxy clusters showed that the gravitational

force of visible matter alone could not sufficiently explain the distributions of hot gas in clusters. Moreover, in the 1990s, observations of gravitational solid lensing provided evidence about some invisible mass sources [5]. Astronomers observed that the gravitational lensing effect was so strong that it required more mass than the mass of the cluster that caused it.

With technological improvements, more large-scale observations were made in the 1990s and 2000s. Astronomers observed the large-scale structures in the universe (distribution of the galaxy clusters) and detected that the distribution was uneven (anisotropic). Further studies showed that the fluctuation from a uniform distribution is not random. Therefore, some unobserved (invisible) mass should exist to explain these nonrandom patterns. Additionally, some temperature fluctuations were detected in cosmic microwave background radiation, which also does not seem random, similar to the distribution of galaxies on a large scale in 1992 by the Cosmic Background Explorer (COBE) satellite. Scientists think these variations are caused by the density changes near the beginning of the universe, which may imply the existence of dark matter.

Although these discoveries revealed much detail about dark matter and many observational milestones achieved by astronomers, dark matter still preserves its mysterious nature. Currently, there are many continuing observations and experiments that aim to understand the true nature of dark matter. The Dark Energy Survey and the Large Hadron Collider are examples of such observations and experiments.

Observational Information Dark Matter

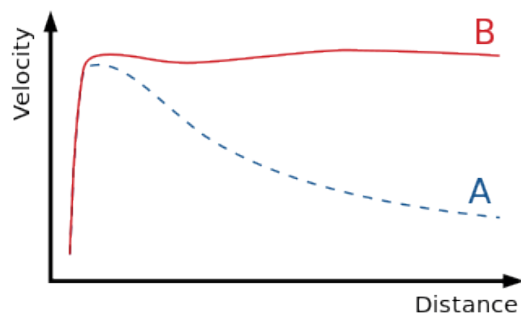
Because Dark matter does not interact with photons (light and any electromagnetic radiation), which is the greatest challenge in observing dark matter, it is impossible to observe it directly. Dark matter does not emit, absorb, or reflect electromagnetic radiation but interacts with gravity. Therefore, an inference of its existence can only be made by observing its gravitational effects on visible matter. There is much observational evidence that confirms its existence and reveals some of its aspects:



Figure 1. Shining light on dark matter (Credit: NASA)

Rotation curves of spiral galaxies: The rotation curve of a galaxy is a graph that shows the orbital velocity of stars/planets in the galaxy on the y-axis and the distance from the galactic centre on the x-axis. Spiral galaxies' arms orbit around the galaxy's centre with all the matter they contain (gas, stars, planets). Based on observations, most of the mass of these galaxies clustered in the centre because we can directly see that centre is more luminous, and we observe more incoming electromagnetic radiation. Hence, we deduce that there is more mass. Therefore, in an ordinary spiral galaxy, the stars and gas in the outer regions of the arms should be moving more slowly compared to matter in closer regions of the galactic centre, according to Kepler's second law (the area swept should be equal). See Figure 2. below.

On the contrary, the observations (which are shown in the graph approximately A is the expected values and B is the observed values) about the orbital speeds of arms of spiral galaxies show that the orbital velocities do not change when the distance from the galactic



centre increases [6]. Since Kepler's laws work perfectly in the solar system, if we make an analogy between the solar system and spiral galaxies based on the distribution of mass, then the only explanation for this contradiction is the existence of some invisible mass in the dark (non-luminous) around the arms

of the galaxy. Although there are some suggested alternative explanations for this phenomenon, like modified Newtonian dynamics [7], the anomaly in rotation curves of spiral galaxies is considered one of the most vital pieces of evidence for the existence of dark matter [8].

Gravitational lensing: Gravitational lensing occurs when an incredibly massive object bends the curvature of space-time and changes the direction of photons from the distant light source (another object). Gravitational lensing causes shape distortions in the image of the light source and even causes its image to appear in two or more places. Astronomers can infer the object's mass (black hole or galaxy cluster) by analysing the distortions in the apparent image. In many observations of gravitational lensing events [11], it is seen that the visible mass is not enough to create such a lensing effect. Astronomers further analysed these effects and even managed to map the distribution of the dark matter to cause such gravitational lensing effects. The current observations about areas whose dark matter distribution is mapped showed that the amount of gravitational lensing and the distortions of the related images can be explained sufficiently by the dark matter map [12].



Figure 3. Gravitational lensing (Credit: NASA)

Velocity dispersion in elliptical galaxies: velocity dispersion is the deviation of each star's velocity from the mean velocity of the stars in the context of a galaxy. When astronomers analyse elliptical galaxies by observing their velocity dispersions, they detect that the visible mass in those galaxies is far less to create a force that causes observed velocity deviations from the mean [9] [10]. Therefore, they theorised that there should be an invisible mass that caused these deviations. Moreover, the dispersion amounts are so high that if the theory is correct, the mass of dark matter should be much more than that of visible matter.

Large-scale structure of the universe: The distribution of galaxies and galaxy clusters on the largest scales of the universe also provides evidence for the existence of dark matter. The distribution of visible matter alone cannot account for the observed patterns of large-scale structure, suggesting that there must be additional mass in the form of dark matter.

The ordinary matter in the universe is not distributed uniformly; it is grouped and creates larger structures like planets, stars, galaxies, clusters and superclusters, and also creates significant gaps (voids). Extensive observations about space prove that the pattern that stars and galaxies create is not random but a repeated, correlated pattern called “filament of galaxies” [15]. The reason for these structures can be traced back to the universe’s beginning. According to our current knowledge, the universe is homogeneous at the beginning (Friedmann Solutions for General Relativity) [16].

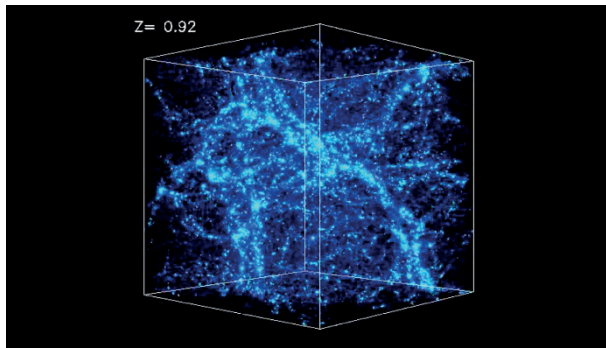


Figure 4 Large-scale structure.(CrediT:NASA)

Therefore, there should be an external force that distorts this homogeneity and causes the formation of greater structures [17]. The interactions between ordinary matter and the dense radiation in the early universe are an excellent reason for this distortion. Still, the universe had not been long enough in that situation for dense radiation to cause such distortions intense enough to create the large structures we observe today. However, dark matter is a better candidate for this anisotropy because it is not affected by radiation and is not necessarily distributed uniformly. It affects ordinary matter by gravity to create such significant structures as galaxy filaments and the correlated pattern of these megastructures in the universe.

Interestingly, the observations show that in some directions, some galaxies' peculiar velocity, there is no visible object observed which can cause an acceleration towards that direction by gravitational force. The 2dF Galaxy Redshift Survey which also includes strong evidence about dark matter and reveals possible dark-matter ordinary matter relationships is such an example for these observations [18]. To conclude, the only explanation for this phenomenon is the existence of dark matter to cause acceleration towards the movement direction of these galaxies by gravity.

Hot gas distribution in galaxy clusters: Observations about the behaviour of hot gas in superclusters are also considered as evidence of the existence of dark matter. From the X-ray emission of such gases and the redshifts, scientists can analyse the spectrum and estimate the temperature, density, and velocity of gases. According to observations, the gas in these clusters moves with velocities that are too high to be held together by the gravitational force of the visible matter alone, similar to the case in rotation curves of spiral galaxies. Therefore, it is thought that additional dark matter mass causes hot gas to reach such high velocities.

Fluctuations in cosmic microwave background radiation: Cosmic microwave background radiation is electromagnetic radiation strongest in the microwave spectrum and is observed from anywhere in space. It is thought that the residual energy after the Big Bang [13]. The cosmic microwave background radiation is nearly uniform. However, some fluctuations in the temperature are observed [14], which have a repeated pattern that cannot be random. Since cosmic microwave background radiation can be detected from anywhere in space, including the areas with no visible matter, there has to be another source that causes these fluctuations. The only explanation is a small gravitational lensing effect that distorts the direction of photons and causes these fluctuations. Because we can observe these fluctuations in space areas with no visible matter, the reason must be the existence of dark matter in those areas to provide enough gravitational force that causes the lensing effect. Moreover, current observations perfectly match the theorised dark matter model very well [15], which makes the anisotropy of cosmic microwave background radiation another robust evidence for the existence of dark matter.

Bullet Cluster Observations: The Bullet Cluster is a supercluster of galaxies in which other galaxy clusters collide. Currently, these observations are considered the strongest evidence for the existence of dark matter [19] because none of the alternative models that exclude dark matter, like Modified Newton Dynamics, can explain the observed events in the Bullet Cluster, which are explained by dark matter [20]. During the collision, the gas in galaxies is heated so much that it emits X-rays, enabling astronomers to observe collision, estimate the velocities and where visible matter is moving. The masses in those galaxies are expected to merge in the middle due to

gravitational force, as most of the collision events in celestial bodies in space.

However, two main gravitational lensing effects are observed around the hot gas, which is seen in this picture Figure 7). The pink area shows the X-ray emissions from the hot gas, and the blue areas show the region under the effect of gravitational lensing. Suppose only visible matter exists in those galaxies. In that case, most of the mass should accumulated in the middle (the pink region), and the gravitational lensing effect should have been observed in that region. However, these gravitational lensing areas undoubtedly show that most of the system's mass accumulated here, which can only be explained by dark matter in those regions. The calculated centre of mass of the system using only visible matter is far different from the calculated centre of mass using all matter (visible matter and dark matter are supposed to be in blue areas) [19].

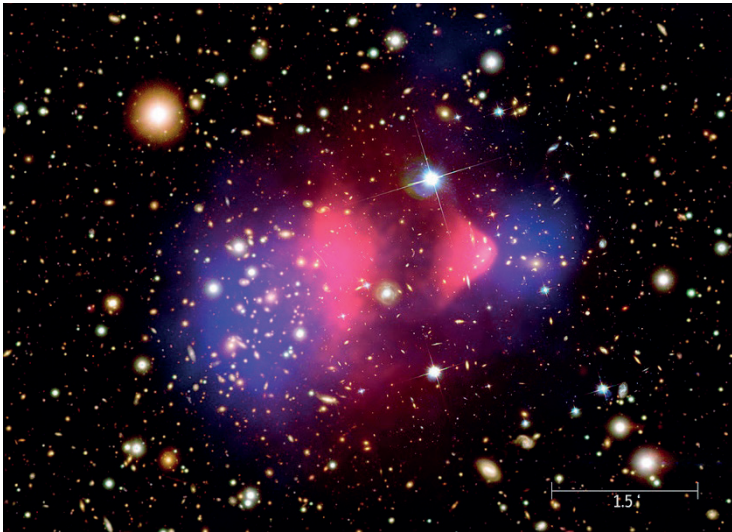


Figure 7. Two main gravitational lensing effects (Credit: NASA)

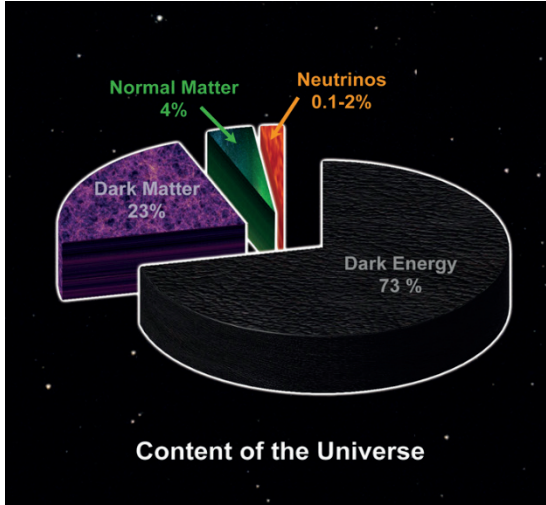
Theoretical Aspects of Dark Matter

Although many observations and experiments about dark matter have been made, there is no direct observation or evidence for its existence. Therefore, we are still far from completely understanding the true nature of dark matter. However, many ideas about dark matter's behavior are theorized, and new theories are continuing to develop with the incoming information from new experiments and observations.

Nature of Dark Matter in Standard Model

The model that is most successful in explaining the current knowledge about the universe and achieving consensus among authorities is the Standard

Model (Lambda-CDM Model). This model is mainly based on General Relativity theory and assumes it is entirely correct. According to the standard model for cosmology (Lambda-CDM Model), the theoretical properties of dark matter are:



1. Dark matter is called “dark” because it does not interact with light or other forms of electromagnetic radiation. So, even if there is a consensus about its existence by observations about the gravitational effects, it cannot be directly observed with any astronomical instruments used by astronomers.

2. Dark matter is a significant component of the universe. Using the incoming information from observations, the Lambda-CDM model predicts that dark matter is composed of 25% of the universe and is responsible for 85% of the total mass of matter. Other parts of the universe are 70% dark energy and 5% ordinary matter [21].

3. The distribution of dark matter in the universe is approximately uniform. However, the concentration of dark matter is higher in regions where galaxies and galaxy clusters form, but it is still distributed more homogeneously compared to ordinary matter.

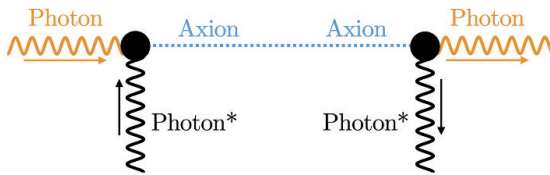
4. The particles that form dark matter have very low velocities compared to light speed. Therefore, dark matter can't escape from the gravitational force of other particles since they are not fast enough to beat centrifugal force. Moreover, this feature of dark matter successfully explains the dark matter accumulations in specific regions, allowing the formation of large structures in the observed universe. Since temperature is defined as the overall kinetic energy of the particles, and the particles of the dark matter are relatively slow, the dark matter is referred to as “cold” in the Lambda-CDM model. Additionally, due to its non-interacting nature with photons, dark matter cannot be heated by absorbing or being cooled by emitting photons.

5. Dark matter is believed not to be composed of atoms and not to contain electrons, protons, and neutrons. Because the matter we observed mostly includes baryons (three quark particles like proton and neutron), dark

matter is often referred to as “non-baryonic matter.” The non-baryonic nature of dark matter is an important aspect because it successfully explains why it does not interact with any kind of electromagnetic radiation.

6. Dark matter particles don't collide with any particle. Since dark matter particles only interact with each other and ordinary matter particles via gravitational force, they cannot collide with any particle. The collisionless nature of dark matter also enables it to clump together and hence contribute to creating the large-scale structure of the universe without disturbing any structure by the effect of collisions.

Other Theories about Dark Matter



1) Weakly Interacting Massive Particles





(WIMPs): WIMP is a hypothetical elementary particle thought to be an elementary particle of dark matter (similar to proton and neutron-ordinary matter relation) such that

it only interacts with other particles via weak nuclear force and gravitational force. WIMPs are called massive particles because their estimated mass is 10^{-21} kg to 10^{-17} kg, much heavier than protons and neutrons. WIMPs are one of the most popular theories about dark matter because there is a probability of the creation of such particles at the beginning of the universe without violating the Standard Model (they can be created in the same way that other baryonic particles are created) [22] and also some extensions of Standard Model like supersymmetry imply that existence of such particles [23]. Although there are no direct observations or evidence to indicate its existence, WIMPs perfectly explain the nature of dark matter.

2) **Axions:** Axion is another hypothetical particle considered a solution for the “CP Problem” in physics. It is possible that axions can be created in the early stages of a universe without violating the Standard Model [25]. Axions are extremely light hypothetical particles with a mass of 10^{-34} kg to 10^{-31} kg, making them much lighter than protons and electrons [24]. They interact with other particles only via electromagnetic and strong nuclear force. Scientists later noticed that axions can also be an explanation for dark matter. Because axions' interaction with electromagnetic force is fragile due to their small mass, zero charge, and low energy, and although their mass is shallow, they may be clumped in some regions that act as gravitational fields. Therefore, axions are also considered a potential explanation for dark matter since their behaviour is similar to dark matter.

Desperately seeking sterile

The three known types of neutrino might be "balanced out" by a bashful fourth type

ELECTRON NEUTRINO	MUON NEUTRINO	TAU NEUTRINO	STERILE NEUTRINO
			
MASS	< 1 electronvolt		> 1 electronvolt
FORCES THEY RESPOND TO	Weak force Gravity		Gravity
DIRECTION OF SPIN	All three "left handed"		"Right handed"

3) Sterile Neutrinos:

Sterile neutrinos are another hypothetical particle that only interacts with other particles via gravitational force. Their mass is not known precisely. Although other active neutrinos in the Standard Model are not likely to be the elementary

particle of dark matter, sterile neutrinos are significantly more probable to be a candidate [26] in some terms. Neutrinos in the Standard Model have tiny masses, which makes them fast and hard to clump together to create the gravitational effect of dark matter. Moreover, if the neutrino in the Standard Model creates dark matter, it would be hot because the particles have negligible mass and hence can have high speeds. However, the current theories about dark matter suggest that it is more likely cold than in the Standard Model. On the other hand, there is no concrete upper bound on the mass of sterile neutrinos, considering that they can only interact via gravitational force. Hence, they have weak interactions with ordinary matter; sterile neutrinos are good potential candidates for dark matter.

Conclusions

Although we have plenty of evidence to support the existence of dark matter and there is a long history of research, the true nature of dark matter cannot be understood. However, many experiments are continuing, such as the Large Hadron Collider and the Dark Energy Survey, to search for the mystery of the nature of dark matter. These experiments provide new insights into the properties of dark matter, and day by day, our knowledge about dark matter increases. Understanding dark matter may reveal many mysteries and unsolved problems about the beginning of the universe, the large-scale structure, and our understanding of gravity with the general relativity theory.

I would like to thank Mert Nardal for his help during the preparation of this summary.

REFERENCES

1. “A History of Dark Matter” – Gianfranco Bertone and Dan Hooper
2. Lundmark, K. (1 January 1930). “Über die Bestimmung der Entfernungen, Dimensionen, Massen und Dichtigkeit für die nächstgelegenen anagalactischen Sternsysteme”
3. Zwicky, F. (1937). “On the Masses of Nebulae and of Clusters of Nebulae”
4. Rubin, Vera C.; Ford, W. Kent Jr. (February 1970). “Rotation of the Andromeda Nebula from a Spectroscopic Survey of Emission Regions”.
5. Randall, Lisa (2015). Dark Matter and the Dinosaurs: The Astounding Interconnectedness of the Universe.
6. Corbelli, E.; Salucci, P. (2000). “The extended rotation curve and the dark matter halo of M33”.
7. For an extensive discussion of the data and its fit to MOND see Milgrom, M. (2007). “The MOND Paradigm”
8. Hammond, Richard (May 1, 2008). The Unknown Universe: The Origin of the Universe, Quantum Gravity, Wormholes, and Other Things Science Still Can't Explain
9. Faber, S.M.; Jackson, R.E. (1976). “Velocity dispersions and mass-to-light ratios for elliptical galaxies”. *The Astrophysical Journal*.
10. Binny, James; Merrifield, Michael (1998). *Galactic Astronomy*.
11. Taylor, A.N.; et al. (1998). “Gravitational lens magnification and the mass of Abell 1689”.
12. Wu, X.; Chiueh, T.; Fang, L.; Xue, Y. (1998). “A comparison of different cluster mass estimates: consistency or discrepancy?”.
13. Sunyaev, R. A. (1974). “The thermal history of the universe and the spectrum of relic radiation”
14. <https://www.astro.ucla.edu/~wright/CMB-DT.html>
15. Coil, Alison L. (2013). “The Large-Scale Structure of the Universe”
16. G. F. R. Ellis; H. van Elst (1999). “Cosmological models (Cargèse lectures 1998)”
17. Jaffe, A.H. “Cosmology 2012: Lecture Notes”
18. Peacock, J.; et al. (2001). “A measurement of the cosmological mass density from clustering in the 2dF Galaxy Redshift Survey”
19. Markevitch, M.; Randall, S.; Clowe, D.; Gonzalez, A. & Bradac, M. (16–23 July 2006). Dark Matter and the Bullet Cluster
20. Siegel, Ethan (9 November 2017). “The Bullet Cluster proves dark matter exists, but not for the reason most physicists think”

21. https://www.esa.int/Science_Exploration/Space_Science/Extreme_space/What_is_the_Universe_made_of#:~:text=In%20the%20currently%20popular%20model,matter%20and%205%25%20normal%20matter.
22. Garrett, Katherine (2010). “Dark matter: A primer”
23. Jungman, Gerard; Kamionkowski, Marc; Griest, Kim (1996). “Supersymmetric dark matter”
24. Peccei, R. D. (2008). “The Strong CP Problem and Axions”
25. Redondo, J.; Raffelt, G.; Viaux Maira, N. (2012). “Journey at the axion meV mass frontier”
26. Ibarra, Alejandro (2015-07-15). “Neutrinos and dark matter”



Chapter 2

QUANTITATIVE ANALYSIS OF MARKET VALUE PREDICTORS IN TURKISH SÜPER LIG: A PCA AND REGRESSION APPROACH

Mohammed ADEM¹

Mehmet Ali CENGİZ²

1 Ondokuz Mayıs Üniversitesi, Lisansüstü Eğitim Enstitüsü Müdürlüğü, İstatistik Anabilim Dalı, Veri Bilimi. ORCID ID: 0000-0002-1945-7735

2 Prof., Ondokuz Mayıs Üniversitesi, Fen Fakültesi, İstatistik Bölümü, Uygulamalı İstatistik Anabilim Dalı. ORCID ID: 0000-0002-1271-2588

Introduction

Football, also referred to as soccer in some countries, is acclaimed as the world's most popular sport, a status attributed to its widespread appeal and accessibility. According to a FIFA survey, over 240 million people regularly play football in more than 200 countries, which underscores its global reach (FIFA, 270 million people active in football., 2007). Its universal popularity can be partly attributed to the minimal equipment and infrastructure requirements, making it accessible to people from various socioeconomic backgrounds. The simplicity of the game, combined with its ability to foster community and national pride, further contributes to its widespread appeal. Additionally, major football events like the FIFA World Cup have a unifying effect, transcending cultural and national boundaries and fostering a global community of fans and players alike. This phenomenon is reflected in the viewership of the FIFA World Cup; the 2006 World Cup final alone was watched by an estimated 715.1 million people worldwide, which was about a ninth of the entire population of the planet at the time (FIFA, TV Data, 2007). The sport's ability to connect people across different cultures and regions is a testament to its powerful social and cultural influence.

Football has undergone significant evolution since its codification in England in the 19th century. The sport's development is closely tied to the industrialization and urbanization of Britain, where it rapidly spread among the working class, eventually becoming the nation's most popular sport by the end of the 19th century (Goldblatt, 2014). The creation of standardized rules by the Football Association in 1863 marked a pivotal moment, distinguishing football from rugby and other similar games. This standardization facilitated the sport's international spread, particularly within Europe and South America. By the 20th century, football had become ingrained in the cultural fabric of numerous nations, catalyzing the establishment of professional leagues and international competitions, most notably the FIFA World Cup inaugurated in 1930. The latter half of the 20th century witnessed further evolution, with advancements in broadcasting technology expanding football's reach and commercial value (Boyle & Haynes, 2004). This period also saw significant changes in gameplay and tactics, influenced by global exchanges of ideas and the increasing professionalization of coaching (Wilson, 2018). Today, football continues to evolve, shaped by technological innovations like VAR (Video Assistant Referee), Data based analysis of the game and an ever-growing global fan base, reflecting its status as a dynamic, globally interconnected sport.

The study aims to dissect the relationship between football players' market values and their on-field performances in the Turkish Süper Lig. Utilizing principal component analysis (PCA) and multiple regression analysis, the research identifies key performance indicators that significantly impact players' market valuations. The methodology involves distilling a

large set of performance metrics into principal components that succinctly capture the essential statistical features contributing to players' market value. This quantitative approach not only enhances understanding of value determination in football but also aids stakeholders in refining player evaluation and making strategic decisions in recruitment and development.

Additionally, the study integrates a clustering analysis to categorize players into distinct groups based on their performance attributes. By applying the K-Means clustering algorithm to the principal components derived from PCA, players are segmented into clusters that reflect similar playing styles and roles. This segmentation allows for a more nuanced analysis of market value, as each cluster represents a subgroup of players with comparable skill sets and roles within their teams. The clustering thus provides a framework for assessing market value dynamics within specific player categories, facilitating targeted analytical insights.

The findings of this study are expected to offer practical applications for club managers, sports analysts, and financial advisors in football. By quantifying the impact of various performance metrics on market values, the research highlights the most financially valued skills and attributes in the league. Moreover, the clustering approach enables a tailored analysis of player valuation, suggesting that market value is not only a reflection of individual performance but also of how those performances align with the roles and expectations defined by player clusters. This holistic view could significantly influence strategic decision-making in player signings, contract negotiations, and team assembly in professional football.

Theory and Literature

The integration of data analysis in football has revolutionized decision-making processes, ranging from player signings to tactical preparations. The modern football club utilizes vast amounts of data to assess player performance, potential, and value, optimizing strategies both on and off the field. Systematic analysis of player statistics and trends enables clubs to make informed decisions that align with long-term goals, such as squad building and match preparation.

Principal Component Analysis (PCA) is a key statistical technique in football analytics for reducing the dimensionality of large data sets. By simplifying datasets with many variables into principal components, PCA helps identify the most influential factors impacting player performance and market value. This aids clubs in focusing on key attributes that define successful players in specific contexts.

K-Nearest Neighbors (KNN) is employed in predictive analytics within sports for player classification and predicting game outcomes based on

historical data. This method's reliance on proximity to make predictions is apt for scenarios like scouting, matching player characteristics with specific playing styles, or tactical setups.

Regression analysis is another critical tool, utilized to understand relationships between variables like player attributes and market values. Models built through regression help predict outcomes based on input variables, assisting clubs in financially sound decision-making concerning player trades or signings.

The theoretical framework for using data analysis in football not only emphasizes the application of these techniques but also the strategic integration of the insights they provide into decision-making processes. Clubs effectively incorporating data analytics are more likely to achieve a competitive advantage and financial stability.

The literature reveals a dynamic shift in football driven by data analytics, machine learning (ML), and technological advancements, affecting player evaluation, team building, and strategic decision-making. Studies range from evaluating sports metrics to algorithmic approaches in talent identification and analyzing player transfer dynamics.

Franks et al. (2016) introduced "meta-metrics" to assess sports metrics, emphasizing the need to discern between relevant and irrelevant metric variations, refining decision-making in sports analytics. Barron et al. (2018) demonstrated the potential of ML in enhancing traditional scouting methods by identifying key performance indicators from technical performance data.

Advancements in decision support systems, crucial in football management, utilize ML to optimize player positioning and team formation, enhancing team performance strategies. For instance, a thesis by Al-Asadi (2018) showcases a system that employs ML methods effectively in this realm.

Studies such as Liu et al. (2016) dissect the intricate dynamics of the player transfer market, revealing that substantial investments generally lead to enhanced team performance. Aydemir et al. (2022) combined various data sources to predict player transfer values, highlighting the complex nature of the transfer market.

In sum, the literature underscores how data-driven methods are revolutionizing football, providing new insights into player performance, recruitment strategies, and club management, fostering a new era of intelligent football management aligned with robust analytical evidence.

Data and Methodology

In the exploration of the complex relationship between football players' performance metrics and their market values, the study leverages

an extensive dataset sourced from the Turkish Süper Lig for the 2018-2019 season. This dataset, acquired from Sofascore, encompasses both general player information and detailed performance data across 115 distinct metrics, illustrating a comprehensive view of player capabilities and contributions on the field. The dataset includes every player from all 20 teams participating in the season, ensuring a broad and inclusive data foundation for robust analysis. The data spans multiple dimensions:

General Information: Player name, age, position, team, and contract details provide basic yet vital information.

Performance Metrics: Extensive in-game statistics such as goals scored, assists, defensive actions, passing accuracy, and more that quantitatively describe a player's game influence.

Market Value: An estimation of the player's worth in the transfer market, serving as a critical outcome variable for the analyses.

In the provided code snippet, effective metrics are computed from various performance indicators in football matches, encompassing defensive and offensive actions such as duels, crosses, dribbles, and passes. These metrics quantify the effectiveness of players in specific aspects of the game by considering both the frequency of their actions and their success rates. For instance, Effective Defensive Duels per 90 is determined by multiplying the number of defensive duels per 90 minutes by the percentage of defensive duels won, while Effective Passes per 90 is derived from the product of passes per 90 and the accuracy of those passes. After calculating these metrics, irrelevant columns are removed from the dataset to streamline the data for further analysis and interpretation.

Analytical Techniques Applied

The study applied multiple sophisticated statistical and machine learning techniques to extract meaningful insights.

Principal Component Analysis (PCA): Used to reduce the dimensionality of the dataset while capturing most of the variance in the data while retaining 85% of the variance, aiming to create a more concise representation of the data. This approach helped in distilling the information into fewer, more potent indicators of performance and value.

Cluster Analysis: Leveraging K-means clustering facilitated the segmentation of players into distinct groups based on their performance traits, which helps in comparative analysis across different player profiles. The data is first scaled using Standard Scaling to standardize features, ensuring uniformity in feature scales, which is vital for effective clustering. Next, the Elbow Method is employed to identify the optimal number of clusters for the

K-means analysis. By plotting the SSE against different cluster numbers, the point where the rate of decrease slows down is identified, helping to determine the ideal number of clusters for the analysis. This process ensures that the clustering results are accurate and actionable.

Linear Regression Models: Employed to predict market values based on performance metrics, offering insights into the attributes most valued in the transfer market. The regression analysis is conducted for each cluster using linear regression models. For every distinct cluster, the data is filtered accordingly, separating the independent variables (Principal Components) from the dependent variable (Market Value). A constant is added to the model to account for the intercept, and the Ordinary Least Squares (OLS) method is applied to fit the regression model. The results are then summarized, providing insights into the relationship between the Principal Components and Market Value within each cluster. This analysis aids in understanding how different clusters contribute to variations in market values, facilitating targeted strategies for player valuation and management.

The integration of PCA and clustering revealed nuanced player segments, highlighting different aspects of football performance that correlate with market value. For instance, defensive skills, playmaking abilities, and scoring proficiency emerged as key drivers of market value. The linear regression models further quantified these relationships, providing a predictive foundation to estimate a player's market value based on on-field performance metrics.

Results

Principal Component Analysis (PCA)

In this study, Principal Component Analysis (PCA) was utilized to reduce the dimensionality of a dataset comprising 82 detailed football player performance metrics. The PCA transformation distilled these metrics into 15 principal components (PCs) that capture the most significant variance within the data, thus simplifying the complexity of the dataset while retaining essential information that characterizes player performance.

The PCA provides a framework to understand complex player data by reducing dimensions and highlighting the most impactful attributes contributing to a player's overall performance and market value. These components help categorize players into distinct types based on their strongest attributes, facilitating more nuanced scouting, performance assessment, and market valuation in professional football.

PC	Description	Key Metrics
PC1	Precision Passing and Defensive Skills	Accurate crosses, successful attacking actions, minutes played
PC2	Offensive Dynamics and Scoring Potential	Shots on target, xG per 90, successful attacking actions per 90
PC3	Goalkeeping and Defensive Metrics	Save rate, exits per 90, defensive actions
PC4	Comprehensive Attacking Play	Non-penalty goals per 90, shot assists per 90, shots on target
PC5	Speed and Agility	Accelerations per 90, successful defensive actions per 90
PC6	Long-Range and Aerial Play	Average long pass length, aerial duels won
PC7	Playmaking and Midfield Dynamics	Successful attacking actions, passes per 90
PC8	Wide Play and Crossing Accuracy	Crosses per 90, accurate crosses, %
PC9	Set Piece and Scoring Efficiency	Free kicks per 90, shots on target, %
PC10	Defensive and Physical Engagement	Sliding tackles per 90, interceptions
PC11	High-Impact Plays	Key passes, dribbles per 90
PC12	Endurance and Experience	Age, minutes played
PC13	Transitional and Versatile Play	Received passes per 90, successful defensive actions
PC14	Specialized Roles in Offense and Defense	Fouls suffered per 90, defensive duels
PC15	Targeted Offensive Contributions	Shots per 90, non-penalty goals

Table1: Summary Of Principal Components Derived From PCA

Cluster Analysis

The cluster analysis in this study was conducted using the K-means clustering algorithm. This method was chosen for its efficiency and effectiveness in grouping data points (players) based on the similarity of their performance metrics derived from the PCA. The goal was to identify distinct groups of players with similar attributes to facilitate targeted analysis and decision-making in player management and team composition. Before applying the K-means algorithm, the data underwent a standardization process using the StandardScaler method to ensure that all variables contributed equally to the analysis, eliminating bias due to the scale of the variables. The optimal number of clusters was determined using the Elbow Method, which involves plotting the sum of squared distances of samples to their closest cluster center and identifying the 'elbow' point where the rate of decrease sharply shifts. This method suggested that four clusters would provide the most meaningful segmentation.

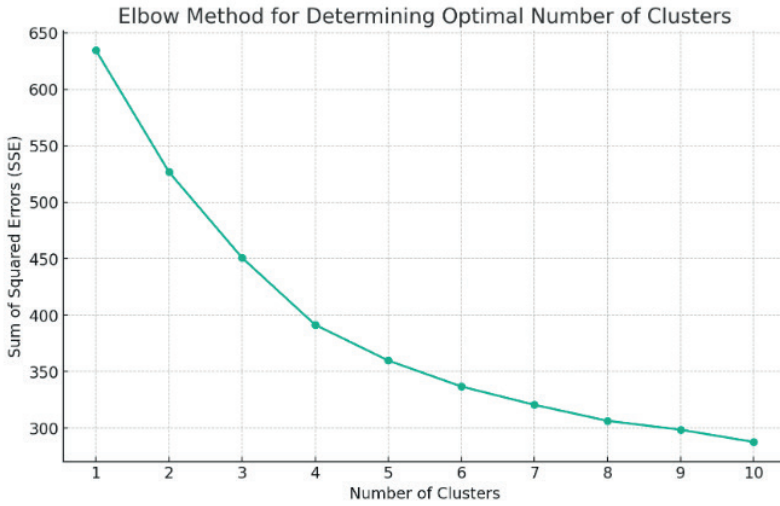


Fig1: Elbow Method

Based on the results from the K-means clustering, players were segmented into five distinct clusters, each representing unique playing styles and abilities. The following bar chart illustrates the distribution of players across five distinct clusters identified in the cluster analysis.

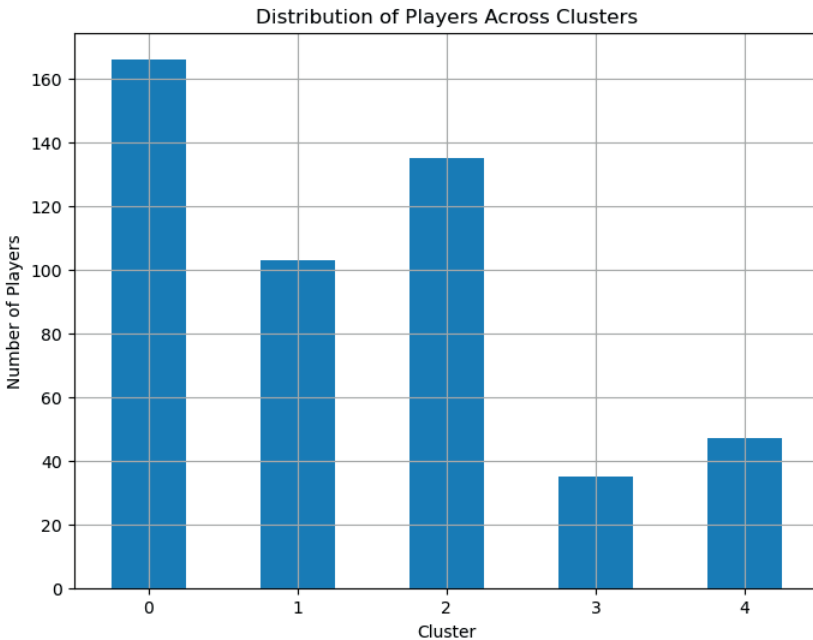


Fig 2: Distribution Of Players Across Clusters

Cluster 0: Precision Passing and Defensive Skills

Players in this cluster are primarily midfielders or defenders known for their defensive capabilities and precise passing. They excel in maintaining possession and effectively distributing the ball under pressure, evidenced by high scores in metrics like successful passes per 90 and pass completion rates. Defensively, their skills are underscored by metrics such as interceptions per 90, tackles won, and clearances. In their teams, these players are foundational, ensuring stability in defensive situations and aiding in the transition from defense to offense through meticulous ball distribution.

Cluster 1: Offensive Dynamics and Scoring Potential

This cluster includes forwards and attacking midfielders who drive the offensive thrust of their teams. They demonstrate a potent offensive presence on the field, engaging in goal-scoring and creating significant play opportunities. The cluster is characterized by high values in goals per 90, xG, assists, and successful dribbles. These players are crucial in pivotal game moments, often becoming the focal points of their teams' attacking strategies and marketing campaigns due to their ability to alter the course of matches with their skills.

Cluster 2: Comprehensive Attacking Play

Cluster 2 consists of versatile players who contribute widely across the attacking spectrum. These players blend playmaking with scoring, making them invaluable in dynamic offensive setups. They exhibit a balanced mix of assists, key passes, shots on target, and successful offensive duels, often demonstrating a high work rate that sees them actively participating across the entire pitch. Their adaptability allows them to fit into multiple tactical formations, making them essential connectors between the midfield and attack.

Cluster 3: Goalkeeping and Defensive Metrics

Specialized for goalkeepers and defensive players, this cluster focuses on metrics pivotal to defensive and goalkeeping roles. Noticeably smaller than the other clusters, players here are integral to their teams' defensive structures, highlighted by metrics such as save percentage, clean sheets, saves per game, and successful exits. They also excel in one-on-one defensive situations, including aerial duels. These players often assume leadership roles within the squad, organizing the defense and initiating play from the back, thus forming the core of the team's defensive strategy.

Cluster 4: Specialized Roles in Offense and Defense

Cluster 4 includes players who perform specialized tasks critical to both offensive and defensive phases. These players, often occupying roles like wing-backs or defensive midfielders, are noted for their dual capabilities.

Defensively, they are reliable, as indicated by metrics like blocks per 90 and successful tackles. Offensively, they contribute through crosses per 90 and key passes from wide areas. Their ability to engage effectively in both attacking and defensive duels underscores their versatility, making them key tactical elements in matches requiring nuanced strategies. These players ensure the team’s balance, supporting offensive plays without compromising defensive solidity, and are pivotal in managing transitions and set-piece scenarios.

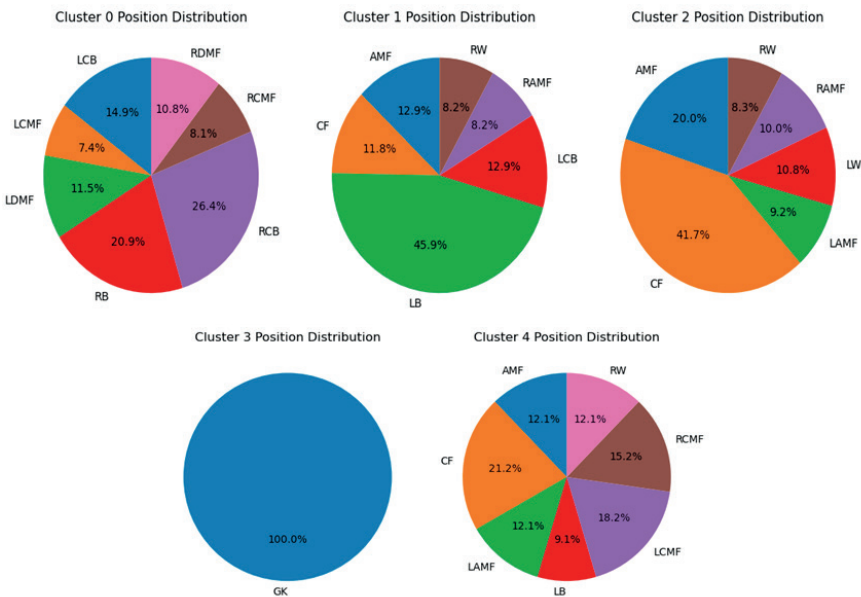


Fig 3: Cluster - Position Distribution

Understanding the clusters helps in tactical planning, such as identifying players who can fulfill specific roles within a team’s strategy or adjusting training programs to enhance underrepresented skills in certain clusters. Clusters assist in profiling potential signings to ensure they fit into the desired playing style or tactical setup. They also help in identifying players with similar attributes to those who are performing well. By analyzing the attributes of each cluster, coaching staff can tailor development programs to help players evolve attributes that may allow them to transition into clusters that align better with team needs or their career aspirations.

In conclusion, cluster analysis provides a nuanced view of the player landscape, revealing patterns and groupings that are not immediately apparent through traditional analysis. This approach allows for a more strategic application of player data in team management and player evaluation, enhancing the ability to make data-driven decisions in the competitive environment of professional football.

Regression Findings

PC	Coefficient	P-value
PC7	-3.026e+06	0.017
PC9	+3.267e+06	0.012

Table 2: Cluster 0 Regression Results

The regression analysis conducted for each cluster revealed nuanced insights into how performance metrics influence players' market values, with significant predictors varying across different clusters.

In Cluster 0, which focuses on precision passing and defensive skills, the model explained approximately 23.5% of the variance in market values. Among the significant predictors, PC7, which represents defensive engagements and physicality, showed a negative relationship with market value, suggesting that increased defensive actions might correlate with lower market values. In contrast, PC9, representing impactful playmaking, positively affected market values, highlighting the value placed on effective playmaking abilities.

PC	Coefficient	P-value
PC1	-6.648e+06	0.012
PC2	-2.669e+06	0.016
PC3	+2.23e+06	0.038
PC4	-9.403e+06	0.023
PC5	+2.99e+06	0.009
PC6	+8.415e+06	0.000
PC7	-4.033e+06	0.000
PC11	-3.786e+06	0.042

Table 3: Cluster 1 Regression Results

Cluster 1 demonstrated a strong model with an R-squared of nearly 0.489, indicating it could explain almost half of the variance in market values. This cluster, characterized by long-range and aerial play, found significant predictors in PC1 and PC6—both positively impacting market value. These components, emphasizing long-range capabilities and aerial prowess, underscore the premium on players who excel in these areas, reflecting their critical role in influencing market values.

PC	Coefficient	P-value
PC2	-8.322e+07	0.043
PC6	+5.412e+06	0.036
PC7	-3.735e+06	0.016
PC9	+4.074e+06	0.027

Table 4: Cluster 2 Regression Results

In Cluster 2, focused on offensive dynamics and scoring potential, the model's R-squared was 0.286. This indicates a moderate relationship between the performance metrics and market values, capable of explaining about 28.6% of the variance. The most noteworthy predictor was PC6, which underscores the importance of scoring potential. This component positively correlates with market value, reinforcing the significance of offensive capabilities and goal-scoring skills in determining a player's market worth.

Cluster 3, which includes precision passing and defensive skills along with goalkeeping metrics, presented a substantial model effectiveness with an R-squared of 0.484. This suggests a significant correlation between players' metrics and their market values, indicative of effective predictability. The presence of goalkeeping metrics in this cluster suggests a specific market niche for players excelling in these roles, highlighting the specialized nature of these positions in football.

Cluster 4, however, demonstrated the lowest effectiveness in predicting market values based on the measured performance metrics, with an R-squared of only 0.209. This cluster's results indicate limited predictive success, suggesting that the comprehensive attacking play metrics captured might not fully encompass the broad range of skills impacting market values, or possibly the influence of high-profile outliers.

Overall, the regression findings across clusters illustrate the diverse and complex factors influencing player valuations in professional football. While offensive capabilities, defensive actions, and specialized skills like long-range shooting and aerial abilities significantly drive market values in some clusters, other clusters show a more scattered or nuanced set of influential factors. This diversity highlights the tailored approaches needed in player evaluation and management, reflecting the specialized and varied nature of player roles and their respective market dynamics.

Discussion

The analysis conducted presents a nuanced understanding of the relationship between player performance metrics across various clusters and their corresponding market values in professional football. Our results suggest that different clusters of players, as defined by their on-field roles and effectiveness in specific areas such as offense, defense, or specialized skills, influence their market value in distinct ways. For example, in Cluster 1, offensive dynamics and scoring potential were significantly related to higher market values, indicating that players who contribute directly to scoring and creating goal opportunities are highly valued. In contrast, Cluster 2 highlighted the importance of defensive contributions and versatile playmaking, reflecting a valuation approach that appreciates versatile players who contribute across multiple facets of the game.

Despite these insights, the analysis has several limitations. The adjusted R-squared values for some clusters suggest that the models explain a relatively small portion of the variance in market values. This could be due to the complex nature of market value determination, which is influenced by factors beyond on-field performance, including marketability, contract situations, and external economic factors. Additionally, the presence of multicollinearity, particularly in Clusters 3 and 4, where no significant predictors were identified, suggests that the relationships between variables are complex and may require more sophisticated modeling techniques to disentangle.

The findings have significant implications for club management and scouting departments. By understanding which attributes translate into perceived financial value, clubs can better strategize their player development, scouting, and transfer activities. For instance, investing in players with high offensive metrics might yield better returns in transfer markets, as seen in Cluster 1. However, the importance of defensive skills and versatility should not be underestimated, as demonstrated by Clusters 2 and 4, indicating a balanced approach might be more sustainable.

Future research could address these limitations by incorporating additional data such as player popularity on social media, sponsorship deals, and fan base size to capture more aspects of 'market value'. Advanced statistical techniques, such as machine learning models or neural networks, could be employed to handle the multicollinearity better and improve the predictive power of the models. Furthermore, longitudinal studies could explore how these relationships change over time, providing insights into the dynamics of the football market.

In conclusion, this study illuminates the complex interplay between player performance metrics and market value in professional football. By leveraging cluster analysis and regression models, we have identified specific performance metrics that significantly impact player valuation in different clusters. This research not only enhances our understanding of market dynamics in football but also offers practical guidance for stakeholders in making informed decisions related to player investments. Future work expanding on these methodologies and incorporating broader data sets promises to refine these insights further and drive the strategic development of football clubs globally.

References

- Al-Asadi, M. (2018). Decision Support System for a Football Team Management by Using Machine Learning Techniques. *SELÇUK UNIVERSITY GRADUATE SCHOOL OF NATURAL SCIENCES*.
- Aydemir, A. E., Temizel, T. T., & Temizel, A. (2022). A Machine Learning Ensembling Approach to Predicting Transfer Values. *SN COMPUT. SCI.* 3.
- Barron, D., Ball, G., Robins, M., & Sunderland, C. (2018). Artificial Neural Networks and Player Recruitment in Professional Soccer. *PLoS ONE*.
- Boyle, R., & Haynes, R. (2004). *Football in the New Media Age*. Routledge.
- FIFA. (2007). *270 million people active in football*. FIFA Magazine.
- FIFA. (2007). *TV Data*. fifa.com: <https://web.archive.org/web/20090830065721/http://www.fifa.com/aboutfifa/marketing/factsfigures/tvdata.html> adresinden alındı
- Franks, A. M., D'Amour, A., Cervone, D., & Bornn, L. (2016). Meta-analytics tools for understanding the statistical properties of sports metrics. *J. Quant. Anal. Sports*, 151–165.
- Goldblatt, D. (2014). *The Age of Football: The Global Game in the Twenty-first Century*. Macmillan.
- Konefał, M., Chmura, P., Zając, T., Chmura, J., Kowalczyk, E., & Andrzejewski, M. (2019). A New Approach to the Analysis of Pitch-Positions in Professional Soccer. *Journal of Human Kinetics*, 143-153.
- Liu, X. F., Liu, Y.-L., Lu, X.-H., Wang, Q.-X., & Wang, T.-X. (2016). The Anatomy of the Global Football Player Transfer Network: Club Functionalities versus Network Properties. *The Anatomy of the Global Football Player Transfer Network: Club Functionalities versus Network Properties*.
- van Dooren, K. (2023). Predictors of Football Player Performance at sub-top Eredivisie clubs. *Twente University*.
- Wilson, J. (2018). *Inverting The Pyramid: The History of Soccer Tactics*. Orion.



Chapter 3

CONDURITOLS: PIONEERING SYNTHETIC MARVELS WITH PROFOUND BIOLOGICAL SIGNIFICANCE

Sedat Sadi İNCİ¹

Hülya ÇELİK²

1 Ağrı İbrahim Çeçen Üniversitesi Eczacılık Fakültesi sedokurplani@gmail.com

2 Doç. Dr.; Ağrı İbrahim Çeçen Üniversitesi Eczacılık Fakültesi Temel Eczacılık Bilimleri Bölümü
hycelik@agri.edu.tr ORCID No: 0000-0003-0805-0523

INTRODUCTION

Conduritol

The conduritol compound, known by its chemical name as 1,2,3,4-cyclohexenetrol, is a compound that is seen as a derivative of cyclohexene, which carries 4 hydroxyl groups in terms of its formation. There are 6 different compounds in the group, they are separated according to their position in the mean plane of the ring. These are A, B, C, D, E, F. The synthesis of conduritol for the first time was made by K. Kübler in 1908. Many synthesis methods have been proposed for the chonduritol compound, which has six different formats in diastereomeric form. The A-F order of these isomers also refers to the synthesis/isolation order. Of these six isomers, the presence observed in nature is A and F. Although conduritol A is observed to be limited, conduritol F is observed in almost all green plants.

In this synthesis, Kübler used the plant *Marsdenia cundurango*, which is native to South America and Peru. It has been established that the plant encompasses cyclitol or cyclic polyol structures.

In addition, chondritols, cyclohexanedols (such as proto-quercitol) and cyclohexanhexols (such as myo-inositol) are important intermediate compounds in the formation of molecules that are not of synthetic origin and show biological activity.

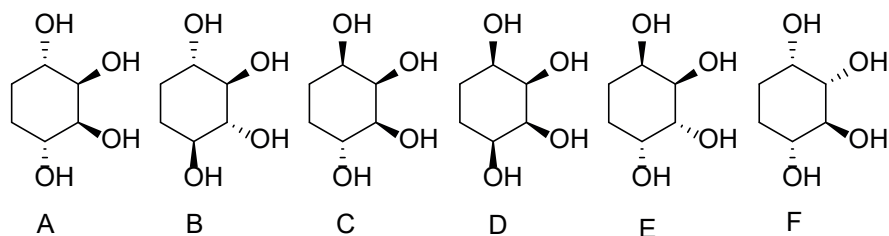


Figure 1. *Chonduritol derivatives*

Marsdenia condurango is an alcohol isolated in 1908 using vine bark. This alcohol was recorded by Kübler as conduritol, but what Kübler found was not an optically active compound and had an unsaturated cycle. In their studies, Dangschat and Fischer examined its structure and determined it as Conduritol A. Chonduritols, which have six diastereomers, are named in a sequential manner as A-B-C-D-E-F due to the absence of confusion. In 1962, as a result of Plouvier's work, a new isomer of conduritol was discovered from the plant *Crysanthemum Leucanthemum* and named *L-Leucanthemol*, Conduritol F.

The Concept and Discovery of Conduritol

These compounds, which we call conduritol, are a group that has been popular with people working in the scientific world because they are synthetic and biologically active. It has been determined by studies that epoxides and amino chondritols of this group inhibit the HIV virus and the enzyme glicosidase, and some of its derivatives even control the release of insulin in the human body. Apart from these, it is known that some conduritol derivatives are used as intermediates in the synthesis of some antibiotics, these antibiotics are pancratistatine, licoridine and aminoglycoside antibiotics. It is known that some of the compounds we call conduritol are also used in chemotherapy, which is the treatment of cancerous cells, because they inhibit the enzyme activities involved in the formation of oligosaccharides. Chonduritol, which are used as inhibitors of glycoside enzymes, are involved in the treatment of diabetes, cancer and AIDS. (Kilbas and Balci, 2011).

Of the conduritol compounds, A and F are already present in nature. Due to the double bond present in the structures of these compounds, it participates in the addition reactions with low activity and can then be transformed into another functional group. Compounds A and F are useful intermediates of organic syntheses, but they are irreversible in some reactions. As we mentioned before, conduritol is the compound that attracts attention in the scientific world, as well as derivatives of this compound, called halochonduroles, have gained importance in recent years due to their α -glycosidase inhibitors. Of these, the use of bromine-chonduritol is included in AIDS studies. The reason why it has attracted attention so quickly in the scientific world is the biological missions they have undertaken in recent years. These missions are to be used as a model for insulin-regulating action and release. The double bonds in this structure are oxidized and are important compounds that form the structure of kersitol and inositol, which are their parent analogues. The importance of these compounds is that they act as inhibitors of pseudo-sugars and glycosidases, which contain queritol and inositol structures.

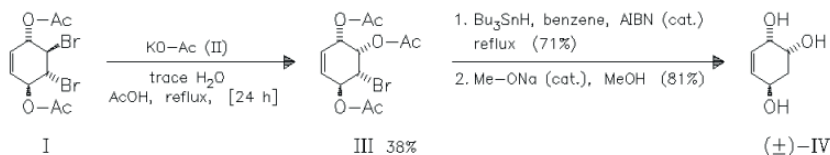


Figure 2. First known synthesis of the conduritol compound

The 1,4 benzoquinone contained in this part is formed as a result of six-step reactions. The key reaction in this synthesis is the displacement of the monohalide by the anchimeric means. The functions of the Dibromo (I) compound here are important. (III) compound, and subsequent O-acetylation

to form the expected deoxy-chonduritol (Haines *et al.* 1998). The interest in these compounds is increasing day by day, and the reason for this interest is;

- ✓ The conversion of conduritol compounds into different functionalities by addition reactions can be easily realized and can be used as an important molecule in the formation of compounds such as natural and synthetic.
- ✓ In addition, chonduritol compounds act as insulin regulators as biological activity and have an important place in the development of insulin drugs.
- ✓ The biological activity of bromochonduritol and chonduritol epoxide derivatives originating from or containing the conduritol skeleton is also observed as glycosidase inhibitors.

A large number of inositol derivatives are synthesized from chonduritols by functionalizing their double bonds. The transformation of benzene derivatives into 3-5, cyclohexadene-cis-1,2-diol 8 compounds in bacterial culture medium started in the 1980s and accelerated in the following 20-year period. (Brown *et al.* 1993; Hudlicky *et al.* 1999). In addition, an example is given in Figure 1.3 regarding the synthesis of inositol derivatives 12 and 15 starting from ketal 9 prepared from diol 8, which was synthesized using the microbiological method, and following the conduritol derivatives 10, 14 scheme (Hudlicky *et al.* 1996).

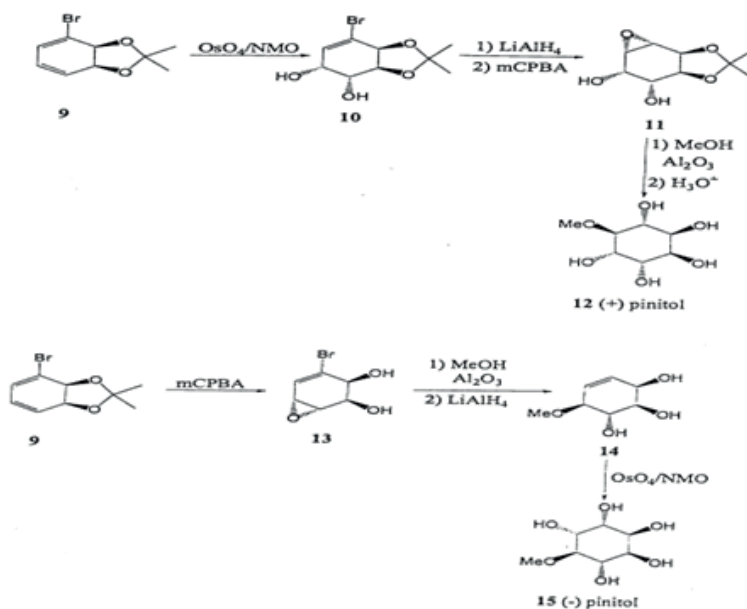


Figure 3. Synthesis of inositol derivatives

The discovery of the anti-diabetes effect of our compound emerged with a mouse experiment in the 1930s. In an experiment conducted in 1930, Indian syrup prepared from *Gymena syvestre*, which has been used for thousands of years for the treatment of diabetes, was found to significantly change and reduce the sugar level at a dose of 4 grams applied to each patient. After this experiment, the Japanese research group discovered that Konduritol A was found in this preparation and had an important place, *and Konduritol A was isolated from its leaves using Gymena syvestre*. Then, isolated Konduritol A was given to the running subject mice and sugar level measurements were examined, and after this study, it was determined that the effect of Choduritol A on sugar was very important.

A different research group, Billington and his colleagues, have carried out a strange experiment related to Conduritols in recent years. In this experiment, he tested the levels of onduritol analogues to affect insulin secretion (Billington *et al.* 1998). In this experiment, it was determined that the level of conduritol connection with insulin exchange rates was carried out under in vitro conditions.

<u>Konduritol izomeri</u>	<u>2.8 mM glikozdaki % deęişim</u>	<u>16.7 mM % deęişim</u>
Konduritol A	+45	-30
Konduritol B	+41	+50
Konduritol C	+27	-20
Konduritol D	0	0
Konduritol E	+12	+15
Konduritol F	+9	-3
Dihidroconduritol A	-16	-13

Figure 4. *Conduritol isomers and their changes in glucose*

As seen in the changes in glucose levels, the effect of chonduritol A and chonduritol B increased the level of glucose at low levels but also decreased those at high levels. After examining these data, the research team suggested that these compounds could be used in the synthesis of drugs used in the treatment of diabetes based on the effect of conduritols on insulin secretion.

According to the data obtained in the total synthesis experiment of the new chonduritol, which can modulate insulin secretion, published by another research team, it was recorded that conduritol A and B altered insulin release from isolated pancreatic islets. Based on these records and the known hypoglycemic activity of conduritol A, a number of polycyclic analogues of chonduritol A have been synthesized, and the insulin release capabilities of these synthesized substances have been examined (Balcı 1997; Kindl 1964)

Types of Conduritol

Conduritol A

It is known that Konduritol A, a natural product, was first isolated by Kübler. The first successful non-stereospecific synthesis of this compound was carried out by Nakajima et al. In these studies, trans-diacetate-10 was used for the synthesis of chonduritol isomers 3 for the first time. These compounds, which were formed as a result of the oxidation of diacetate 10 with perbenzoic acid, formed a mixture of 11 and 12. Without separation, this mixture was hydrolyzed and produced three isomeric chonduritols; A, B and E, 4, 5, 8 were obtained. Its molecular formula is $C_6H_{10}O_4$.

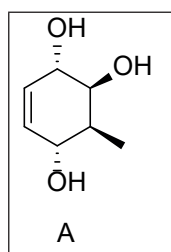


Figure 5. Conduritol A chemical structure

Konduritol A is a chonduritol in the 2nd, 3rd and 4th states of the hydroxy groups in the trans, trans, cis- relationship with the one in position 1. UIPAC Name (1S,2R,3S,4R)-cyclohex-5-en-1,2,3,4-tetrol. Its function is metabolic. Conduritol A is a natural conduritol found in *Marsdenia tomentosa*, *Gymnema sylvestre*, and *Wattakaka volubilis*, whose information is found to be constant

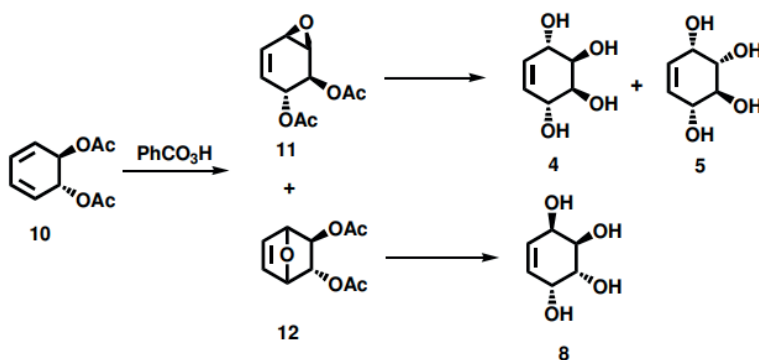


Figure 6. Choduritol A synthesis

Pharmacological and Biochemical Properties: They are compounds that inhibit or block the activity of glycoside hydrolases such as Alpha-amylases and Alpha-glucosidases.

Hypoglycemic Effect of Conduritol A Compound

In an experiment, weight changes in mice were observed as a result of a 14-day observation. In order to detect the excretion of glucose, the liver is taken and HE, the pancreas is taken to perform immune histochemical staining, then pancreatic islet beta cells are shown. The index of the thymus, pancreas, splenica is calculated.

As a result of the experiment, diabetic model mice were compared, and it was determined that fasting blood glucose was significantly reduced in rats exposed to high and moderate doses of conduritol A. Compared to the diabetic model group, the cell structure and form of chonduritol A were somewhat improved. Immunohistochemistry results showed that the number of beta cells of the pancreas in each group of chonduritol A was greater than in the model group.

As a result, the properties of Konduritol A may have an effect on the ability to level blood lipid metabolism, scavenge free radicals, increase antioxidant ability, and strengthen immune function. It has been shown to promote hepatic synthesis to reduce fasting blood sugar (Kaplan 2015; Kayard, 2011). Stereoselective synthesis has been reported as a new method for the chonduritol-A compound, starting from P-benzoquinone and a different anthracene derivative (Kayardi 2011). Today, ring-closure olefin metathesis (RCM) has come to the fore as an innovative method related to asymmetric chonduritol synthesis. Using this method, conduritol-A, E and F were synthesized independently. Diene 26 was synthesized starting from galactitol, D-mannitol, and D-glusitol, respectively. These studies have led to the production of Conduritol-A (4) with 99% efficiency.

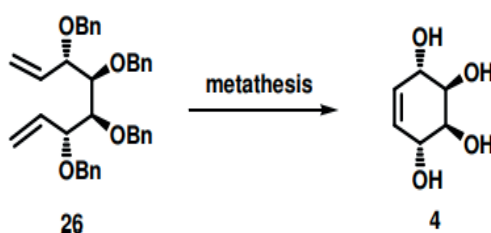


Figure 7. *Synthesis of Conduritol-A (4)*

Konduritol B

Conduritol B is a natural product found in *Leptadenia arborea*, *Asclepias curassavica* and *Cynanhum bungei*. Its molecular formula is $C_6H_{10}O_4$.

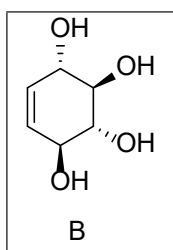


Figure 8. Chemical structure of Konduritol B

Many studies on the synthesis of conduritol and its derivatives, starting from cyclitols by substituting under appropriate conditions, have been published in the literature. To give an example, Müller synthesized conduritol-B from the pentaacetate of 6-bromoquercitol (28) by treating it with zinc in acetic acid. The results of this synthesis were once again examined by two scientists, McCasland and Horswill. They formed two different bromoquercitols 28 and 29 by the reaction of myo-inositol (27) with acetyl bromide. With the destruction of the bromine atoms, hydrolysis yielded the tetraacetate of conduritol-B (30), and its acetyl group, Conduritol B, was successfully synthesized.

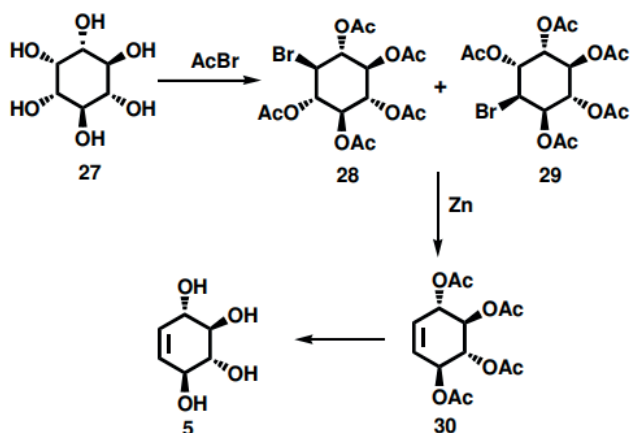
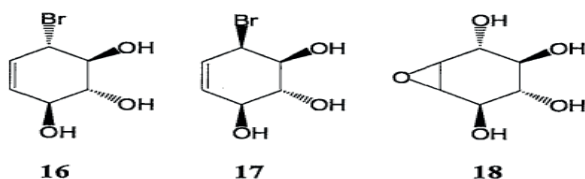


Figure 9. Chonduritol B synthesis

In the studies carried out, the stereospecific synthesis of chonduritol B starting from oxepine-benzene oxide has also been recorded. Epoxy diol was formed by the addition of oxygen functionality to molecule 40. Subsequently, epoxy diol⁴² was converted to epoxy diacetate structure and yielded Conduritol B tetraacetate by the opening reaction of the catalyzed ring (Balci 2007).

Chonduritol B Epoxide Formation and Biological Significance

Although conduritol compounds have a rich structure, there are two active synthetic chonduritols that act as glucose inhibitors that can be biologically active and used, these are Epoxide 18, which is a mixture of 16 and 17 mentioned.



Şema 3

Figure 10. *Chonduritol B derivatives*

Conduritol B Epoxide compound, known as CBE, is a naturally occurring derivative of chonduritol B, as mentioned. The reason why CBE is important for scientists is that it acts as a covalent inhibitor of the catalytic site of acid beta-glucosidase¹ and alpha-glucosidase². In addition, it is a compound that provides the formation of ceramide from beta-glucosidase and glucosylceramide compounds. The cause of lysosomal storage disease, known as Gaucher disease, is damaging mutations in acid betaglusidase. CBE is an important compound used in Gaucher disease because it is a compound that accelerates the duration of the effects. CBE causes glucocerebrocyte accumulation in neurons in Gaucher patients during their treatment, and it has been noted that CBE has no effect on dendrite development (Grabowski *et al.* 1985; Yang *et al.* 1985; Premkumar *et al.* 2005; Grabowski *et al.* 1986)

Bromochonduritol Formation and Biological Activity

Conduritol B, known as bromochonduritol, is a diastereomeric mixed-like structure formed by exposing B to hydrogen bromide. The first known synthesis of this structure was when conduritol B was exposed to 48% HBr, and then it was seen in chromatography in experimental activities after the waiting phase (Legler *et al.*1977).

In recent years, bromo-chonduritols have attracted the attention of people working in this field with their use as glycosidase inhibitors and the production of halogenochonduritols.

As a result of these researches, these reactions were recorded by visibly converting halogenobenzene derivatives into halogeno-cis-diol 1 compounds

in an antibacterial working environment. The compounds we are talking about have a wide range of activation areas with the obtaining of polyols.

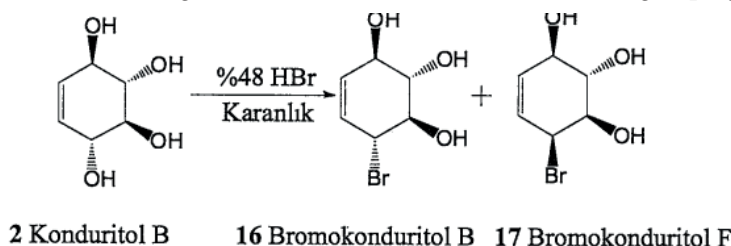


Figure 11. *Conduritol B derivatives*

It has been recorded that this mixture obtained is then recrystallized and when they are kept in ethanol, it transforms and an isomer mixture is formed.

By using these methods, the use of which was determined correctly, the synthesis of halichondritol from halogenobenzene and pinitol by oxidation reaction of halogenochonduritol showed a common framework of action (Brown, 1993).

In addition to the fact that these compounds have a strong effect on research in the AIDS treatment process, they are also a powerful bioactive agent used in undesirable conditions caused by blood sugar levels known as diabetes. 150 of the nearly 3000 enzymes known in nature consist of glycosidases. The task of these enzymes, known as glycosidase, has been recorded as an enzyme that provides hydrolysis in N-S glycoside bonds together with mono-oligo and polysaccharides depending on the substrate feature.

The stereospecificity of the enzymes used has been determined by the glycosidases we have mentioned, which break either the α -glycoside bond or the β -glycoside bond. Stereospecific is the direct effect of the stereochemistry structure of the reacting reagent on the structure of the product.

The most important of these are α -glycosidase (maltase), β -glucosidase, β -galactosidase (sucrase, invertase), β -glycofurinase and amylases. α - Glycosidase actually cleaves the α glycoside bonds in maltose. β -glycosidase hydrolyzes β -methyl glycoside, amygdalin, and celllobiose β -glycosides. B-galactosidase (lactase) specifically cleaves the β -glycoside bond of lactose, forming galactose and glucose. B-fructosidase breaks down sucrose into glucose and fructose, as well as hydrolyzes furanoid β -fructosides. β -Glucuronidase breaks down glucuronides, including mucoids. Amylases break down starch and glycogen (Beyer 1996).

Conduritol C

The first recorded synthesis of the compound known as conduritol C was carried out by McCasland and Reeves, starting with epi-inositol. 6-bromoquercitol pentaacetate is formed by taking epi-inositol to a warm environment and exposing it to acetyl bromide and acetic anhydride. This formed compound is also treated with zinc-acetic acid, forming the tetraacetate of Conduritol C. Its molecular formula is $C_6H_{10}O_4$.

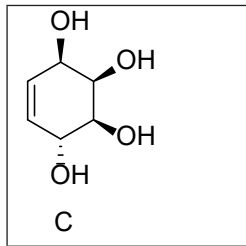


Figure 12. Conduritol C chemical structure

After the first synthesis, Nakajima and his group synthesized Choduritol C based on trans-benzene-diol (Nagabhushan 1970).

Biocatalysis is performed using monosubstituted benzenes as a useful and objective perspective on the synthesis of chonduritol C. Chemo enzymatic methods obtain the desired molecules Choduritol C, Bromo Chonduritol C and Methyl Chonduritol C (Balcı 1990; McCasland *et al.* 1955; Nakajima *et al.* 1957; Yurey *et al.* 1961; Le Drian *et al.* 1989).

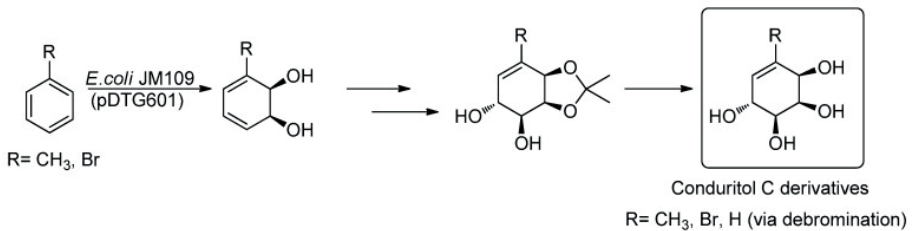


Figure 13. Reaction on the preparation of Conduritol C

Conduritol D

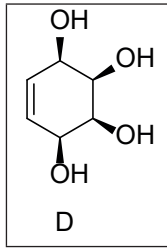


Figure 14. *Conduritol D chemical structure*

The first recorded synthesis of the compound we refer to as Konduritol D was carried out by Angyal and Gilham in the literature. This compound is derived from di-O-isopropyl derivatives. With this method, 67 were separated from neighboring groups and two groups of iodide ions were eliminated. After this process of isopropylene groups, Chonduritol D was obtained. Its molecular formula is $C_6H_{10}O_4$.

Conduritol E

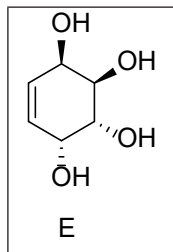


Figure 15. *Conduritol E chemical structure*

The first recorded synthesis of our Konduritol E compound was carried out by Nakajima et al. This first synthesis was not useful because it was stereospecific and, as mentioned, it was shown by Angyal et al. as the starting material for the synthesis of conduritol d. They also used a method close to the aforementioned method for the synthesis of conduritol e. Its molecular formula is $C_6H_{10}O_4$ (Cantekin 2006).

Conduritol F

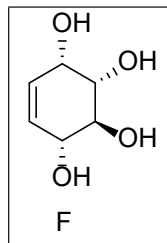


Figure 16. *Chemical structure of Konduritol F*

Conduritol F compound, which was first synthesized by Nakajima et al., was synthesized from diacetate tetrachlorocyclohexenone compound in 1959, when it was not yet discovered in nature. Its molecular formula is $C_6H_{10}O_4$ (Balci 1997).

Halochonduroles and Double Bond Substituted Conductors

As close to conduritol compounds, halochondurites and double bond-substituted chonduritols are also among the popular ones in research. For example, bromochondritols are effective molecules in AIDS studies because they are covalent α -glucosidase inhibitors for the active site. Hudlicky et al. and Carless introduced the synthesis of double bond-substituted conduritols based on halobenzenes (Cantekin 2006).

Biological Significance and Activity of Conduritols

The main reason why conduritol and its derivatives are of great interest among scientists is that they have many biological activities, from herbicidal and anti-microbial, on the other hand, to glycosidase inhibition and mediation of cellular communication. Glycosidase enzyme inhibitors, which have an important place in the diagnosis and treatment process of AIDS and similar diseases, are also important in diabetes and cancer types. The importance of this disease in the research, diagnosis and treatment process of metabolic disorder known as Gaucher has been proven by various researches. It has been shown that the activity of our cyclohexenone compound, which we refer to as conduritol, is inhibitory for glycosidases and prevents feeding. Apart from these, they have antibiotic, anti-leukemic and various activities on the development of cells. To give an example, our konduritol-A compound can be obtained pure from the leaves of the *Gymnema sylvestre* plant, which is used in the treatment of diabetes today. Chonduritols also form the building blocks of various biologically important compounds. Of these, Amarillidasin is a favorite member of this alkaloid group, while pankratistatin is an aminochonduritol skeleton. The pankratistatin in question is obtained from the roots of the *Pancreas littorale* plant, a Hawaiian plant, and it is known that it was used in the treatment of diseases by the leading medical people of the city in a period dating back to ancient Greece, which is a distant history. The pankratistatin compound is mentioned as important in known sources, and the reason is that its biological activity, inhibition of protein synthesis and ovarian sarcoma, and lymphocytic leukemia, which was later discovered, have an antineoplastic effect (Cantekin, 2006).

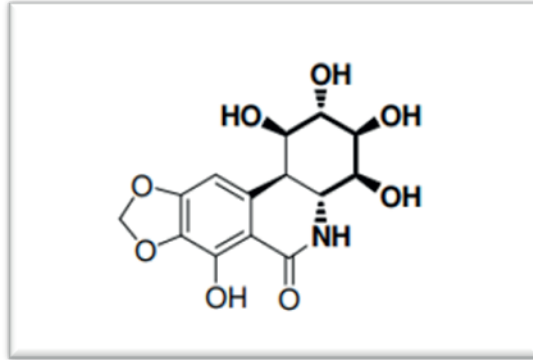


Figure 17. *Chemical structure of pancratistatin*

In figure 2.15, which is shown as lycoricidine, our compound completed its synthesis after nine steps using conduramine-A. The fact that this compound has an inhibitory effect on enzymes that process oligosaccharides to a high degree and that it is involved in various branches of cancer treatment known as chemotherapy and that it is compatible with this treatment makes this compound important from a biological point of view. These two compounds, which we refer to as lycoricidin and pankratistatin, are also used as inhibitors on the glycosidase enzyme, so they have an important place in the diagnosis and treatment of various types of cancer and the treatment of various disorders and diseases such as AIDS.

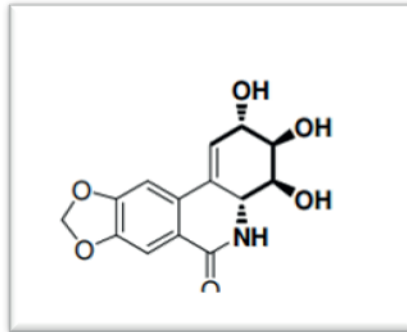


Figure 18. *Chemical structure of Konduramin-A*

These compounds, which we refer to as oligosaccharides, have faced high interest in the scientific world in terms of their physiological roles and therefore their therapeutic potential. Some of their synthetic derivatives have enzyme inhibitor activity in glycolysis (Balcı 1997).

RESULTS AND DISCUSSION

The conduritol compound is a compound that can be obtained both naturally and synthetically, which has been met with increasing attention in recent years. Although there are some of its effects that have not yet been discovered, it is expected to gain greater importance in the future in the light of the researches. In particular, the discovery of its hypoglycemic effect has accelerated scientists' research and development on chonduritol. Furthermore, the anticancer effect of conduritol shows that it is also effective in studies conducted in many European countries.

In general, these compounds, called natural or synthetic, are of great importance in the world of health and will increase in importance in the future. Therefore, research and development work on chonduritol is expected to continue, which will allow for the emergence of potential new treatments and products in the healthcare field.

This study was examined in depth to emphasize the synthetic and biological importance of conduritol compounds. Conduritol has played a leading role in synthetic chemistry and have been proven to have many biological activities. In particular, it is noted for its hypoglycemic effect, its potential for use in Gaucher disease, and its effects in the diagnosis and treatment of AIDS disease. However, conduritol can also be used as intermediate compounds in biological enzyme mechanisms, making them a versatile and valuable area of research.

Kübler's first synthesis in 1908 and subsequent studies have established conduritol in the scientific world. With the discovery of these compounds, new possibilities have emerged in the diagnosis and treatment of many diseases. Conduritol's properties, such as their antibiotic and anticancer effects, will continue to be the focus of future research.

In conclusion, it is clear that conduritol is of great importance from a synthetic and biological point of view. It is hoped that these studies can have positive effects on future drug development and disease treatments.

Conduritol compound is a natural and synthetically obtainable compound that has gained importance in recent years. Although some of the effects of conduritol have been discovered, they will gain greater importance in the future in line with the studies conducted. Thanks to the discovery of its hypoglycemic effect, scientists have accelerated the study and development of conduritol. Thanks to its anticancer effect, conduritol is also effective in studies in most European countries. As a result, these compounds, which we call natural or synthetic, are of great importance in the health world and it is seen that they will increase in the future.

ACKNOWLEDGEMENTS: This study was prepared by my student Sedat Sadi İNCİ from Agri İbrahim Cecen University Faculty of Pharmacy research project thesis.-

REFERENCE

- Arif, A., 2021. Synthesis and study of biological activities of some novel cyclohexitol, halogenochondritol, and carbon sugars that may be biologically important.175,18,12
- Aydemir, S., 2005. Gaucher disease; two facts.” Journal of Academic Gastroenterology 4.1.60-63.
- Aydin, G., 2016. Synthesis and characterization of oxygen-condensed cyclitols.
- Balci, Metin, 1997. “Synthesis of conduritols and related compounds.” *Pure and applied chemistry* 69.1: 97-104
- Balci, M., 2007. Synthesis of cyclitols: conduritol, conduramin and quersitols.178,18
- Balci, M., Sütbeyaz, Y., Seçen, H., 1990. Tetrahedron , 46, 3715.
- Bertholet, A.M., Delerue, T., Millet, A.M., Moulis, M.F., David, C., Daloyau, M., Arnaune-Pelloquin, L., Davezac, N., Mils, V., Miquel, M.C., 2016. Mitochondrial fusion/fission dynamics in neurodegeneration and neuronal plasticity. *Neurobiol.*90, 3–19.
- Cantekin, S., 2006. The development of the novel synthesis for conduritols..
- Cantekin, S., 2006. New methods for synthesizing chonduritol derivatives.79.11
- Caliskan, R., 2008. New methods in the synthesis of conduritol derivatives.189,1
- Ekmekçi, Z.Balcı M., 2018 . New synthetic methods for aminocyclitols.
- Goker, O., Schiffmann, R., Park J.K., Stubblefield, B.K., Tayebi, N., Sidransky, E., 2013. Phenotypic continuum in neuronopathic gaucher disease: an intermediate phenotype between type 2 and type 3. *J pediatr.*143:273–276.
- Grabowski, G., 1985. Gaucher disease types 1, 2 and 3: differential mutations of the active site of acid beta-glucosidase identified by chonduritol b epoxide derivatives and sphingosine *Jhum Genet.*, vol. 37 pp. 499-510
- Hatefi, Y.,1985. The mitochondrial electron transport and oxidative phosphorylation system. *Annu. Rev. Biochem.*54, 1015–1069.
- Held, N.M., Houtkooper, R.H., 2015. Mitochondrial quality control pathways as determinants of metabolic health. *Bioessays* 37, 867–876.
- İlhan, M., 2019 Pharmacognostic research on the efficacy of herbs used in gynecological disorders among the people.190,11
- Kaplan D., 2015. Synthesis of methyl-substituted methoxy conduritols.48.1
- Kaya, N., 2009. The synthesis of hydroxymethyl containing cyclitol derivatives.169,28
- Kaya, S., Kilbas B., Balcı M., 2019. A novel method of synthesis of halochondritol.128-15
- Kayaardı, İ., 2011.Synthesis of conduritol B derivatives with nitrate.49.11

- Kegalj, K., 2019. Renal phenotype of chemically induced mouse model for Gaucher's disease.
- Keinicke, L., Madsen, R., 2015. A concise, synthetic route to the conduritols from pentoses, *Org.Biomol.Chem.*, 3, 4124-4128
- Kindl H., Hoffmann, O., Fortschritt O., 1964, *organ. Akturst.* 24, 149.
- Kübler, K., 2008. *Arch. Phann. About. Stsch. Pharm.* 246,620.
- Le Drian, C., Vieira, E., Vogel, P., 2017. Conduritol C synthesis (1L-cyclone-5-ene-1,2,3,4-tetrol) *Helv.*72.338–347.
- McCasland G.E., Reeves J.M., 2008. Bromination of Epi-Inositol. *Conduritol-CJ.*77:1812–1814.
- Nakajima M., Tomida I., Takei S., 1957. Zur Chemie des Benzolglykols., 3.4.5.6tetrahydroksi-glikloheksen (Konduriten) *Eur. J. Inorg. Kimya* 90:246–250.
- Podeschwa, M., 2003. Synthesis of natural products based on inositol based on para-benzoquinone.
- Settembre, C., Fraldi, A., Medina, D.L., Ballabio, A., 2013. Signals from the lysosome: a control centre for cellular clearance and energy metabolism. *Nat. Rev. Mol. Cell Biol.*14, 283–296.
- Shanmugasundaram, K.R., Panneerselvam, K., Samudram, P., Shanmugasundaram, R.P., 1983. *J. Ethnobotanik*, 7, 205.
- Topal, R., 2015. Synthesis of cyclohexanoid compounds, 180-190
- Uçar, Ş., 2008 Gaucher disease and iron deficiency anemia. *Aegean Journal of Medicine* 47.3.197-200
- Vitner, E.B., Platt, F.M., Futerman, A.H., 2010. Common and uncommon pathogenic cascades in lysosomal storage diseases. *J. Biol. Chem.*285, 20423–20427.
- Yang, S., 1985. Inactivation of alpha-glucosidase by the active site-directed inhibitor, chonduritol b epoxide," *Biochim Biophys Acta, Skin.* 828(3) pp. 236-240,
- Premkumar, L., 2005. X-ray structure of human acid-beta-glucosidase covalently bound to conduritol-b-epoxide implications for gaucher disease," *the Journal of Biological Chemistry*, vol. 280(25) pp. 23815-23819,
- Grabowski, G., 1986. Human acid beta-glucosidase. Use of Chonduritol B epoxide derivatives to investigate catalytically active normal and Gaucher disease enzymes *The Journal of Biological Chemistry*, Vol. 261(18) pp. 8263-8269
- Korkotian, E., 1999. Elevated intracellular levels of glucosylceramide result in an increase in endoplasmic reticulum density and functional calcium stores in cultured neurons," *the journal of biological chemistry*, vol. 274(31) pp. 21673-21678
- Yurev, Y.K., Zefmv K., 2016. New stereospecific synthesis method of hexahydroxy cyclohexane.31,685–686.



Chapter 4

HISTORY OF ASTRONOMY

E. Nihal Ercan¹

¹ Prof. Dr., Boğaziçi University, Physics Department

Introduction

Astronomy is a branch of science that has existed since the beginning of human history and has accelerated as humanity progresses. It has been a mirror of mankind's view of the universe and life, undergoing significant changes for thousands of years from ancient times to the present. Compared to other natural sciences, astronomy is the first natural science to have developed and predicted. In ancient times, humanity directed its curiosity to the sky because it was intriguing and enchanting with its countless shining dots. Since the Sun, Moon, planets and stars move regularly in their orbits, humanity, which started to observe the sky at night, began to find an order in chaos as time passed.

The other reason astronomy was more developed than other natural sciences at the beginning of human history was that astronomy was intertwined with mathematics. In ancient Greece, astronomy was seen as a branch of mathematics. Although mathematics is considered a complex science, the rapid development of astronomy in Ancient Babylon and Ancient Greece is that the movements of the planets can be expressed mathematically. Astronomy has duration and continuity. Each civilisation has contributed to its development until today by preserving and adding to the contribution of the previous civilisation to astronomy. As with all sciences, astronomy is a cumulative science, but beyond that, the astronomical tradition has an impressive duration. Even when the closest star to us, the Sun, is 150 million kilometres away, a significant amount of time and continuity is needed to obtain information about the movements, positions, structural features and similar information of other celestial bodies. Astronomy has developed since the first day humanity turned its face to the sky. And all humanity has contributed to this development. The continuation of the study includes part of the history of astronomy from the very beginning to the present.

Prehistory and antiquity



Prehistory[1]

Since the early ages, humanity has painted and sculpted all kinds of objects, living things, or events that concern it. There are thousands of petroglyphs from the Bronze Age. Apart from pictures of horned animals and tools used for hunting,

the Sun also has a clear image. They portrayed the rays of the sun in the form of a circle. According to the views of some scientists, they also painted two images of the star group known as the Pleiades. A circular bronze plate with seven small gold dots representing the crescent-shaped Moon, possibly the

Sun (perhaps the Full Moon) and the Pleiades constellation, dating from 1600 BC, have been found in Germany. Links to astronomy in prehistoric times are also evident in monuments and tombs. Structures designed as burial chambers in the Stone Age culture (called Stonehenge) usually face east. Stonehenge's central axis is aligned to coincide with the direction of sunrise at the summer solstice. Many archaeoastronomers accept some astronomical alignments at Stonehenge.

We know that prehistoric humans noticed and followed the Sun and the Moon. However, we will not be able to learn how he attributed meanings to the astronomical events he experienced before the article.

Mesopotamia[2]

The most complex relationship with astronomy emerged in Central Mesopotamia. There are three different reasons why Mesopotamia has a complex relationship with astronomy. The first reason is that astronomy had a crucial social position in Mesopotamia. According to their beliefs, the Gods sent signs from the sky to warn of calamities, epidemics or impending wars that would become their kings. To receive these warnings, a mechanism was established to receive the signs in the sky at the beginning of the 2nd millennium BC. The kingdom used the sky, while the ordinary people tried to understand sure signs by inferring from the movements of animals. This brought astronomy to a socially important point. The second reason for the complex relationship with astronomy was that public service in Mesopotamia dealt with astronomical events. Priests, who served as temple clerks, watched the sky every night to remain closely informed on what was going on. They also recorded their conclusions as a result of his observations. The third and last reason was that they had a regular system to record the data they obtained in Mesopotamia. They recorded their data on clay tablets and kept them in temples for safekeeping. Loss of information was prevented by re-copying damaged tablets. These three reasons made Mesopotamia the first civilisation to establish the closest connection with astronomy. In the 7th century BC, the results of observations made day and night by temple astronomers in Mesopotamia were recorded. A few generations later, Mesopotamian astronomers could predict the behaviour of the Moon and planets. Around 300 BC, temple scribes furthered astronomers' predictive ability to obtain a more sophisticated method for predicting planetary behaviour based on arithmetic theories.

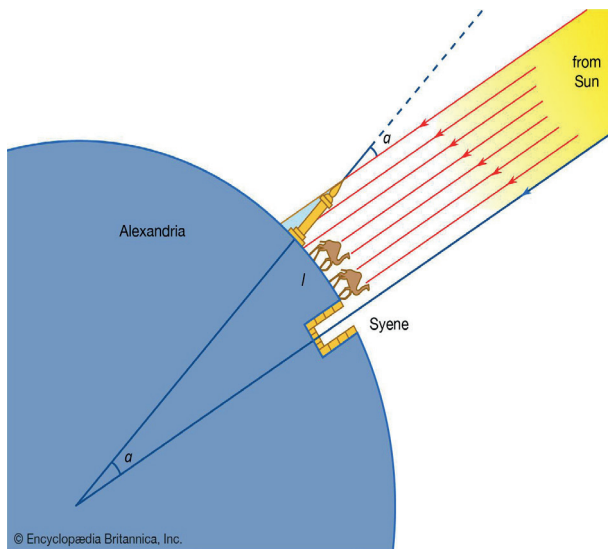
Ancient Greece[3]

Astronomy in Ancient Greece has existed since the beginning of Greek literature. Homer mentions stars and constellations in his Iliad and Odyssey, including Orion, the Ursa Major, and Sirius. Other literary works also contain detailed astronomical information. Hesiod, who produced important works in Ancient Greece, explained in his book Works and Days that it is necessary to look at the movements in the annual cycles of some important stars to have a safe journey, to do daily chores, or to determine the seasons. Much of Hesiod's astronomical knowledge paralleled that of modern Mesopotamia.

Applying geometry[3]

When geometry was applied to astronomical problems in ancient Greece, a new era began in Greek astronomy. Aristotle, who claims that the world is spherical in his work On the Heavens, supports this claim with a solid argument. Aristotle also mentions that the Earth's shadow on the Moon during a lunar eclipse is circular and the changes that occur in the stars in the sky as you go from north to south on Earth.

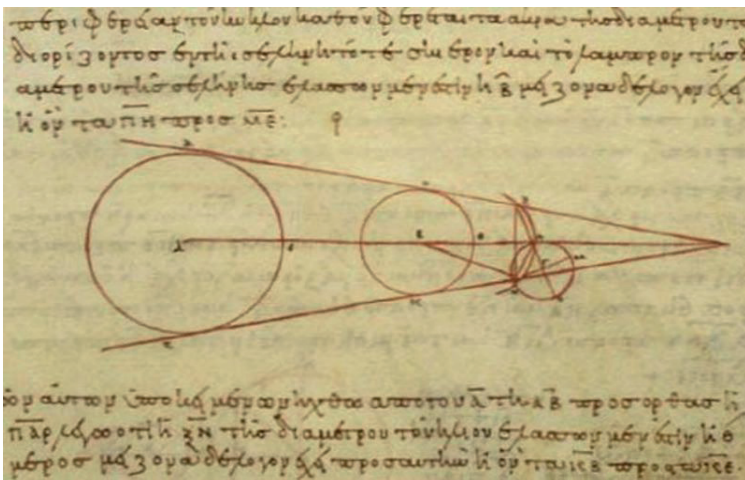
The oldest surviving measurement of the Earth's size is that of Eratosthenes, made in the 3rd century BC. Eratosthenes said the Sun was directly overhead at noon on the summer solstice at Syene, now a town above the Nile in Egypt. That same day, he noticed Alexandria's sun was below 90 degrees. He made a rough estimate using the distance between these two different places.



With this rough measurement, he found a value close to the actual value of the world.

In the same century, Aristarchus of Samos used geometry to estimate the distances of the Sun and Moon in his book On the Sizes and Distances of the

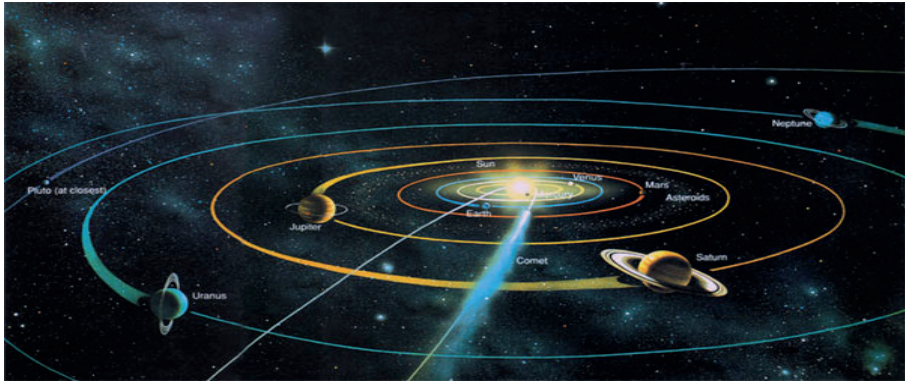
Sun and Moon. For example, he assumed that the angle between the Sun and the Moon is 87° when viewed from the Earth on the fourth of the Moon. From this, the distance from the Sun is about 19 times that of the Moon from us (The actual ratio is about 389). He found that the diameter of the Moon is between 0.32 and 0.4 times the diameter of the Earth and that the Sun is between 6.3 and 7.2 times the diameter of the Earth. At the time of Hipparchus of Bithynia (2nd century BC), the methods developed by Aristarchus allowed reaching essential values for the size and distance of the Moon. However, although Aristarchus used the parallax method to calculate the distance between the Earth and the sun and the moon between the earth, its importance was not understood at that time. The 19 to 1 ratio that Aristarchus found was not seriously questioned until the 17th century.



The motion of the planets[3]

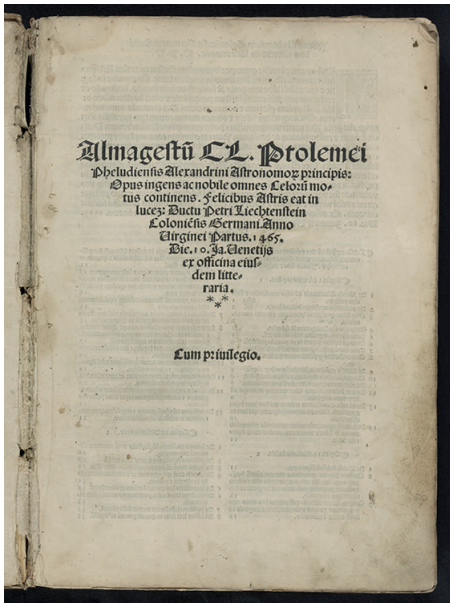
Around 400 BC, thoughts about the movements of the planets begin to emerge. Eudoxus established the first known Greek theory of planetary motion, and in a book called *On Velocities*, he acknowledges that each celestial body is carried on a concentric sphere. Eudoxus suggested doing it with four spheres to account for the three different motions of the planets. He modelled these four spheres by assigning the motions of the planets. This theory is sometimes called the theory of concentric spheres. Greek astronomers during this period were more concerned with providing possible physical calculations of the universe and proving geometric theorems rather than finding planetary motions numerically. Eudoxus' theory of concentric spheres was criticised for its inability to explain that the cycles of some planets, especially Mars and Venus, are brighter than other planets at some times, and this theory was abandoned after a while. However, it exerted a powerful influence in cosmology, as the cosmos continued to be regarded as a series of concentric spheres until the

Renaissance. Alternative models based on external loops and eccentric circles were developed at the end of the 3rd century BC.



In Eudoxus' theory of concentric spheres, he ignored the fact that the Sun accelerates and decelerates throughout the year around the zodiac when assessing the Sun's motion. It is assumed that the Sun still moves at a constant speed around a regular circle. However, the centre of the circle is slightly away from the Earth. Hipparchus was the first to calculate the amount and direction of decentralisation based on the measured lengths of the seasons. The eccentric circle theory was an essential model in explaining the observed motion of the Sun and was accepted until the 17th century. Hipparchus played a crucial role in introducing numerical parameters from Mesopotamia to Greek astronomy. It changed the Greeks' view of astronomy quite a bit.

Ptolemy[4]



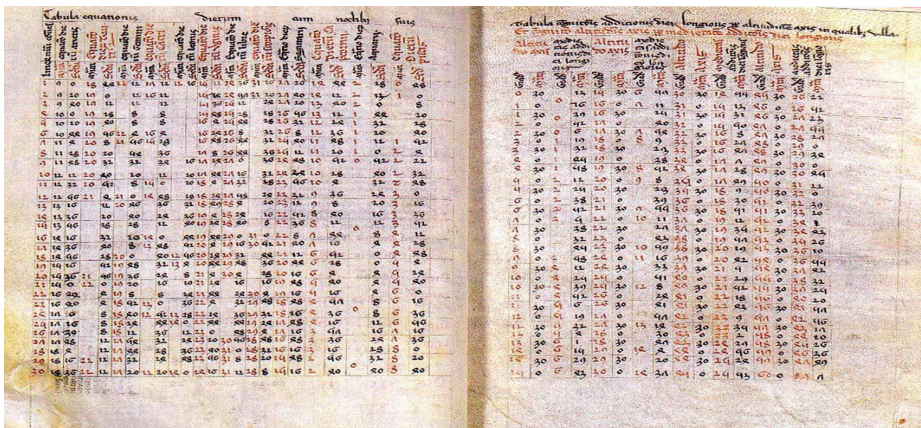
Ptolemy brought Greek astronomy to its zenith with his *Almagest*. His work based on the work of Hipparchus made significant progress and made the old work of planets superfluous.

His first new theorem in the *Almagest* is the equant point. In planetary theories of Hipparchus' time, a planet moves uniformly around its outer orbit with a constant velocity, while the center of the outer orbit moves in an off-center orbit around the Earth. However, in Ptolemy's theory, the movement of the center of the outer orbit speeds up and slows down. This theory caused a

conducted. Mesopotamian astronomy was adopted in Persia and India using original and native Indian methods. Greek geometrical planetary theories developed between the Ptolemy and Hipparchus periods were also the subject of study in India. Indian astronomy came to life as a combination of Greek and Mesopotamian astronomy.

The Islamic World

Arab Muslim astronomers have reached a complex level of knowledge of astronomy and have begun to work on it. He contributed to developing al-Khwārizmī's hand table containing astronomical tables and instructions for using them. The ancient prototype of this hand table is the hand table containing paintings by Ptolemy. The Almagest has been translated into Arabic at least four times. Arab astronomers tried to master and develop the Greek planetary theory. Al-Battani's hand table advanced on Ptolemy's planetary theory and made necessary calculations for some parameters, such as the magnitude and direction of the Sun's eccentricity. Hundreds of Arabic astronomical hand tables have been preserved from the 9th to the 15th centuries. Most of these tables are based on Ptolemy's Almagest and hand tables. A very influential hand table in the development of European astronomy is the Toledan Tables, edited by a group of Muslim and Jewish astronomers in Spain, finalised by Ibn al-Zarkallu, and later translated into Latin.



Over time, astronomers could conduct new studies, including slow changes in the sky. In the 9th century, Baghdad astronomers observed that the value of the ecliptic curvature given in Ptolemy's Almagest decreased. Between Ptolemy's time and the present, the degree of ecliptic curvature is about 25 per cent less. Arab astronomers also observed that the length of the seasons varied slightly from the values recorded by Ptolemy. With this new information, he revealed that the solar apogee was slowly moving eastward.

Ibn al-Haytham expressed his doubts about Ptolemy's planetary theory. Thanks to this, he became a source of inspiration for the Marāghēh observatory,

now in Azerbaijan, in the 13th century. Astronomers of that time created creative mathematical models.

Nasir al-Din al-Tusi identified that standard mechanisms, including Ptolemy's theories of Mercury and the Moon, appear to oscillate. He used a mechanism called the Tusi couple to produce a physical model suitable for this.



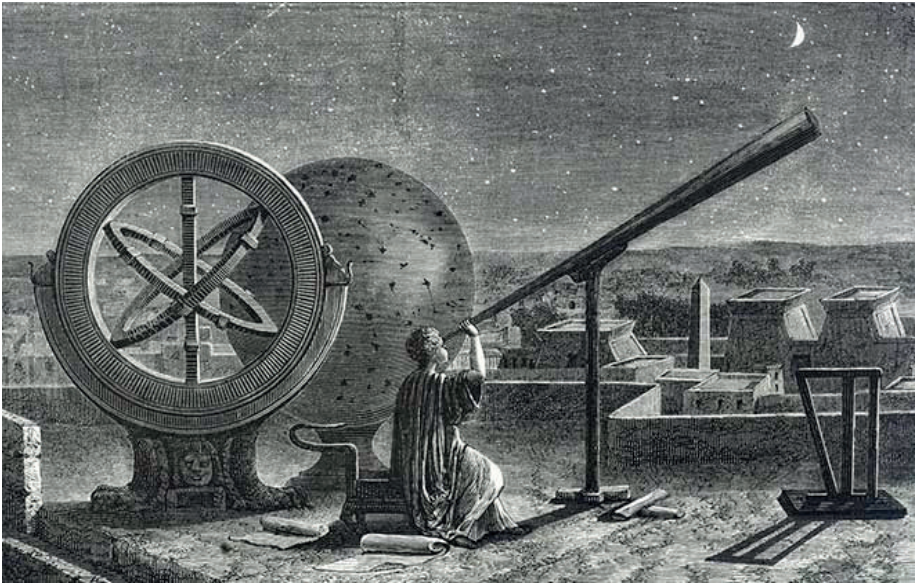
Nasirüddin al-Tusi could explain planetary motion in Ptolemy's geocentric theory of the universe without shifting the centre of the universe, that is, without using eccentric modelling, which is against Aristotle's physics. His student al-Shīrāzī took this modelling further by using a small outer loop to eliminate the need for the equant point.

China

Although there are bones of oracles in China that give information about the emergence of a new star and about solar and lunar eclipses dating back to two thousand BC, astronomy reports were concentrated around 200 BC.

While astronomy had a social function in ancient Greece, it had an imperial function in China. The son of the emperor is considered as the son of heaven. Therefore, developments in astronomy are reflected in the emperor, for better or worse. Astronomical summaries are often written with the rise of a new emperor. These astronomical summaries generally drew attention to the lunar-solar calendar. However, later on, he began to include tables such as Ptolemy's hand table to predict the planets' movements and eclipses. Chinese astronomy is more similar to Mesopotamian astronomy than Greek

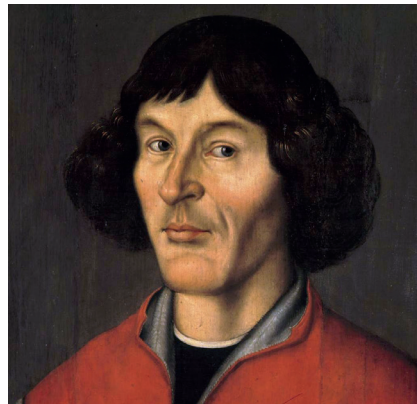




astronomy. Since the Chinese were less attached to cosmological theories and natural laws, they were more interested in singular events such as comets, nova, meteor showers and solar eclipses.

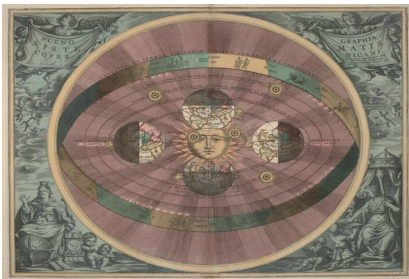
Renaissance[6]

Astronomy in Europe was thanks to Georg von Peurbach, a mathematician and astronomer, and his student Johannes Müller von Königsberg. His comments on Ptolemy's works enabled a later generation to learn about Ptolemy. Known and criticised in Arabic astronomy, Ptolemy's theory of the Moon was mentioned for the first time in the West.



Known and criticised in Arabic astronomy, Ptolemy's theory of the Moon was mentioned for the first time in the West.

Copernicus[6][7]



Copernicus *De Revolutionibus Orbium Coelestium Libri VI* explained the motion of the Earth. While putting forward this theory, he did not rely on his observations, but on Ptolemy's *Almagest*. Because Ptolemy explained the essential tips in the *Almagest*. The *Commentariolus*, an early draft of the Copernicus heliocentric theory of the

universe, was circulated in manuscripts in small astronomical societies from 1510 onwards but was not published until the 19th century.

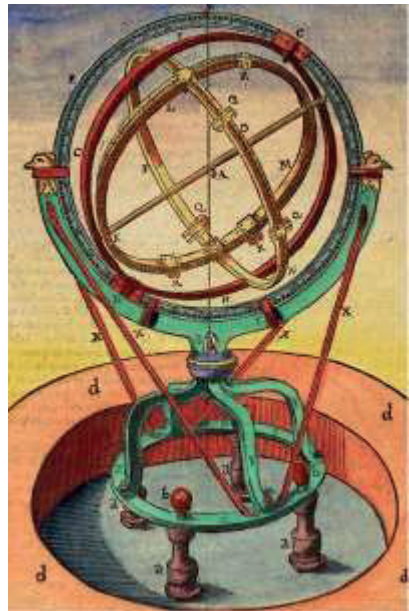
With his foresight and mathematical calculations, Copernicus was envied and strangled by the astronomers of my time.

Tycho[6][7]

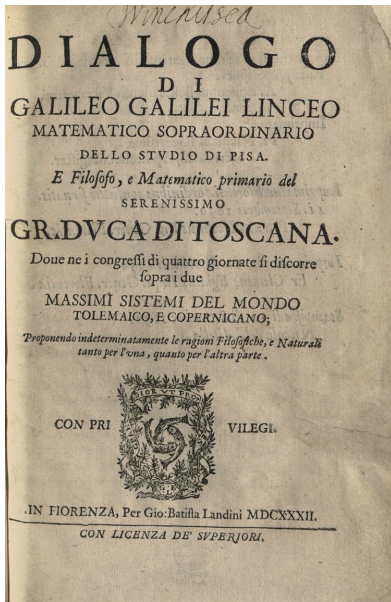


One of the astronomers who admired Copernicus was Tycho Brahe. Tycho, who admires Copernicus's connection of all the movements of the planets with the Sun, is one of those who cannot accept the movement of the Earth. So, he developed an alternative cosmology called the Tychonic system. According to this system, the Moon and the Sun revolve around the Earth, but all other planets revolve around the Sun. By changing the theory that the Earth revolves around the Sun in Copernicus's heliocentric universe theory, he modelled that the Earth is still in the centre.

Like other astronomers, Tycho was impressed by the bright star in Cassiopeia in 1572. He made extensive observations to determine whether its position relative to neighbouring stars had changed. It became even more critical for Tycho to research the bright comet in 1577. In ancient and medieval times, comets were considered atmospheric phenomena. That's why Aristotle considered them in meteorology, not in the sky. He thought it would pass with time anyway. But Tycho could model the comet by putting it in an orbit around the Sun. He pointed out that the comet is sometimes closer to the Earth and sometimes further away.



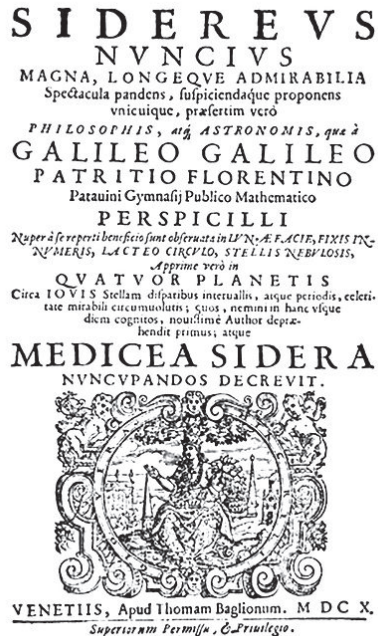
Galileo[6][7]

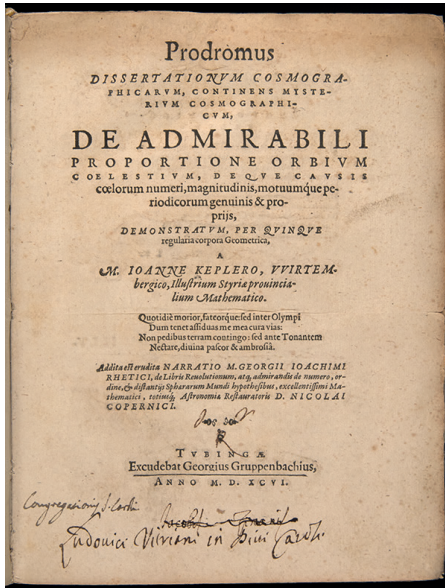


Galileo Galilei designed his telescope, inspired by an invention made in the Netherlands in 1609. He studied the Moon with this telescope. He found that the Moon was not smooth, contrary to rumours, but had mountains and craters. Galileo even measured the heights of the Moon's mountains using the lengths of their shadows. Galileo's most exciting discovery was the discovery of Jupiter's four moons. He announced these discoveries in his book *Sidereus Nuncius* (1610). Although it did not directly support Copernicus' heliocentric theory, Jupiter's moons indicated that there was another centre of revolution outside of Earth. It also showed that a moving planet can carry its moons with it.

In 1616, the Roman Catholic Church put Copernicus' *De Revolutionibus* among the banned works. He also published a list of books that dealt with the movement of the Earth and that had chapters that should be deleted. He also warned Galileo that Copernicus was not teaching his theories correctly. On the other hand, when Copernicus and his theories were excluded, astronomers had to stick to the Tychonic system.

Despite warnings, Galileo decided to take advantage of this when a more liberal pap took office. Accordingly, he wrote *Dialogue Concerning the Two Chief World Systems*—Ptolemaic and Copernican. He was prosecuted for what he wrote in this work and was asked to take back what he wrote. Despite all these pressures, the trial of Galileo did not stop him. He continued to move forward and do work to support his theories.





Kepler[6][7]

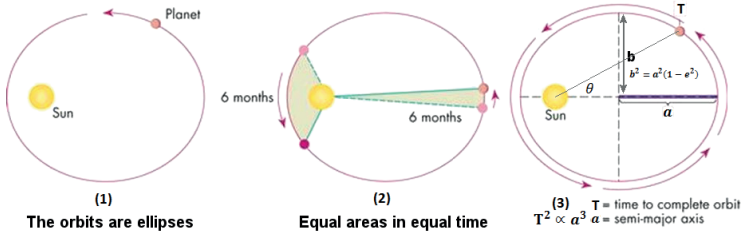
Kepler accepted Copernicus's theories. He took an interest in cosmology while trying to understand the solar system. He used the geometry of regular solids and musical harmonies to explain various aspects of the universe.

While looking for a logical answer to the question of why there are six planets in the universe, he thought that God created six planets because there are only five regular solids for the objects created between the planetary spheres while designing the architecture of the universe. He wrote the work *Mysterium*

Cosmographicum about this. As a result of this book, he received an invitation to work from Tycho Brahe.

Kepler goes to Prague in hopes of getting better planetary parameters than Tycho. Arriving in Prague, Tycho and his assistants learned that he was joining the watchdogs of Mars, which was approaching Earth at the time. This observation was an excellent opportunity for him because only the Maars and Mercury orbits had eccentricities large enough to detect the deviations from circularity. Since Mercury was so close to the Sun, observing Mars was pretty challenging, but observing Mars was also quite important in its own right. Collaboration was short-lived as Tycho died in 1601, but after Tycho's death, he gained access to his observational records. It had to analyse many observations to make it usable. He put the sun at the centre of his system, as he joined Copernicus's heliocentric theory of the universe. But he used Ptolemy's works for technical details. Against his will, he was forced to re-examine the foundations of planetary motion. This strain led to the first two of Kepler's laws published in *Astronomia Nova*(1609). According to the first law, the paths of the planets are ellipses with a focus on the Sun. The second law of the line drawn from the Sun to any planet is sweeping equal areas at equal times. His last published law is that the square of a planet's orbital period is directly proportional to the cube of the major axis length of the ellipse it orbits.

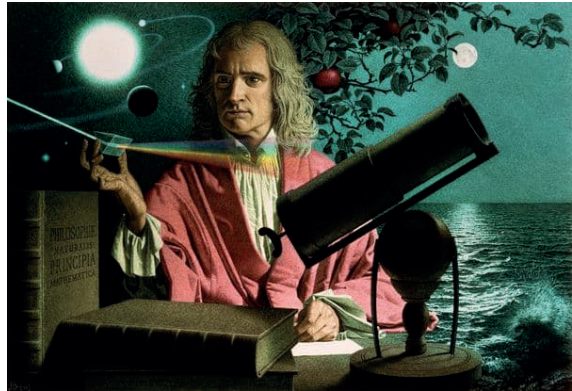
Kepler's 3 Laws of Planetary Motion



Enlightenment

Newton[8]

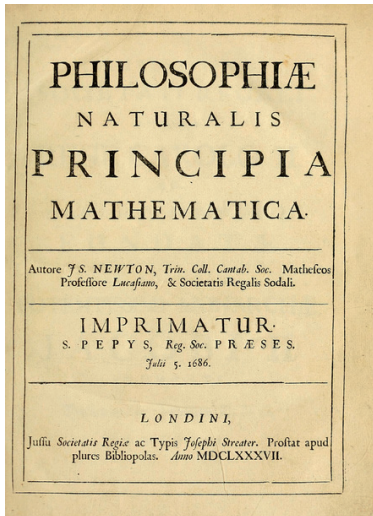
Kepler's laws were physically explained by the publication of the English physicist and mathematician Newton's *Philosophiæ Naturalis Principia Mathematica* (1687). Newton laid down his laws of motion and explained the law of universal gravitation.



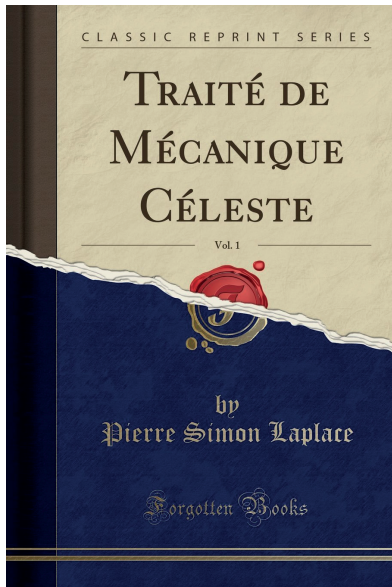
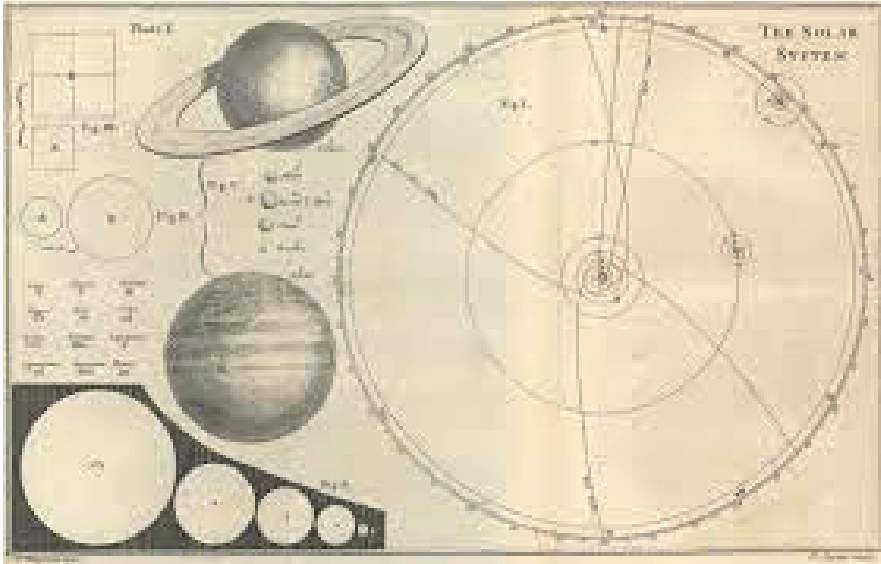
He used Newton's laws to reproduce Kepler's laws. Thanks to Newton, planetary theory became a branch of physics for the first time. He then used the laws to explain other astronomical phenomena.

Testing Newton's theory[8]

In the first half of the 18th century, Newton's inverse square law was put to severe tests. Newton argued that the Earth's rapid rotation on its axis causes it to move away from perfect sphericity. He said it should be a flat sphere instead of a perfect sphere. As proof of what Newton said, the example of Jupiter, which saw a visible flattening when viewed through a telescope, was used. Another piece of evidence is that in 1672, Jean Richer measured the speed of a pendulum clock near the Earth's equator and showed that this clock was slower than the one in Paris. Later, more extensive research proved that Newton was right.



Newton could not calculate the point in the orbit of the Moon at which it was closest to the Earth. A prominent mathematician in the 18th century tried to solve the problem but failed. In 1747, the French mathematician Clairaut proposed changing Newton's law of gravity. Instead of a pure inverse square law, he argued that to accurately represent the motion of the Moon when it was closest to Earth, adding a small term proportional to the inverse fourth power of the distance was necessary. Later, in another study, he showed that Newton's inverse square law was utterly sufficient.



Laplace[9]

Every planet is subject to gravitational force by both the Sun and all other planets. Therefore, Newton, who thought that the orbit of the planets could not be a simple ellipse, as Kepler said, adopted the idea that the planetary system had to be recalibrated. Lagrange and Laplace, who invented mathematical methods to correct some distortions in the 18th century, showed that the solar system is inherently relatively stable in orbit. Each planet is subject to influences from other planets, but in the end, they continue to move in the same orbits, and there is no escape from this movement.



Laplace wrote the *Traité de mécanique céleste*, which contained an intensely mathematical totality, and his popularization work, the *Exposition du système du monde*. It appeared in different editions between 1796 and 1824. Laplace explained the solar system in simple language so ordinary readers could understand it. He did this by explaining the history of astronomy from antiquity to his own time.

The nebula hypothesis, in which Laplace imagines planets condensed from a primitive stellar atmosphere that extends far beyond the solar system boundaries, is seen in the natural sciences as an early example of evolutionary theory. It is also notable that evolution entered astronomy long before it became important in the social sciences.

The Age of Observation

Herschel and the New Planet [10]

William Herschel was the most important observational astronomer of his time. He devoted all his free time to amateur astronomy, which he developed. By making his telescopes, he soon had better equipment than his competitors. In 1781, he was scanning the sky for double stars. He saw an object in the sky that he thought was a comet or cloudless star and thought he had discovered a comet.

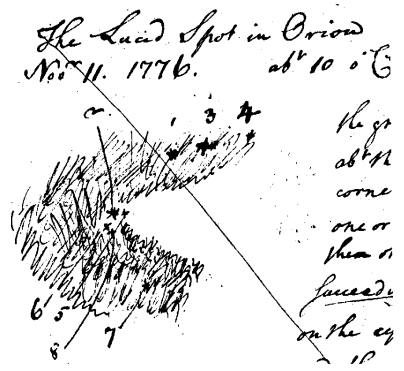
But it was later discovered that the object he thought was a comet was a planet. Continental astronomers disagreed with Herschel's proposed name for the planet.

In 1783, German astronomer Johann Bode proposed the name Uranus.

Herschel and the Milky Way [10]

In the mid to late 18th century, Herschel realised that the Milky Way was a flattened disk. In addition, he tried to decipher the structure of the vast star system of the Milky Way. Herschel was the leading astronomer of his day and a highly creative scientist who devised the assumptions that supported his theories.

In 1785, he drew the first quantitative



picture of the structure of the Milky Way galaxy. However, when he realised that his telescopes were not practical enough to observe the Milky Way correctly, he gave up this picture. However, Herschel's drawing of the Milky Way galaxy was used frequently throughout the 19th century.

Herschel and her sister, Caroline Herschel, have put much effort into cataloguing nebulae. Ancient Greek and Arabic astronomers observed several nebulae, or clusters of nebulae, with the naked eye. In 1755, the philosopher Kant suggested that these nebulae could be compared to the Milky Way galaxy. In 1771, Charles Messier published a list of 45 nebulae. This list of 45 nebulae was increased to 103 in 1784. He used one of Herschel Messier's lists. Caroline Herschel used the telescope her brother built to scan for comets and found nebulae that were not on Messier's list.

The Herschel brothers increased the known nebulae to about 2,500 in 20 years.



Conclusions

From prehistoric times to the present, thousands of people from many different civilisations have contributed to astronomy thanks to their curiosity about the sky. The only thing that has not changed is the unstoppable development of astronomy;

In contrast, on the right path, astronomy is curious to understand the world and the universe we live in, from when astronomy was interested in mythological reasons. Astronomy shows much better how the natural sciences relate to each other. Astronomy's adventure, which started in Mesopotamia, made significant progress, especially with Ptolemy. In the future, many civilisations will read books and try to understand their theories. All the other scientists that followed built the foundations of astronomy by superimposing the knowledge they obtained.

I want to thank Kübra Şen for her assistance in preparing this search.

References

- [1] Prehistoric astronomers. Ancient knowledge created by modern myth, Emilia Pasztor (2011)
- [1] Foundations of Astronomy, 9th ed. (2007)
- [1] The History and Practice of Ancient Astronomy (1988)
- [1] Astronomy in Prehistoric Britain and Ireland (1999)
- [2] Astronomy-Astrology in Mesopotamia, Brown (2001)
- [2] Eclipse prediction in Mesopotamia, JM Steele (2000)
- [3] The material culture of Greek astronomy, J Evans (1999)
- [3] Visual aspects of the transmission of Babylonian astronomy and its reception into Greek astronomy, J Evans (2011)
- [3] Life and thought in the Greek and Roman world, M Cary (1941)
- [3] Applied historical astronomy: an historical perspective, JM Steele (2004)
- [4] Copernicus and the Critics of Ptolemy, P Barker (1999)
- [4] Saving the phenomena: The background to Ptolemy's planetary theory, BR Goldstein (1997)
- [4] The first non-Ptolemaic astronomy at the Maragha School, G Saliba (1997)
- [4] The trouble with Ptolemy, O Gingerich (2002)
- [5] Early Arabic critique of Ptolemaic cosmology: A ninth-century text on the motion of the celestial spheres, G Saliba (1994)
- [5] India: THE PURĀNAS AND JYOTIḤŚĀSTRĀ: ASTRONOMY, D Pingree (2014)
- [5] The teaching of astronomy in India, MN Anandaram (2001)
- [5] Book Review: Astronomy in the Western Islamic World, Astronomy and Astrology in Al-Andalus and the Maghrib, G Saliba (2009)
- [5] A history of Arabic astronomy: Planetary theories during the golden age of Islam, G Saliba (1995)
- [5] The locales of islamic astronomical instrumentation, F Charette (2006)
- [5] Chinese studies in the history of astronomy, X Zezong(1949-1979) [5] A History of Arabic Astronomy: Planetary Theories During the Golden Age of Islam (1994)
- [5] History of Astronomy in India, 2nd ed. (2000)
- [6] Roman Astronomy and Cosmology in the Carolingian Renaissance (2007)
- [6] The Places of Astronomy in Early-Modern Culture, Nicholas Jardine(1998)
- [6] Selected Papers on Medieval and Renaissance Astronomy, J Samsó (2011)

- [6] A scholarly intermediary between the Ottoman Empire and Renaissance Europe, R Morrison (2018)
- [7] Copernicus and the Origin of his Heliocentric System, BR Goldstein(2002)
- [7] The telescope before Galileo, E Sluiter (1997)
- [7] Keplerian astronomy after Kepler: Researches and problems, W Applebaum (1996)
- [7] Kepler's Fabricated Figures: Covering up the Mess in the *New Astronomy*, W. H. Donahue (2000)
- [7] New light on Tycho's instruments, VE Thoren (1973)
- [8] Astronomy Explained Upon Isaac Newton's Principles: And Made Easy to Those Who Have Not Studied Mathematics, J Ferguson(1794)
- [8] Isaac Newton and his work in astronomy and optics, RH Curtiss (1927)
- [8] Planetary Astronomy from the Renaissance to the Rise of Astrophysics, Part A, Tycho Brahe to Newton, R Taton (2003)
- [9] The Laplace resonance in the Kepler-60 planetary system, K Goździewski, C Migaszewski (2015)
- [9] Pierre-Simon Laplace: 1749-1827 a life in exact science, CC Gillispie, Grattan-Guinness (2000)
- [10] "On the power of penetrating into space": the telescopes of William Herschel, JA Bennett (1976)
- [10] William Herschel and the nebulae, part 2: 1785–1818, M Hoskin (2011)
- [10] Schaffer, Simon (1981). "Uranus and the Establishment of Herschel's Astronomy". *Journal for the History of Astronomy*.



Chapter 5

A STUDY ON TZITZEICA HYPERSURFACES IN EUCLIDEAN 4-SPACE \mathbb{E}^4 *

Emrah Tunç¹

Bengü Bayram²

1 Ph.D., Balıkesir University, Faculty of Arts and Sciences, Department of Mathematics, Balıkesir.
ORCID: 0000-0002-7630-0996

2 Prof. Dr., Balıkesir University, Faculty of Arts and Sciences, Department of Mathematics, Balıkesir.
ORCID: 0000-0002-1237-5892

* Produced from Emrah Tunç's doctoral thesis titled "A Characterization of Tzitzeica Curves and Surfaces (Balıkesir University, 2021)"

** Supervisor: Prof. Dr. Bengü Bayram

1. Introduction

Tzitzeica introduced a class of surfaces [14], nowadays called Tzitzeica surfaces in 1907 and a class of curves [15], called Tzitzeica curves in 1911. For a Tzitzeica surfaces with negative Gaussian curvature, the asymptotic lines are Tzitzeica curves [7,8]. This class of surfaces has been generalized to hypersurfaces as follows. A Tzitzeica hypersurface is a hypersurface satisfying the condition (Tzitzeica condition)

$$K(x) = a_1 \cdot d^{n+2}(x) \quad (1)$$

where $K(x)$ denotes the Gaussian curvature at a point x , $d(x)$ is the distance between the origin and the hyperplane tangent to the hypersurface at x and a_1 is a real constant [17]. Distance function $d(x)$ is defined by

$$d = \langle \zeta, X \rangle \quad (2)$$

where ζ is the unit normal vector field of the hypersurface at x and X is the position vector of the hypersurface. In [3,4], authors studied Tz-curve and Tz-surfaces in Euclidean 3-Space \mathbb{E}^3 and in [12,13], studied Tz-curves in Euclidean 4-Space \mathbb{E}^4 . In [17], Vilcu gave necessary and sufficient condition for Cobb-Douglas factorable hypersurface to be Tzitzeica hypersurface. A new Tzitzeica hypersurface was obtained in parametric, implicit and explicit forms in [7]. In addition, authors classified translation hypersurfaces which satisfy Tzitzeica condition in [2]. In [16], authors aimed to study the evolutions of Tzitzeica hypersurfaces which appear in understanding the dynamics of some geometric programming problems and reliability optimal allocation problems.

In this study, we express the condition for a hypersurface to be Tzitzeica hypersurface (Tz-hypersurface) in terms of fundamental form coefficients of the hypersurface in the Euclidean 4-Space \mathbb{E}^4 . We investigate different kind of rotational hypersurfaces and factorable hypersurfaces and give some examples.

2. Basic Notations and Concepts

Let $\vec{x} = (x_1, x_2, x_3, x_4)$, $\vec{y} = (y_1, y_2, y_3, y_4)$ and $\vec{z} = (z_1, z_2, z_3, z_4)$ be three vectors in \mathbb{E}^4 . Then the inner product and triple vector product are given by

$$\langle \vec{x}, \vec{y} \rangle = x_1y_1 + x_2y_2 + x_3y_3 + x_4y_4 \quad (3)$$

and

$$\begin{aligned} \vec{x} \times \vec{y} \times \vec{z} &= \det \begin{pmatrix} e_1 & e_2 & e_3 & e_4 \\ x_1 & x_2 & x_3 & x_4 \\ y_1 & y_2 & y_3 & y_4 \\ z_1 & z_2 & z_3 & z_4 \end{pmatrix} \\ &= (x_2y_3z_4 - x_2y_4z_3 - x_3y_2z_4 + x_3y_4z_2 + x_4y_2z_3 - x_4y_3z_2, \\ &\quad -x_1y_3z_4 + x_1y_4z_3 + x_3y_1z_4 - x_3z_1y_4 - y_1x_4z_3 + x_4y_3z_1, \\ &\quad x_1y_2z_4 - x_1y_4z_2 - x_2y_1z_4 + x_2z_1y_4 + y_1x_4z_2 - x_4y_2z_1, \\ &\quad -x_1y_2z_3 + x_1y_3z_2 + x_2y_1z_3 - x_2y_3z_1 - x_3y_1z_2 + x_3y_2z_1) \quad (4) \end{aligned}$$

respectively.

Let M and \tilde{M} be differentiable manifolds in m -dimensional and $(m+d)$ -dimensional, respectively. A differentiable mapping $f: M \rightarrow \tilde{M}$ is said to be an *immersion* if $df_p: T_p(M) \rightarrow T_{f(p)}(\tilde{M})$ is injective for all $p \in M$. If, in addition, $f: M \rightarrow f(M)$ is a homeomorphism, then f is called *embedding*. If $M^m \subseteq \tilde{M}^{m+d}$ and $f: M \rightarrow \tilde{M}$ is an embedding then M is said to be *immersed submanifold* of \tilde{M} . Moreover, f is an *isometric immersion* if f , which is an immersion, satisfies the condition

$$\langle df_p(X_1), df_p(Y_1) \rangle_{f(p)} = \langle X_1, Y_1 \rangle_p \quad (5)$$

for all $X_1, Y_1 \in T_p(M)$ [6].

Let $X = X(u, v, w)$ be an isometric immersion of a hypersurface M^3 in \mathbb{E}^4 . The unit normal vector field of the hypersurface is

$$\zeta = \frac{X_u \times X_v \times X_w}{\|X_u \times X_v \times X_w\|}. \quad (6)$$

The first fundamental form coefficients of the hypersurface are

$$\begin{aligned} E &= \langle X_u, X_u \rangle & F &= \langle X_u, X_v \rangle & G &= \langle X_v, X_v \rangle \\ A &= \langle X_u, X_w \rangle & B &= \langle X_v, X_w \rangle & C &= \langle X_w, X_w \rangle \end{aligned} \quad (7)$$

and the second fundamental form coefficients are

$$\begin{aligned} L &= \langle X_{uu}, \zeta \rangle & M &= \langle X_{uv}, \zeta \rangle & N &= \langle X_{vv}, \zeta \rangle \\ P &= \langle X_{uw}, \zeta \rangle & T &= \langle X_{vw}, \zeta \rangle & V &= \langle X_{ww}, \zeta \rangle. \end{aligned} \quad (8)$$

Furthermore Gaussian curvature of the hypersurface is defined by

$$K = \frac{(LN - M^2)V + 2MPT - P^2N - T^2L}{(EG - F^2)C + 2ABF - A^2G - B^2E} = \frac{\det II}{\det I} \quad (9)$$

where

$$\begin{aligned} \det I &= \det \begin{pmatrix} E & F & A \\ F & G & B \\ A & B & C \end{pmatrix} = (EG - F^2)C + 2ABF - A^2G - B^2E, \\ \det II &= \det \begin{pmatrix} L & M & P \\ M & N & T \\ P & T & V \end{pmatrix} = (LN - M^2)V + 2MPT - P^2N - T^2L \quad [9]. \end{aligned}$$

Let M be differential manifold, $f: M^m \rightarrow \mathbb{E}^{m+d}$; $f(u) = (f_1(u), f_2(u), \dots, f_{m+d}(u))$; $u = (u_1, u_2, \dots, u_m) \in M^m$ is an isometric immersion and $g: S^n(1) \rightarrow \mathbb{E}^{n+1}$

$$\begin{aligned} &g(v_1, v_2, \dots, v_n) \\ &= \left(\prod_{i=1}^n \cos v_i, \prod_{j=2}^n \sin v_1 \cos v_j, \prod_{k=3}^n \sin v_2 \cos v_k, \dots, \sin v_{n-1} \cos v_n, \sin v_n \right) \end{aligned}$$

is an embedding. Then, for all $u \in M^m; f_1(u) \neq 0$ and $v \in S^n$, X rotational embedding is defined by the parametrization

$$X: M^m \times S^n(1) \rightarrow \mathbb{E}^{m+n+d}$$

$$(u, v) \rightarrow X(u, v) = (f_1(u), f_2(u), \dots, f_{m+d-1}(u), f_{m+d}(u).g(v)) \quad (10)$$

[11].

Let $\gamma: I \subset \mathbb{R} \rightarrow \Pi \subset \mathbb{E}^2$ be a plane curve and ℓ be a line in Π in \mathbb{E}^4 . A rotational hypersurface in \mathbb{E}^4 is a hypersurface rotating a profile curve γ about axis ℓ . ℓ is spanned by $(0,0,0,1)$ and orthogonal matrix $Z(v, w)$ is defined by

$$Z = \begin{pmatrix} \cos v \cos w & -\sin v & -\cos v \sin w & 0 \\ \sin v \cos w & \cos v & -\sin v \sin w & 0 \\ \sin w & 0 & \cos w & 0 \\ 0 & 0 & 0 & 1 \end{pmatrix} \quad (11)$$

with $v, w \in \mathbb{R}$. Matrix Z supplies: $Z \cdot \ell = \ell$, $Z \cdot Z^t = Z^t \cdot Z = I_4$, $\det Z = 1$.

Definition 2.1 If the profile curve is given by $\gamma(u) = (u, 0,0, \varphi(u))$ where $\varphi(u): I \subset \mathbb{R} \rightarrow \mathbb{R}$ is differentiable function for all $u \in I$, then the rotational hypersurface spanned by the vector $(0,0,0,1)$ can be given with the parametrization

$$X(u, v, w) = Z(v, w). \gamma(u) . \quad (12)$$

In addition, from the equation (12), we write

$$X(u, v, w) = (u \cos v \cos w, u \sin v \cos w, u \sin w, \varphi(u)) \quad (13)$$

where $u \in \mathbb{R} - \{0\}$ and $v, w \in [0,2\pi)$ [10].

Definition 2.2 Let $X: \mathbb{E}^3 \rightarrow \mathbb{E}^4$ be a Monge hypersurface in \mathbb{E}^4 given with the parametrization

$$X(u, v, w) = (u, v, w, f(u, v, w)) \quad (14)$$

where $f = f(u, v, w)$ is differentiable function [1]. If $f(u, v, w) = f_1(u) \cdot f_2(v) \cdot f_3(w)$ then Monge hypersurface is called *factorable hypersurface* and equation (14) becomes

$$X(u, v, w) = (u, v, w, f_1(u) \cdot f_2(v) \cdot f_3(w)). \tag{15}$$

3. Tzitzeica Hypersurfaces in \mathbb{E}^4

Definition 3.1 Let $X: M^3 \rightarrow \mathbb{E}^4$ be a hypersurface in \mathbb{E}^4 . If M^3 satisfies the condition

$$a_1 = \frac{K(x)}{d^5(x)} \tag{16}$$

then M is called *Tzitzeica hypersurface* (*Tz-hypersurface*) in \mathbb{E}^4 .

Theorem 3.2 Let $X: M^3 \rightarrow \mathbb{E}^4$ be a hypersurface in \mathbb{E}^4 given with the parametrization

$X(u, v, w) = (f(u, v, w), g(u, v, w), h(u, v, w), z(u, v, w))$. M is a Tz-hypersurface if and only if, the relation

$$\frac{\begin{vmatrix} L & M & P \\ M & N & T \\ P & T & V \\ E & F & A \\ F & G & B \\ A & B & C \end{vmatrix}}{\begin{vmatrix} f & g & h & z \\ f_u & g_u & h_u & z_u \\ f_v & g_v & h_v & z_v \\ f_w & g_w & h_w & z_w \end{vmatrix}} = a_1 \cdot \frac{1}{W^5} \tag{17}$$

holds, where a_1 is non-zero real constant, $W = \|X_u \times X_v \times X_w\|$; A, B, C, E, F, G and L, M, N, P, T, V are first and second fundamental form coefficients of the hypersurface which define at (7) and (8) respectively.

Proof By taking derivatives of the position vector X with respect to u, v and w and using equation (6) we get the unit normal vector field ζ . From equation (2), we find

$$d = \frac{1}{W} \{ f(g_u h_v z_w - g_u z_v h_w - h_u g_v z_w + h_u z_v g_w + z_u g_v h_w - z_u h_v g_w) \}$$

$$\begin{aligned}
 &+g(-f_u h_v z_w + f_u z_v h_w + h_u f_v z_w - h_u f_w z_v - f_v z_u h_w \\
 &\quad + z_u h_v f_w) \\
 &+h(f_u g_v z_w - f_u z_v g_w - g_u f_v z_w + g_u f_w z_v + f_v z_u g_w \\
 &\quad - z_u g_v f_w) \\
 &+z(-f_u g_v h_w + f_u h_v g_w + g_u f_v h_w - g_u h_v f_w - h_u f_v g_w \\
 &\quad + h_u g_v f_w)\} \\
 &= \frac{1}{W} \cdot \begin{vmatrix} f & g & h & z \\ f_u & g_u & h_u & z_u \\ f_v & g_v & h_v & z_v \\ f_w & g_w & h_w & z_w \end{vmatrix}, \tag{18}
 \end{aligned}$$

where $W = \|X_u \times X_v \times X_w\|$. In addition, from equation (9), using the Gaussian curvature and equation (18) in (16) we get the result.

Definition 3.3 Let $f: M^2 \rightarrow \mathbb{E}^3$, $f(u, v) = (f_1(u, v), f_2(u, v), f_3(u, v))$ be an isometric immersion and $g: S^1(1) \rightarrow \mathbb{E}^2$, $g(\theta) = (\cos\theta, \sin\theta)$ be an embedding. Then, for all $(u, v) \in M^2$; $f_1(u, v) \neq 0$ and $\theta \in S^1(1)$, *rotational hypersurface*, defined by the parametrization

$$\begin{aligned}
 X: M^2 \times S^1(1) &\rightarrow \mathbb{E}^4 \\
 X(u, v, \theta) &= (f_1(u, v), f_2(u, v), f_3(u, v). \cos\theta, f_3(u, v). \sin\theta). \tag{19}
 \end{aligned}$$

Theorem 3.4 Let M^3 be a rotational hypersurface given with the parametrization (19). Then M^3 is a Tz-hypersurface if and only if

$$a_1 = \frac{(LN - M^2)}{(EG - F^2)} \cdot \frac{-c(a^2 + b^2 + c^2)^2}{f_3(af_1 + bf_2 + cf_3)^5} \tag{20}$$

where

$$\begin{aligned}
 a(u, v) &= f_{2_u} f_{3_v} - f_{3_u} f_{2_v} \\
 b(u, v) &= f_{3_u} f_{1_v} - f_{1_u} f_{3_v} \\
 c(u, v) &= f_{1_u} f_{2_v} - f_{2_u} f_{1_v} \tag{21}
 \end{aligned}$$

are differentiable functions.

Proof Let M^3 be a rotational hypersurface given with the parametrization (19). By taking derivative of (19) with respect to u , v and θ and using the equation (6) we find the unit normal vector field of M^3 as

$$\zeta = \frac{(a, b, c \cos \theta, c \sin \theta)}{\sqrt{a^2 + b^2 + c^2}}. \quad (22)$$

Then from equation (2) we get the distance function

$$d = \frac{1}{\sqrt{a^2 + b^2 + c^2}}(af_1 + bf_2 + cf_3).$$

We obtain the first and the second fundamental form coefficients from equations (7) and (8) and using these coefficients in equation (8), we get Gaussian curvature of M^3 as

$$K = \frac{-c(LN - M^2)}{f_3 \sqrt{a^2 + b^2 + c^2}(EG - F^2)}$$

where

$$a(u, v) = f_{2u}f_{3v} - f_{3u}f_{2v}$$

$$b(u, v) = f_{3u}f_{1v} - f_{1u}f_{3v}$$

$$c(u, v) = f_{1u}f_{2v} - f_{2u}f_{1v}$$

are differentiable functions. Consequently, by substituting K and d in (16), we get the result.

Example 3.5 Let us take $S^2(r)$ instead of M^2 in equation (19). Then we get $f(u, v) = (r \cos u \cos v, r \cos u \sin v, r \sin u)$ and the parametrization of the rotational hypersurfaces as

$$X: S^2(r) \times S^1(1) \rightarrow \mathbb{E}^4,$$

$$X(u, v, \theta) = (r \cos u \cos v, r \cos u \sin v, r \sin u \cos \theta, r \sin u \sin \theta) \quad (23)$$

This hypersurface is a Tz-hypersurface and Tz-constant is $a_1 = \frac{-1}{r^8}$.

By taking the derivative of (23) with respect to u , v and θ and by the use of (21), we get

$$a(u, v) = -r^2 \cos^2 u \cos v$$

$$b(u, v) = -r^2 \cos^2 u \sin v$$

$$c(u, v) = -r^2 \sin u \cos u.$$

From the equation (7) and (8) the first and second fundamental form coefficients of M^3 are

$$E = r^2, F = 0, G = r^2 \cos^2 u, A = 0, B = 0, C = r^2 \sin^2 u,$$

and

$$L = r, M = 0, N = r \cos^2 u, P = 0, T = 0, V = r \sin^2 u$$

respectively. If we substitute these values in (20), then we get $a_1 = \frac{-1}{r^8}$. So the rotational hypersurface given with the parametrization (23) is Tz-hypersurface.

Definition 3.6 Let $f: M^1 \rightarrow \mathbb{E}^2$, $f(\theta) = (f_1(\theta), f_2(\theta))$ be an isometric immersion and $g: S^2(1) \rightarrow \mathbb{E}^3$, $g(u, v) = (\cos u \cos v, \cos u \sin v, \sin u)$ be an embedding. Then, for all $\theta \in M$; $g_1(u, v) = \cos u \cos v \neq 0$ and $(u, v) \in S^2(1)$, *rotational hypersurfaces* is defined by the parametrization

$$X: M^1 \times S^2(1) \rightarrow \mathbb{E}^4,$$

$$X(\theta, u, v) = (f_1(\theta), f_2(\theta) \cos u \cos v, f_2(\theta) \cos u \sin v, f_2(\theta) \sin u). \quad (24)$$

Theorem 3.7 Let M^3 be a rotational hypersurface given with the parametrization (24). Then M^3 is a Tz-hypersurface if and only if

$$a_1 = \frac{f_1'^2 (f_1' f_2'' - f_1'' f_2')}{f_2^2 (f_1' f_2 - f_1 f_2')^5} \quad (25)$$

holds.

Proof Let M^3 be a rotational hypersurface given with the parametrization (24). By taking the derivative of (24) with respect to u , v and θ and using the equation (6) we obtain unit normal vector field of the hypersurfaces

$$\zeta = \frac{1}{\sqrt{f_1'^2 + f_2'^2}} (-f_2', f_1' \cos u \cos v, f_1' \cos u \sin v, f_1' \sin u).$$

Then from equation (2) we find the distance function

$$d = \frac{f_1' f_2' - f_1 f_2'}{\sqrt{f_1'^2 + f_2'^2}}.$$

After that, from equations (7) and (8) we find the first and the second fundamental form coefficients and by using of these coefficients in (9) we get Gaussian curvature

$$K = \frac{f_1'^2 (f_1' f_2'' - f_1'' f_2')}{f_2'^2 \left(\sqrt{f_1'^2 + f_2'^2} \right)^5}.$$

Consequently, by substituting K and d in (16), we find the result.

Example 3.8 Let us take $S^1(r)$ instead of M^1 at (24), then f becomes $f(\theta) = (r \cos \theta, r \sin \theta)$ and the parametrization of the rotational hypersurfaces becomes

$$X: S^1(r) \times S^2(1) \rightarrow \mathbb{E}^4,$$

$$X(\theta, u, v) = (r \cos \theta, r \sin \theta \cos u \cos v, r \sin \theta \cos u \sin v, r \sin \theta \sin u). \quad (26)$$

This hypersurface is a Tz-hypersurface and Tz-constant is $a_1 = \frac{-1}{r^8}$.

Example 3.9 Let us take $f(\theta) = (\cosh \theta, \sinh \theta)$ instead of M^1 at (24), then the parametrization of the rotational hypersurfaces becomes

$$X: M^1 \times S^2(1) \rightarrow \mathbb{E}^4,$$

$$X(\theta, u, v) = (\cosh \theta, \sinh \theta \cos u \cos v, \sinh \theta \cos u \sin v, \sinh \theta \sin u).$$

This hypersurface is a Tz-hypersurface and Tz-constant is $a_1 = 1$.

Theorem 3.10 Let M^3 be a rotational hypersurface given with the parametrization (13). Then M^3 is a Tz-hypersurface if and only if $\varphi(u) = \frac{c}{u^3}$ where c is non-zero real constant.

Proof From the derivative of equation (13) with respect to u, v and w , after some calculations, we find the unit normal vector field

$$\zeta = \frac{1}{\sqrt{1+\varphi'^2}}(\varphi' \cos v \cos w, \varphi' \sin v \cos w, \varphi' \sin w, -1).$$

By the use of equation (2) we find the distance function

$$d = \frac{u\varphi' - \varphi}{\sqrt{1 + \varphi'^2}}.$$

After that, from equations (7) and (8) we find the first and the second fundamental form coefficients and by using of these coefficients in (9) we get Gaussian curvature

$$K = \frac{-\varphi'^2 \varphi''}{u^2(1 + \varphi'^2)^{\frac{5}{2}}}$$

Consequently, by substituting K and d in (16),

$$a_1 = \frac{-\varphi'^2 \varphi''}{u^2(u\varphi' - \varphi)^5} \quad (27)$$

is obtained.

If the rotational hypersurface given with the parametrization (11) is Tz-hypersurface then a_1 is non-zero real constant at (27). Thus we have

$$\left(\frac{-\varphi'^2 \varphi''}{u^2(u\varphi' - \varphi)^5} \right)' = 0. \quad (28)$$

Calculating and rearranging (28), we get

$$u\varphi'(u\varphi' - \varphi)^4(-2u^2\varphi'\varphi''^2 - u^2\varphi'^2\varphi''' + 2u\varphi\varphi''^2 + u\varphi\varphi'\varphi''' + 2u\varphi'^2\varphi'' - 2\varphi\varphi'\varphi'' + 5u^2\varphi'\varphi''^2) = 0. \tag{29}$$

Because of being undefined of denominator of (28), the first and the third terms of (29) that is u and $(u\varphi' - \varphi)$, respectively and besides, because of the condition $a_1 \neq 0$, the second term of (29) that is φ' must be different from zero. Consequently, the fourth term of (29), that is

$$-2u^2\varphi'\varphi''^2 - u^2\varphi'^2\varphi''' + 2u\varphi\varphi''^2 + u\varphi\varphi'\varphi''' + 2u\varphi'^2\varphi'' - 2\varphi\varphi'\varphi'' + 5u^2\varphi'\varphi''^2$$

must be equal to zero. After some calculations,

$$3u^2\varphi'\varphi'' + 2u\varphi\varphi'' + 2u\varphi'^2 - 2\varphi\varphi' = 0 \wedge \varphi''' = 0 \tag{30}$$

simultaneous conditions are obtained. Differentiating first part of (29) with respect to u and substituting second part of (29) that is $\varphi''' = 0$ in this differentiation taken, $4\varphi' + u\varphi'' = 0$ equation is obtained. By solving this differential equation, $\varphi(u) = \frac{c}{u^3}$ is found. The proof is complete.

Corollary 3.11 Let M be rotational Tz-hypersurface given with the parametrization (13) so that is $\varphi(u) = \frac{c}{u^3}$. Hence, Tz-constant of this hypersurface is $a_1 = \frac{27}{256c^2}$.

Theorem 3.12 The factorable hypersurface given with the parametrization $X(u, v, w) = (u, v, w, f_1(u) \cdot f_2(v) \cdot f_3(w))$ is Tz-hypersurface if and only if

$$a_1 = \frac{f_1 f_2 f_3 (f_1 f_1'' f_2'^2 f_3'^2 + f_1'^2 f_2 f_2'' f_3'^2 + f_1'^2 f_2'^2 f_3 f_3'' - 2(f_1' f_2' f_3')^2 - f_1 f_1'' f_2 f_2'' f_3 f_3'')}{(u f_1' f_2 f_3 + v f_1 f_2' f_3 + w f_1 f_2 f_3' - f_1 f_2 f_3')^5}$$

holds.

Proof By taking the derivative of (15) with respect to u , v and w and using the equation (6) we obtain unit normal vector field of the factorable hypersurfaces

$$\zeta = \frac{1}{\sqrt{1 + (f_1' f_2 f_3)^2 + (f_1 f_2' f_3)^2 + (f_1 f_2 f_3')^2}} (f_1' f_2 f_3, f_1 f_2' f_3, f_1 f_2 f_3', -1).$$

By the use of equation (2) we find the distance function

$$d = \frac{u f_1' f_2 f_3 + v f_1 f_2' f_3 + w f_1 f_2 f_3' - f_1 f_2 f_3}{\sqrt{1 + (f_1' f_2 f_3)^2 + (f_1 f_2' f_3)^2 + (f_1 f_2 f_3')^2}}.$$

After that, from equations (7) and (8) we find the first and the second fundamental form coefficients and by using of these coefficients in (9) we get Gaussian curvature

$$K = \frac{f_1 f_2 f_3 (f_1 f_1'' f_2'^2 f_3'^2 + f_1'^2 f_2 f_2'' f_3'^2 + f_1'^2 f_2'^2 f_3 f_3'' - 2(f_1' f_2' f_3')^2 - f_1 f_1'' f_2 f_2'' f_3 f_3'')}{(1 + (f_1' f_2 f_3)^2 + (f_1 f_2' f_3)^2 + (f_1 f_2 f_3')^2)^{5/2}}$$

Consequently, by substituting K and d in (16), we find the result

Example 3.13 The hypersurface given with the parametrization $X(u, v, w) = \left(u, v, w, \frac{1}{u.v.w}\right)$ in \mathbb{E}^4 is well known Tzitzeica hypersurface [5] and it is factorable hypersurface with the Tz-constant $a_1 = \frac{1}{256}$.

REFERENCES

- [1] M. Altın, A. Kazan, H. B. Karadağ, “Monge hypersurfaces in euclidean 4-space with density”, *Journal of Polytechnic*, vol. 23, no 1, p. 207-214, 2020.
- [2] M. E. Aydın, A. Mihai, “Translation hypersurfaces and Tzitzeica translation hypersurfaces of the Euclidean Space”, *Proceedings of the Romanian Academy, Series A*, vol. 16, no 4, p. 477-483, 2015.
- [3] B. Bayram, E. Tunç, K. Arslan, G. Öztürk, “On Tzitzeica Curves in Euclidean 3-Space IE^3 ”, *Facta Universitatis Ser.Math. Inform*, vol.33, no 3, p. 409 – 416, 2018.
- [4] B. Bayram, E. Tunç, “On Tzitzeica Surfaces in Euclidean 3-Space IE^3 ”, *BAUN Fen Bil.Enst.Dergisi*, vol. 23, no 1, p. 277 – 290, 2021.
- [5] E. Calabi, “Complete Affine Hyperspheres I”, *Symposia Mathematica (Convegno di Geometria Differenziale, INDAM, Rome, 1971)*, Academic Press, London, vol. X, p. 19-38, 1972.
- [6] B. Y. Chen, “Geometry of Submanifolds”, *Courier Dover Publications*, 2019.
- [7] O. Constantinescu, M. Craşmareanu, “A new Tzitzeica hypersurface and cubic Finslerian metrics of Berwald type”, *Balkan Journal of Geometry and Its Applications*, vol. 16, no 2, p. 27-34, 2011.
- [8] M. Craşmareanu, “Cylindrical Tzitzeica curves implies forced harmonic oscilators”, *Balkan Journal of Geometry and Its Applications*, vol. 7, no 1, p. 37-42, 2002.
- [9] E. Güler, A. Gümüşok Karaalp, “Dini-type helicoidal hypersurface in 4-space”, *Ikoniion Journal of Mathematics*, vol. 1, no 1, p. 26-34, 2019.
- [10] E. Güler, “Rotational hypersurfaces satisfying $\Delta^1 R = AR$ in the four-dimensional Euclidean space”, *Journal of Polytechnic*, vol. 24, no 2, p. 517-520, 2021.
- [11] N. H. Kuiper, “Minimal total absolute curvature for immersions”, *Inventiones Mathematicae*, vol. 10, p. 209-238, 1970.
- [12] E. Tunç, B. Bayram, “A New Characterization of Tzitzeica Curves in Euclidean 4-Space”, *Fundamentals of Contemporary Mathematical Sciences*, vol. 4, no 2, p. 77-86, 2023.
- [13] E. Tunç, B. Bayram, “A Note on Tzitzeica Curves in Euclidean 4-Space IE^4 ”, *International Theory, Research and Reviews in Science and Mathematics, Serüven Yayınevi*, p. 141-166, October 2023.

- [14] G. Tzitzeica, “Sur une nouvelle classe de surfaces”, *Comptes Rendus des Séances de l’Académie des Sciences Paris*, vol. 144, no 1, p. 1257-1259, 1907.
- [15] G. Tzitzeica, “Sur certaines courbes gauches”, *Annales scientifiques de l’École Normale Supérieure*, vol. 28, no 3, p. 9-32, 1911.
- [16] C. Udriște, I. Tevy, A. S. Rasheed, “Evolution of Tzitzeica Hypersurfaces”, *AAPP Physical, Mathematical, and Natural Sciences*, vol. 28, no 3, p. A7.1-A7.8, 2018.
- [17] G. E. Vilcu, “A geometric perspective on the generalized Cobb-Douglas production function”, *Applied Mathematics Letters*, vol. 24, no 5, p. 777-783, 2011.



Chapter 6

ON QUATERNIONS AND THEIR MATRICE REPRESENTATIONS WITH COMPLEX MATRICES*

*Ali Atasoy*¹

* Note: This study is derived from a section of the doctoral thesis titled "Quaternions and Some Applications of Quaternionic Functions" by the author Ali ATASOY (YÖK thesis no: 337862; Dumlupınar University-2013, <https://acikbilim.yok.gov.tr/handle/20.500.12812/609977>, Supervisor: Doç. Dr. Erhan Ata).

¹ Dr. Asst. Prof., Kırıkkale University, Keskin Vocational School, Kırıkkale, Türkiye, <https://orcid.org/0000-0002-1894-7695>

1. Introduction

Quaternions and their matrix representations are fundamental in various fields of mathematics and physics due to their ability to handle rotations and other transformations in three-dimensional space. This mathematical framework, originally developed by Hamilton (Hamilton, 1843), extends complex numbers to higher dimensions and provides powerful tools for representing and manipulating spatial orientations and rotations (Atasoy, 2013).

Split quaternions, also known as hyperbolic quaternions, modify these rules to align with the geometry of Minkowski space rather than Euclidean space. In split quaternions, the units satisfy slightly different multiplication rules, which reflect their application in special relativity and other spacetime theories (Ata and Yaylı, 2009).

Split quaternions are similarly applied in contexts requiring transformations in Minkowski space, such as in the formulation of Lorentz transformations in special relativity. The distinct multiplication rules of split quaternions make them suitable for modeling hyperbolic rotations and boosts, essential for understanding relativistic effects (Bekar and Yaylı, 2013).

Let us denote the set of real numbers by IR . The vector space of quaternions defined over IR will be denoted by IH . For $a, b, c, d \in IR$, a quaternion is defined as a vector in IH in the form:

$$q = a + bi + cj + dk \in IH$$

Here, the following equalities hold:

$$i^2 = j^2 = k^2 = -1, \quad ijk = -1$$

The real part of this quaternion q is given by:

$$Req = a$$

and the imaginary part is:

$$\text{Im}q = bi + cj + dk$$

The conjugate of q is defined as:

$$\bar{q} = q^* = a - bi - cj - dk$$

and its norm is given by:

$$|q| = \sqrt{q^*q} = \sqrt{a^2 + b^2 + c^2 + d^2}$$

If $|q| = 1$, then q is called a unit quaternion (Hacısalıhoğlu, 1983). It should be noted that quaternion multiplication is non-commutative.

2. Preliminaries

Quaternions can be represented as 4×4 matrices. This representation leverages the algebraic properties of quaternions to facilitate their application in linear algebra and computational contexts. The matrix form of a quaternion $q = a + bi + cj + dk$ is given by:

$$q = \begin{pmatrix} a & -b & -c & -d \\ b & a & -d & c \\ c & d & a & -b \\ d & -c & b & a \end{pmatrix}$$

This matrix representation preserves the quaternion multiplication properties, enabling efficient computation of quaternion products, inverses, and other operations using standard matrix algebra techniques.

Theorem 2.1. Let $x, y, z \in IH$. The following properties hold:

1. $x^*x = xx^*$, hence $|x| = |x^*|$.
2. $|x| = 0 \Leftrightarrow x = 0$.

$$|x + y| \leq |x| + |y|$$

$$|xy| = |yx| = |x||y|$$

$$3. |x|^2 + |y|^2 = \frac{1}{2}(|x + y|^2 + |x - y|^2)$$

$$4. u = \frac{x}{|x|} \text{ is a unit quaternion.}$$

$$5. \text{ For any complex number } c, jc = \bar{c}j \text{ or } jcj^* = \bar{c}.$$

$$6. (xy)^* = y^*x^*.$$

$$7. (xy)z = x(yz)$$

$$8. x^* = x \Leftrightarrow x \in IR$$

$$9. \text{ For any } x \in IH,$$

$$ax = xa \Leftrightarrow x \in IR.$$

$$10. x^{-1} = \frac{x^*}{|x|^2} \text{ for } x \neq 0 \text{ and } |x^{-1}| = \frac{1}{|x|}.$$

11. Any quaternion q can be expressed as $q = c_1 + c_2j$ where $c_1, c_2 \in \mathbb{C}$. (Zhang, 1997).

Proof:

$$5. \text{ Let } c = x + iy \in \mathbb{C} \text{ where } x, y \in IR.$$

$$\left. \begin{aligned} jc &= j(x + iy) = jx - ky \\ \bar{c}j &= (x - iy)j = xj - ky \end{aligned} \right\}$$

Hence, the equality holds. Similarly,

$$jcx^* = j(x + iy)(-j) = (jx - ky)(-j) = x - iy = \bar{c}.$$

$$6. \text{ Let } x = x_0 + x_1i + x_2j + x_3k \text{ and } y = y_0 + y_1i + y_2j + y_3k.$$

$$\left. \begin{aligned} x^* &= x_0 - x_1i - x_2j - x_3k \\ y^* &= y_0 - y_1i - y_2j - y_3k \end{aligned} \right\}$$

The product is:

$$\begin{aligned} x \cdot y &= (x_0y_0 - x_1y_1 - x_2y_2 - x_3y_3) + (x_0y_1 + x_1y_0 + x_2y_3 - x_3y_2)i \\ &\quad + (x_0y_2 - x_1y_3 + x_2y_0 + x_3y_1)j \\ &\quad + (x_0y_3 + x_1y_2 - x_2y_1 + x_3y_0)k \end{aligned}$$

The conjugate product is:

$$\begin{aligned} y^* \cdot x^* &= (x_0y_0 - x_1y_1 - x_2y_2 - x_3y_3) \\ &\quad - (x_0y_1 + x_1y_0 + x_2y_3 - x_3y_2)i \\ &\quad - (x_0y_2 - x_1y_3 + x_2y_0 + x_3y_1)j \\ &\quad - (x_0y_3 + x_1y_2 - x_2y_1 + x_3y_0)k \end{aligned}$$

Therefore, $(x \cdot y)^* = y^* \cdot x^*$.

$$10. x^*x = |x|^2,$$

$$x^* \underbrace{xx^{-1}}_I = |x|^2 x^{-1}$$

$$x^* = |x|^2 x^{-1} \Rightarrow x^{-1} = \frac{x^*}{|x|^2}$$

and

$$|x^{-1}| = \frac{|x^*|}{||x|^2|} = \frac{1}{|x|}$$

12. A quaternion q can be written as:

$$\begin{aligned} q &= q_1 + q_2i + q_3j + q_4k = \underbrace{(q_1 + q_2i)}_{c_1} + \underbrace{(q_3 + q_4i)}_{c_2}j \\ &= c_1 + c_2j; (c_1, c_2 \in \mathbb{C}) \end{aligned}$$

The proof of the others is clear.

2.2. Similarity of Quaternions

For any $x, y, u \in IH$, if the equality

$$u^{-1}xu = y$$

holds, then the quaternions x and y are said to be similar, denoted by $x \sim y$.

If x and y are similar quaternions, their norms are equal. This is because:

$$x \sim y \Rightarrow u^{-1}xu = y \Rightarrow |u^{-1}||x||u| = |y| \Rightarrow |x| = |y|$$

Let $[x]$ denote the set of equivalence classes of the quaternion x , then, $y \in [x]$ if x and y are similar quaternions. If $x \in IR$, the equivalence class $[x]$ contains only a single element. For any quaternion x , it holds that $x \sim x^*$ (Parker, 2009).

Lemma 2.2.1. For $q = q_0 + q_1i + q_2j + q_3k \in IH$, it holds that

$$q \sim \left(q_0 + \sqrt{q_1^2 + q_2^2 + q_3^2}i \right)$$

(Zhang, 1997).

Theorem 2.2.1. For any $x, y \in IH$,

$$x \sim y \Leftrightarrow \text{Re}x = \text{Re}y \text{ and } |\text{Im}x| = |\text{Im}y|$$

(Brenner, 1951; Au-Yeung, 1984).

Remark 2.2.1. Let $M_2(\mathbb{C})$ denote the ring of 2×2 matrices with complex number entries. The subring $H' \subset M_2(\mathbb{C})$, given by

$$H' = \left\{ \begin{pmatrix} a_1 & a_2 \\ -\bar{a}_2 & \bar{a}_1 \end{pmatrix} : a_1, a_2 \in \mathbb{C} \right\}$$

is essentially identical to IH . Indeed, using the basis $\{1, j\}$ for IH , the map

$$\mu: IH \rightarrow IH' ; \mu(q) = \mu(a_1 + a_2j) = \begin{pmatrix} a_1 & a_2 \\ -\bar{a}_2 & \bar{a}_1 \end{pmatrix} = q'$$

is a bijective isomorphism. Therefore $IH \approx IH'$. Furthermore, $|q|^2 = \det q'$, and the eigenvalues of the matrix q' are $\text{Re}q \pm |\text{Im}q|i$. Since q' is a complex matrix, its eigenvalues are found from:

$$\begin{aligned} q'v = \lambda v &\Rightarrow (q' - \lambda I)v = 0 \Rightarrow |q' - \lambda I| = 0 \Rightarrow \begin{vmatrix} a_1 - \lambda & a_2 \\ -\bar{a}_2 & \bar{a}_1 - \lambda \end{vmatrix} \\ &= 0 \Rightarrow \lambda^2 - \left(\frac{a_1 + \bar{a}_1}{\text{tr}q'} \right) \lambda + \frac{|a_1|^2 + |a_2|^2}{\det q'} = 0 \end{aligned}$$

which are the roots of the quadratic equation. Thus, the eigenvalues are $\lambda = \text{Re}q \pm |\text{Im}q|i$ (Jacobson, 1974).

2.3. Matrix Representation of Split Quaternions

Let Q denote the set of split quaternions. For $q = d + ai + bj + dk \in Q$, the basis elements $\{1, i, j, k\}$ satisfy the following relations $i^2 = -1, j^2 = k^2 = 1, ij = k, jk = -i$ and $ki = j$. For $p, q \in Q$, we define the operator T_q on Q by $T_q(p) = qp$. Considering the action of T_q on the basis elements:

$$T_q(1) = q \cdot 1 = d + ai + bj + dk$$

$$T_q(i) = q \cdot i = di - a - bk + cj$$

$$T_q(j) = q \cdot j = dj + ak + b + ci$$

$$T_q(k) = q \cdot k = dk - aj - bi - cj$$

we can express T_q as the following matrix (Alagöz et al, 2012):

$$T_q \equiv \begin{bmatrix} d & a & b & c \\ -a & d & c & -b \\ b & c & d & a \\ c & -b & -a & d \end{bmatrix}.$$

On the other hand, using the basis elements $\{1, j\}$, we can rewrite $q = d + ai + bj + dk$ as

$$q = \left(\underbrace{d + ai}_w \right) + j \left(\underbrace{b - ic}_v \right)$$

Thus, we obtain:

$$\begin{cases} T_q(1) = q \cdot 1 = w + vj \\ T_q(j) = q \cdot j = v + wj \end{cases}$$

where $w = d + ai$ and $v = b - ic$. Therefore, T_q can also be represented in the complex matrix format as:

$$T_q \equiv \begin{bmatrix} w & v \\ v & w \end{bmatrix}.$$

This approach demonstrates how split quaternions can be handled within different basis frameworks and showcases their versatility. The complex matrix representation, as noted by Masrouri, Yaylı, Faroughi, and Mirshafizadeh, provides a convenient method for computations involving split quaternions (Masrouri, Yaylı, Faroughi ve Mirshafizadeh, 2011).

2.4. Quaternion Matrices and Their Adjoint

Let's denote the set of quaternion matrices of type $m \times n$ as $M_{m \times n}(IH)$. When $m = n$, we simply denote this set as $M_n(IH)$. Given a matrix $A = (a_{st}) \in M_{m \times n}(IH)$ and a quaternion $q \in IH$, we can define

the right and left scalar multiplication as $qA = (qa_{st})$ and $Aq = (a_{st}q)$, respectively.

For $A \in M_{m \times n}(IH)$, $B \in M_{n \times t}(IH)$, and $p, q \in IH$, the following properties hold:

$$(qA)B = q(AB)$$

$$(Aq)B = A(qB)$$

$$(pq)A = p(qA).$$

These properties imply that the set $M_{m \times n}(IH)$ constitutes a left (right) vector space over IH .

The conjugate of a matrix A , denoted as \bar{A} , is given by $\bar{A} = \overline{(a_{st})} = (a_{st}^*)$. The transpose of A , denoted as A^T , is defined as $A^T = (a_{ts}) \in M_{n \times m}(IH)$. The conjugate transpose of A , denoted as A^* , is given by $A^* = (\bar{A})^T \in M_{n \times m}(IH)$.

A matrix $A \in M_n(IH)$ is said to be normal if it satisfies $AA^* = A^*A$. If A satisfies $A^* = A$, it is called Hermitian. If A satisfies $A^*A = I$, it is unitary. A matrix $A \in M_n(IH)$ is invertible if there exists a matrix $B \in M_n(IH)$ such that $AB = BA = I$.

Elementary row and column operations can be applied to quaternion matrices (Birkhoff and MacLane, 1977). These operations provide a foundational framework for manipulating quaternion matrices similarly to matrices over real or complex fields, preserving the structure and properties necessary for various algebraic and geometric applications.

3. Properties of Quaternion Matrices

Let us now present a theorem that encapsulates some of the properties of quaternion matrices.

Theorem 3.1. Let $A \in M_{m \times n}(IH)$ and $B \in M_{n \times t}(IH)$. The following properties hold:

1. $(\bar{A})^T = \overline{(A^T)}$
2. $(AB)^* = B^*A^*$
3. In general, $(AB)^T \neq B^T A^T$
4. $(AB)^{-1} = B^{-1}A^{-1}$
5. In general, $\overline{(AB)} \neq \bar{A}\bar{B}$
6. $(A^*)^{-1} = (A^{-1})^*$
7. In general, $(\bar{A})^{-1} \neq \overline{(A^{-1})}$
8. In general, $(A^T)^{-1} \neq (A^{-1})^T$ (Zhang, 1997).

Proof:

7) Let $A = \begin{pmatrix} i & k \\ 0 & j \end{pmatrix}$. From the equation $A \cdot A^{-1} = I$, we have:

$$\begin{pmatrix} i & k \\ 0 & j \end{pmatrix} \cdot \begin{pmatrix} a & b \\ c & d \end{pmatrix} = \begin{pmatrix} 1 & 0 \\ 0 & 1 \end{pmatrix}$$

From this, it follows that:

$$A^{-1} = \begin{pmatrix} -i & -1 \\ 0 & -j \end{pmatrix}$$

and

$$\overline{(A^{-1})} = \begin{pmatrix} i & -1 \\ 0 & j \end{pmatrix}$$

On the other hand $\overline{(A^{-1})} = \begin{pmatrix} -i & -k \\ 0 & -j \end{pmatrix}^{-1} = \begin{pmatrix} i & 1 \\ 0 & j \end{pmatrix}$. Thus, in general, we observe that $(\bar{A})^{-1} \neq \overline{(A^{-1})}$.

8) Let $A = \begin{pmatrix} i & k \\ 0 & j \end{pmatrix}$. Then:

$$(A^{-1})^T = \begin{pmatrix} -i & 0 \\ -1 & -j \end{pmatrix}$$

while:

$$(A^T)^{-1} = \begin{pmatrix} i & 0 \\ k & j \end{pmatrix}^{-1} = \begin{pmatrix} -i & 0 \\ 1 & -j \end{pmatrix}$$

Therefore, in general, $(A^T)^{-1} \neq (A^{-1})^T$.

The proof of the others is clear.

Proposition 3.1. Let $A, B \in M_n(IH)$. If $AB = I$, then $BA = I$ (Zhang, 1997).

Proof. Since this proposition holds for complex matrices, let $A = A_1 + A_2j$ and $B = B_1 + B_2j$, where A_1, A_2, B_1 and B_2 are complex matrices. We then have:

$$\begin{aligned} AB = I &\Rightarrow (A_1 + A_2j)(B_1 + B_2j) = I \\ &\Rightarrow (A_1B_1 - A_2\overline{B_2}) + (A_1B_2 + A_2\overline{B_1})j = I + 0.j \end{aligned}$$

Thus,

$$\begin{pmatrix} A_1 & A_2 \\ -\overline{A_2} & A_1 \end{pmatrix} \begin{pmatrix} B_1 & B_2 \\ -\overline{B_2} & B_1 \end{pmatrix} = \begin{pmatrix} I & 0 \\ 0 & I \end{pmatrix} = \begin{pmatrix} I & 0 \\ 0 & I \end{pmatrix}.$$

Since complex matrices commute, we can write:

$$\begin{pmatrix} B_1 & B_2 \\ -\overline{B_2} & B_1 \end{pmatrix} \begin{pmatrix} A_1 & A_2 \\ -\overline{A_2} & A_1 \end{pmatrix} = \begin{pmatrix} I & 0 \\ 0 & I \end{pmatrix}.$$

Starting with the given equations $B_1A_1 - B_2\overline{A_2} = I$ and $B_1A_2 + B_2\overline{A_1} = 0$, it follows that

$$(B_1A_1 - B_2\overline{A_2}) + (B_1A_2 + B_2\overline{A_1})j = I \Rightarrow BA = I$$

hence completing the proof.

For $A = A_1 + A_2j \in M_n(IH)$, a $2n \times 2n$ matrix, the adjoint matrix of the quaternion matrix A , denoted as χ_A , is given by the complex matrix

$$\chi_A = \begin{pmatrix} A_1 & A_2 \\ -\overline{A_2} & A_1 \end{pmatrix}.$$

If the matrix A is a complex matrix, i.e., $A = A + 0.j$, then

$$\chi_A = \begin{pmatrix} A & 0 \\ 0 & \bar{A} \end{pmatrix}.$$

Considering the quaternion $q = q_0 + q_1i + q_2j + q_3k = (q_0 + q_1i) + (q_2 + q_3i)j$, for the 2×2 elementary quaternion matrix

$$P = \begin{pmatrix} 1 & q \\ 0 & 1 \end{pmatrix}$$

which ensures $|P| = 1$, it follows that

$$P = \begin{pmatrix} 1 & q_0 + q_1i + q_2j + q_3k \\ 0 & 1 \end{pmatrix} = \underbrace{\begin{pmatrix} 1 & q_0 + q_1i \\ 0 & 1 \end{pmatrix}}_{A_1} + \underbrace{\begin{pmatrix} 1 & q_2 + q_3i \\ 0 & 1 \end{pmatrix}}_{A_2} j.$$

The adjoint of the matrix P is

$$\chi_P = \begin{pmatrix} A_1 & A_2 \\ -\bar{A}_2 & \bar{A}_1 \end{pmatrix} = \begin{pmatrix} 1 & q_0 + q_1i & 0 & q_2 + q_3i \\ 0 & 1 & 0 & 0 \\ 0 & -q_2 + q_3i & 1 & q_0 - q_1i \\ 0 & 0 & 0 & 1 \end{pmatrix}.$$

The determinant $\det(\chi_P) = |\chi_P| = 1$.

More generally, for $\alpha \in IH$ and $A = \begin{pmatrix} 1 & \alpha \\ 0 & B \end{pmatrix}$, the determinant $|\chi_A| = |\chi_B|$. Given, $B = B_1 + B_2j$, we have

$$\begin{aligned} A &= \begin{pmatrix} 1 & \alpha \\ 0 & B_1 + B_2j \end{pmatrix} = \begin{pmatrix} 1 & \alpha \\ 0 & B_1 \end{pmatrix} + \begin{pmatrix} 0 & 0 \\ 0 & B_2 \end{pmatrix} j \Rightarrow |\chi_A| = \begin{pmatrix} A_1 & A_2 \\ -\bar{A}_2 & \bar{A}_1 \end{pmatrix} \\ &= \begin{pmatrix} 1 & \alpha & 0 & 0 \\ 0 & B_1 & 0 & B_2 \\ 0 & 0 & 1 & \alpha \\ 0 & -\bar{B}_2 & 0 & \bar{B}_1 \end{pmatrix}. \end{aligned}$$

Thus,

$$|\chi_A| = \begin{vmatrix} B_1 & 0 & B_2 \\ 0 & 1 & \alpha \\ -\bar{B}_2 & 0 & \bar{B}_1 \end{vmatrix} = B_1\bar{B}_1 + B_2\bar{B}_2.$$

Conversely, $\chi_B = \begin{pmatrix} B_1 & B_2 \\ -\bar{B}_2 & \bar{B}_1 \end{pmatrix}$, we find

$$|\chi_B| = B_1\bar{B}_1 + B_2\bar{B}_2$$

thereby confirming that $|\chi_A| = |\chi_B|$ (Eilenberg and Niven, 1944).

Theorem 3.2. Let $A, B \in M_n(IH)$. Then:

1. $\chi_{I_n} = I_{2n}$
2. $\chi_{AB} = \chi_A \chi_B$
3. $\chi_{A+B} = \chi_A + \chi_B$
4. $\chi_{A^*} = (\chi_A)^*$
5. $\chi_{A^{-1}} = (\chi_A)^{-1}$
6. The matrix χ_A is unitary, Hermitian, or normal if and only if the matrix A is also unitary, Hermitian, or normal (Lee, 1949).

Proof.

1. Consider the identity matrix I_n :

$$I_n = \begin{pmatrix} 1 & 0 & \cdots & 0 \\ 0 & 1 & \cdots & 0 \\ \vdots & \vdots & \ddots & \vdots \\ 0 & 0 & \cdots & 1 \end{pmatrix}_{n \times n} = \underbrace{\begin{pmatrix} 1 & 0 & \cdots & 0 \\ 0 & 1 & \cdots & 0 \\ \vdots & \vdots & \ddots & \vdots \\ 0 & 0 & \cdots & 1 \end{pmatrix}}_{A_1}_{n \times n} + \underbrace{\begin{pmatrix} 0 & 0 & \cdots & 0 \\ 0 & 0 & \cdots & 0 \\ \vdots & \vdots & \ddots & \vdots \\ 0 & 0 & \cdots & 0 \end{pmatrix}}_{A_2}_{n \times n} j.$$

Thus,

$$\chi_{I_n} = \begin{pmatrix} A_1 & A_2 \\ -A_2 & A_1 \end{pmatrix} = \begin{pmatrix} 1 & 0 & \cdots & 0 & 0 & 0 & \cdots & 0 \\ 0 & 1 & \cdots & 0 & 0 & 0 & \cdots & 0 \\ \vdots & \vdots & \ddots & \vdots & \vdots & \vdots & \ddots & \vdots \\ 0 & 0 & \cdots & 1 & 0 & 0 & \cdots & 0 \\ 0 & 0 & \cdots & 0 & 1 & 0 & \cdots & 0 \\ 0 & 0 & \cdots & 0 & 0 & 1 & \cdots & 0 \\ \vdots & \vdots & \ddots & \vdots & \vdots & \vdots & \ddots & \vdots \\ 0 & 0 & \cdots & 0 & 0 & 0 & \cdots & 1 \end{pmatrix}_{2n \times 2n} = I_{2n}.$$

2. For the product $A \cdot B$:

$$\begin{aligned} A \cdot B &= (A_1 + A_2j)(B_1 + B_2j) = A_1B_1 + A_1B_2j + A_2jB_1 + A_2jB_2j \\ &= A_1B_1 + A_1B_2j + A_2\overline{B_1}j - A_2\overline{B_2} \\ &= \underbrace{(A_1B_1 - A_2\overline{B_2})}_{Q_1} + \underbrace{(A_1B_2 + A_2\overline{B_1})}_{Q_2}j. \end{aligned}$$

Thus,

$$\begin{aligned}\chi_{AB} &= \begin{pmatrix} Q_1 & Q_2 \\ -\overline{Q_2} & \overline{Q_1} \end{pmatrix} = \begin{pmatrix} A_1B_1 - A_2\overline{B_2} & A_1B_2 + A_2\overline{B_1} \\ -(A_1B_2 + A_2\overline{B_1}) & A_1B_1 - A_2\overline{B_2} \end{pmatrix} \\ &= \begin{pmatrix} A_1B_1 - A_2\overline{B_2} & A_1B_2 + A_2\overline{B_1} \\ -\overline{A_1B_2} - \overline{A_2B_1} & \overline{A_1B_1} - \overline{A_2B_2} \end{pmatrix}.\end{aligned}$$

On the other hand,

$$\left. \begin{aligned}\chi_A &= \begin{pmatrix} A_1 & A_2 \\ -\overline{A_2} & \overline{A_1} \end{pmatrix} \\ \chi_B &= \begin{pmatrix} B_1 & B_2 \\ -\overline{B_2} & \overline{B_1} \end{pmatrix}\end{aligned}\right\} \Rightarrow \chi_A\chi_B = \begin{pmatrix} A_1B_1 - A_2\overline{B_2} & A_1B_2 + A_2\overline{B_1} \\ -\overline{A_1B_2} - \overline{A_2B_1} & \overline{A_1B_1} - \overline{A_2B_2} \end{pmatrix}$$

Therefore, $\chi_{AB} = \chi_A\chi_B$ is established.

The remaining parts of the proof follow similar procedures, ensuring that the properties of matrices under χ transformations are preserved. Specifically:

4. Given $A = A_1 + A_2j$, it follows that the conjugate of A can be expressed as $\bar{A} = \bar{A}_1 + \bar{A}_2\bar{j} = \bar{A}_1 - \bar{A}_2j$. Consequently, the conjugate transpose A^* can be written as:

$$A^* = (\bar{A})^T = \overline{(A^T)} = \overline{(A_1^T + A_2^Tj)} = (\bar{A}_1)^T + (\bar{A}_2)^Tj$$

This is because A_1 and A_2 are complex matrices. Therefore, we have:

$$\chi_{A^*} = \begin{pmatrix} (\bar{A}_1)^T & (\bar{A}_2)^T \\ -(A_2)^T & (A_1)^T \end{pmatrix} = \begin{pmatrix} \bar{A}_1 & \bar{A}_2 \\ -A_2 & A_1 \end{pmatrix}^T = \begin{pmatrix} \bar{A}_1 & -A_2 \\ \bar{A}_2 & A_1 \end{pmatrix}.$$

Similarly, for χ_A , we have:

$$\chi_A = \begin{pmatrix} A_1 & A_2 \\ -\overline{A_2} & \overline{A_1} \end{pmatrix} \Rightarrow \overline{\chi_A} = \begin{pmatrix} \bar{A}_1 & \bar{A}_2 \\ -A_2 & A_1 \end{pmatrix}$$

Thus,

$$\overline{\chi_A} = \begin{pmatrix} \bar{A}_1 & \bar{A}_2 \\ -A_2 & A_1 \end{pmatrix}$$

Taking the transpose, we get:

$$(\overline{\chi_A})^T = (\chi_A)^* = \begin{pmatrix} \bar{A}_1 & -A_2 \\ \bar{A}_2 & A_1 \end{pmatrix}$$

Therefore, it is shown that:

$$\chi_{A^*} = (\chi_A)^*$$

The proof of the others is clear

Proposition 3.2. Let A and B be $n \times n$ complex matrices. Then,

$$\begin{vmatrix} A & B \\ -\bar{B} & \bar{A} \end{vmatrix} \geq 0.$$

Moreover,

1. For every $C \in M_n(IH)$, $|\chi_C| \geq 0$.
2. $|I + A\bar{A}| \geq 0$.
3. $|A\bar{A} + B\bar{B}| \geq 0$, provided that A and B commute (Zhang, 1997).

Proof.

1. For any $C \in M_n(IH)$, since χ_C is a complex matrix, it follows that $|\chi_C| \geq 0$.
2. $\begin{vmatrix} I & A \\ -\bar{A} & I \end{vmatrix} = |I + A\bar{A}| \geq 0$ (Horn and Johnson, 1985).
3. Let us consider the product $(A^{-1} + 0.j)(A + Bj)$. From this, we derive the following:

$$\begin{pmatrix} A^{-1} & 0 \\ 0 & (\bar{A})^{-1} \end{pmatrix} \begin{pmatrix} A & B \\ -\bar{B} & \bar{A} \end{pmatrix} = \begin{pmatrix} I & A^{-1}B \\ -\bar{A}^{-1}\bar{B} & I \end{pmatrix}$$

Given that $\begin{vmatrix} A & B \\ -\bar{B} & \bar{A} \end{vmatrix} \geq 0$, if A and B commute, then

$$\begin{vmatrix} A & \bar{B} \\ -\bar{B} & \bar{A} \end{vmatrix} = |A\bar{A} + B\bar{B}| \geq 0.$$

This proof demonstrates the stated proposition by utilizing properties of complex matrices and matrix operations to establish the non-negativity of the determinants under the given conditions.

Theorem 3.3. Let $A \in M_n(IH)$. The following conditions are equivalent:

1. A is invertible.
2. The equation $Ax = 0$ has a unique solution.
3. The characteristic polynomial χ_A is invertible, which implies $|\chi_A| \neq 0$.
4. A has a non-zero eigenvalue, i.e., if $Ax = \lambda x$, then $\lambda \neq 0$, where λ is a quaternion and x is a quaternion vector.
5. A is a product of elementary quaternion matrices (Zhang, 1997).

Proof.

1 \Rightarrow 2: If A is invertible, then A^{-1} exists. Considering the $Ax = 0 \Rightarrow A^{-1}Ax = A^{-1} \cdot 0 \Rightarrow x = 0$

Thus, $x = 0$ is the only solution, proving the uniqueness.

2 \Rightarrow 3: Let $A = A_1 + A_2j$ and $x = x_1 + x_2j$, where A_1 and A_2 are complex matrices, and x_1 and x_2 are complex column vectors. Then,

$$\begin{aligned} x &= (A_1 + A_2j)(x_1 + x_2j) = A_1x_1 + A_1x_2j + A_2jx_1 + A_2jx_2j \\ &= (A_1x_1 - A_2\bar{x}_2) + (A_1x_2 + A_2\bar{x}_1)j \end{aligned}$$

For $Ax = 0$:

$$A_1x_1 - A_2\bar{x}_2 = 0$$

$$A_1x_2 + A_2\bar{x}_1 = 0$$

Rearranging, we get:

$$A_1x_1 + A_2(-\bar{x}_2) = 0$$

$$(-\bar{A}_2)x_1 + \bar{A}_1(-\bar{x}_2) = 0$$

This can be written as:

$$\begin{pmatrix} A_1 & A_2 \\ -\bar{A}_2 & \bar{A}_1 \end{pmatrix} \begin{pmatrix} x_1 \\ -\bar{x}_2 \end{pmatrix} = \begin{pmatrix} 0 \\ 0 \end{pmatrix} \Rightarrow \chi_A(x_1, -\bar{x}_2)^T = 0$$

Since the equation $Ax = 0$ has only the trivial solution, it follows that

$|\chi_A| \neq 0$, indicating that χ_A is invertible.

3 \Rightarrow 1: If χ_A is invertible, then there exists a matrix $B = \begin{pmatrix} B_1 & B_2 \\ B_3 & B_4 \end{pmatrix}$ such that:

$$\begin{pmatrix} B_1 & B_2 \\ B_3 & B_4 \end{pmatrix} \begin{pmatrix} A_1 & A_2 \\ -\bar{A}_2 & \bar{A}_1 \end{pmatrix} = \begin{pmatrix} I & 0 \\ 0 & I \end{pmatrix}$$

Let $B = B_1 + B_2j$. Then, $BA = I$, demonstrating that A is invertible by previous equivalence.

1 \Rightarrow 5: If A is invertible, it can be reduced to the identity matrix through a sequence of elementary row and column operations. Consequently, A can be expressed as a product of elementary quaternion matrices, completing the proof.

These equivalence conditions collectively establish the criteria for the invertibility of a quaternion matrix A . This theorem encapsulates essential properties of quaternion matrices, contributing significantly to the understanding of their algebraic structure and applications.

4. Quaternion Multiplication via the Cayley-Dickson Process

Consider the quaternions $p = p_1 + p_2i + p_3j + p_4k$ and $q = q_1 + q_2i + q_3j + q_4k$. According to the Cayley-Dickson construction, these can be redefined as:

$$p = \underbrace{(p_1 + p_2i)}_a + \underbrace{(p_3 + p_4i)}_b j$$

$$q = \underbrace{(q_1 + q_2i)}_c + \underbrace{(q_3 + q_4i)}_d j$$

With these definitions, the quaternion product " $p \cdot q$ " is given by:

$$p \cdot q = (a, b)(c, d) = (ac - \gamma bd^*, da + bc^*)$$

Here, the conjugate of (a, b) is defined as:

$$\overline{(a, b)} = (\bar{a}, -b).$$

In the Cayley-Dickson system, the value of γ determines the type of quaternion multiplication: for standard quaternions, $\gamma = 1$; for split quaternions, $\gamma = -1$; and for real numbers, $\gamma = 0$ (Dickson, 1919).

Example 4.1. Let $p, q \in Q$ be given by $p = 1 + i$ and $q = 1 + k$. The multiplication $p \cdot q$ is calculated as follows:

$$p \cdot q = (1 + i)(1 + k) = (1 + 0i + 1j + 0k)(1 + 0i + 0j + 1k)$$

Rewriting p and q in terms of a, b, c and d :

$$p = \underbrace{(1 + 0i)}_a + \underbrace{(1 + 0i)}_b j$$

and

$$q = \underbrace{(1 + 0i)}_c + \underbrace{(0 + 1i)}_d j$$

Applying the multiplication rule for split quaternions ($\gamma = -1$):

$$p \cdot q = (ac - (-1)bd^*, da + bc^*)$$

Substituting the values:

$$p \cdot q = (1 \cdot 1 + 1(-i), 1 \cdot 1 + 1 \cdot 1) = (1 - i) + (1 + i)j = 1 - i + j + k$$

Example 4.2. Let $p, q \in IH$ be given by $p = 1 + i$ and $q = 1 + k$. The multiplication $p \cdot q$ is calculated as follows:

$$p \cdot q = (1 + i)(1 + k) = (1 + 0i + 1j + 0k)(1 + 0i + 0j + 1k).$$

Rewriting p and q in terms of a, b, c and d :

$$p = \underbrace{(1 + 0i)}_a + \underbrace{(1 + 0i)}_b j$$

and

$$q = \underbrace{(1 + 0i)}_c + \underbrace{(0 + 1i)}_d j.$$

Applying the multiplication rule for quaternions ($\gamma = 1$):

$$p \cdot q = (ac - 1 \cdot bd^*, da + bc^*)$$

Substituting the values:

$$p \cdot q = (1 - (-i), i + 1) = (1 + i) + (1 + i)j = 1 + i + j + k$$

In summary, the Cayley-Dickson process provides a structured approach for quaternion multiplication, where the parameter γ distinguishes between standard, split, and real quaternions, facilitating various algebraic manipulations (Dickson, 1919).

Conclusion

The study of quaternions and their matrix representations reveals a versatile mathematical framework capable of addressing complex problems in three-dimensional rotations and spacetime transformations. Whether using real quaternions for Euclidean space or split quaternions for Minkowski space, these structures provide powerful tools for both theoretical investigations and practical applications in various scientific and engineering disciplines.

References

- Alagöz, Y., Oral, K. H., & Yüce, S. (2012). Split quaternion matrices, *Miskolc Mathematical Notes*, 13(2), 223-232.
- Ata, E., & Yaylı, Y. (2009). Split quaternions and semi-Euclidean projective spaces, *Chaos Solitons Fractals*, 41(4), 1910–1915.
- Atasoy, A. (2013). Quaternions and Some Applications of Quaternionic Functions, *Dumlupınar University Institute of Science, Doctoral Thesis, Kütahya, Türkiye*.
- Au-Yeung, Y. H. (1984). On the convexity of numerical range in quaternionic Hilbert spaces, *Linear and Multilinear Algebra*, 16, 93-100.
- Birkhoff, G., & MacLane, S. (1977), *A Survey of Modern Algebra*, 4th ed., Macmillan.
- Bekar, M., & Yaylı, Y. (2013). Involutions of complexified quaternions and split quaternions, *Advances in Applied Clifford Algebras*, 23, 283-299.
- Brenner, J. L. (1951). Matrices of quaternions, *Pacific J. Math.*, 1, 329-335.
- Dickson, L. E. (1919). On Quaternions and Their Generalization and the History of the Eight Square Theorem, *Annals of Mathematics, Second Series*, 20(3), 155–171.
- Eilenberg, S., & Niven, I. (1944). The fundamental theorem of algebra for quaternions, *Bull. Amer. Math. Soc.*, 50, 246-248.
- Hacısalıhoğlu, H. H. (1983). Hareket Geometrisi ve Kuaterniyonlar Teorisi, Gazi Üniversitesi Fen Edebiyat Fak. Yayınları, Math. No.2, Ankara, Türkiye.
- Hamilton, W. R. (1843). On A New Spaces of Imaginary Quantities Connected with A Theory of Quaternions, *Duplin Proc.*, 2(13), 424-434.
- Horn, R. A., & Johnson, R. C. (1985). *Matrix Analysis*, Cambridge U.P.
- Jacobson, N. (1974). *Basic Algebra I*, W. H. Freeman.
- Lee, H. C. (1949). Eigenvalues of canonical forms of matrices with quaternion coefficients, *Proc. R. I. A.*, 52, 253-260.
- Masroui, N., Yaylı, Y., Faroughi, M. H., & Mirshafizadeh, M. (2011). Comments On Differentiable Over Function of Split Quaternions, *Revista Notas de Matemática*, 7(2), 128-134.
- Parker, J. (2009). *Quaternionic Linear Algebra*, Durham University.
- Zhang, F. (1997). Quaternions and Matrices of Quaternions, *Linear Algebra and Its Applications*, 251, 21-57.



Chapter 7

PRODUCTION FACTORS AFFECTING NANOPARTICLE SIZE AND THE EFFECT OF SIZE ON THERMOPHYSICAL PROPERTIES

Hakan ŞAHAL¹

¹ Dr. Öğr. Üyesi, Munzur Üniversitesi, Tunceli M.Y.O, Gıda İşleme Bölümü, Tunceli, Türkiye, hakansahal@munzur.edu.tr, ORCID: 0000-0001-8714-1735.

INTRODUCTION

A particle with one or more distinctive sizes in the range of 100 nm is referred to as a nanoparticle by the International Union of Pure and Applied Chemistry (IUPAC) (Vert et al., 2012). NPs can have a variety of sizes, shapes, and architectures. They could be irregular or spherical, cylindrical, conical, tubular, hollow core, spiral, etc. (Ealia and Saravanakumar, 2017). NPs can range in size from one to one hundred nm. It is commonly recommended to refer to NPs as atom clusters if their size is less than 1 nm. NPs can contain single or polycrystalline solids and can be crystalline or amorphous. NPs may be grouped together or loose (Machado et al., 2015). NPs can consist of multiple layers or be monotonous. The layers in the second scenario are (I) Surface layer, which is often made up of different tiny molecules, metal ions, surfactants, or polymers. (II) A shell layer composed of a substance distinct chemically from the core layer. (III) The NP's core, or central region, is shaped like a layer (Khan et al., 2019). Owing to their distinct physical, chemical, and biological characteristics, nanoparticles present ground-breaking solutions in a range of industries, including healthcare and medicine, electronics and optoelectronics, energy, environmental applications, food, textiles, construction, defense, and security. Different methods have been devised for the manufacture of nanoparticles since the expected properties vary depending on the field in which they are created. The degree of production at the nanoscale is influenced by variables such the methods involved in their synthesis, the concentration of precursors, the reaction environment, temperature, pressure, reaction time, and stabilizing agents. Significant alterations in the composition's qualities are frequently brought about by variations in a product's nanosize. Both individual and collective nanoparticles are employed in solar systems (Mayer et al., 2011; Neumann dv., 2013; Ding et al., 2014; Klinkova et al., 2014), thermoelectricity (Yang and Caillat, 2006), catalysis (Astruc, 2020), and medical diagnostics. It has several uses in the pharmaceutical industry (Kumar et al., 2013), solar cell manufacture (Aricò et al., 2005), and other industries (Kim et al., 2015;

Konstantatos et al., 2009; Burschka et al., 2013). Many nanoparticles have distinct sizes, shapes, surface chemistries, and quantum effects from their macroscopic counterparts with the same composition, which accounts for the differences in their electrical, optical, magnetic, and catalytic characteristics (Roduner, 2006). Controlling the synthesis of nanoparticles is necessary to manufacture them with exact sizes, shapes, morphologies, and surface chemistries. This is a hard, rigorous, and time-consuming process. The accurate synthesis of nanoparticles is challenging because it frequently requires several chemicals and dependent experimental parameters such reagent concentrations, reaction times, temperatures, and mixing efficiency. The order in which the chemicals are added to the reaction mixture is also important for the successful completion of the synthesis. Typically, trial and error combined with expertise and intuition are used to determine how much each experimental variable contributes to the finished result. This makes figuring out the best recipe and reaction conditions challenging and time-consuming. Therefore, the synthesis of nanoparticles with certain features requires more controlled and efficient methods.

FACTORS INFLUENCING THE SYNTHESIS OF NANOPARTICLES

1. Concentration of Precursors

The nucleation rate, or size formation, under identical heating and synthesizing circumstances for distinct reactions is dependent on the supersaturation and, thus, on the starting concentration of the precursor. To regulate the size of the nanoparticles, the precursor concentration must be changed. Concentration adjustment is achievable, for example, by varying the solvent or precursor quantity. The ratio of surfactant to precursor varies with changes in the concentration of the precursor. Even though higher concentrations of metal precursors typically result in the formation of larger nanoparticles, numerous investigations have shown that increasing concentrations also cause an increase in particle size (Huang et al., 2008; Zeng et al., 2004; Cabrera et al., 2012; Miguel-Sancho

et al., 2012) and may even cause a decrease (Hufschmid et al., 2008; Liv et al., 2001). However, as it may change the pace at which metal ions are reduced, the concentration of reducing agents is also likely to have an effect the size and structure of nanoparticles.

2. Reaction Medium

When synthesizing nanomaterials, the solvent is a crucial parameter. Through their assistance in the nucleation, development, and assembly processes, solvents significantly influence the form and characteristics of the resultant nanomaterial. The size, shape, structure, and stability of the synthesized nanomaterials are ultimately determined by the solvent selection, which also affects the kinetics and thermodynamics of these processes (Abubakar et al., 2023; Mbachu et al., 2023; Egbosiuba, 2022; onu et al., 2023; Egbosiuba et al., 2020). The reactants' solubility and the kinetics of nucleation and development are influenced by the amount or selection of solvent (aqueous or organic). The synthesis of nanomaterials is known to be significantly impacted by all solvent parameters, including polarity, boiling point, and viscosity. Studies show that the stability, size, and form of nanomaterials are among the critical parameters that are mostly controlled by the solvent choice. Smaller nanoparticles can be produced with high polarity solvents like DMF, DMSO, and THF, while bigger nanomaterials can be produced with low polarity solvents like hexane, toluene, and chloroform. Because the nucleation and development of larger nanomaterials will be delayed, solvents with high boiling points, including dodecane and oleic acid, will be used to generate them. Solvents having low boiling points, like acetone and ethanol, will facilitate the nucleation and development of smaller nanomaterials more quickly. Larger nanoparticles are produced by high viscosity solvents like glycerol and PEG (poly(ethylene glycol)) because of slower diffusion and aggregation, whereas smaller nanomaterials are produced by low viscosity solvents like acetone and ethanol because of faster diffusion and aggregation. Smaller nanoparticles are produced by high viscosity solvents

like ethanol and water because they agglomerate and diffuse more quickly. When high surface tension solvents are used, the attraction between nanomaterials and larger aggregates is stronger; however, when low surface tension solvents, like hexane and toluene, are used, the attraction is weaker (Abdulkareem et al., 2023; Kazemi et al., 2023; Taifi et al., 2022; Sobhani., 2023).

Nonetheless, the pH of the reaction medium can affect the size and stability of nanoparticles by changing the charge and reactivity of metal ions and stabilizing agents. Studies have shown that higher pH levels produce smaller-sized nanoparticles than lower pH ones. Nonetheless, it has been noted that varying the pH level might result in distinct forms for both the size and structure of nanoparticles (Alqadi et al., 2014).

3. Temperature

Elevated temperature accelerates the rate of reaction, facilitating the formation of nanoparticles. The Arrhenius equation explains how temperature affects reaction rate; when temperature rises, molecules' kinetic energy rises as well, accelerating the reaction. One essential factor in regulating the size and structure of NPs is temperature. High temperatures typically encourage the development of homogenous, smaller-sized nanoparticles. This has to do with how temperature affects the crystal structure and growth mechanism, which in turn modifies the nucleation and growth processes (Bala et al., 2015). Elevated temperature accelerates the rate of reaction, facilitating the formation of nanoparticles. The Arrhenius equation explains how temperature affects reaction rate; when temperature rises, molecules' kinetic energy rises as well, accelerating the reaction. Temperature is a key element in controlling the shape and size of nanoparticles. High temperatures typically encourage the development of homogenous, smaller-sized nanoparticles. This relates to the way that temperature modifies the crystal structure and growth mechanism, hence changing the nucleation and growth processes (Bala et al., 2015).

4. Pressure

Pressure has an immediate effect on the pace at which chemical reactions take place. The frequency of molecular collisions rises under high pressure, speeding up the rate of reaction. This may make the synthesis of nanoparticles quicker and more effective. Pressure has a major impact on the kinetics and efficiency of reactions, particularly in hydrothermal and supercritical fluid processes (Nadaroğlu, 2017). High pressure can be used to manufacture smaller nanoparticles. This is related to the idea that pressure changes the crystal structure and growth mechanism of nanoparticles, hence modifying their nucleation and growth processes. Furthermore, it is feasible to create more homogeneous and uniformly formed nanoparticles under high pressure. Pressure can induce phase transitions in the creation of nanoparticles by altering the ratios of the solid, liquid, and gas phases. For instance, high pressure facilitates the creation of a homogenous phase in hydrothermal synthesis by making the reactants more soluble. As a result, more pure, single-phase nanoparticles can be produced (Mubayi et al., 2012). Furthermore, the chemical and physiological characteristics of nanoparticles can be impacted by pressure. High pressure-synthesized nanoparticles typically exhibit greater stability and crystallinity. This has a lot of benefits, particularly for applications in biomedicine, energy storage, and catalysis.

5. Reaction Time

The duration of the nanoparticles' incubation takes into account how quickly their morphology and quality change. Nanoparticles are affected by changes in the synthesis method, length of the incubation period, exposure to light, and storage environment. Nanoparticles may shrink or agglomerate after extended incubation (Wang et al., 2021). Enough time is given by the reaction time for the nanoparticles to develop and grow. Higher yields of nanoparticles are produced when reaction periods are extended to allow for complete reaction of the reactants. Due to insufficient nucleation and growth, short-term reactions may result in the creation of irregular and heterogeneous nanoparticles. Reaction time is

a crucial component in controlling the shape and size of nanoparticles. Extended reaction durations promote the production of larger and more uniformly shaped nanoparticles. This facilitates the formation of more organized crystal structures through long-term nucleation and growth processes. Smaller, irregularly shaped nanoparticles can be produced by short-term reactions. In the production of nanoparticles, time can cause phase transitions by shifting the proportions of the solid, liquid, and gas phases. Extended reaction durations facilitate the total dissolution of the reactants and the creation of a uniform phase. Purer, single-phase nanoparticles can be obtained as a result (Salem and Fouda, 2018).

6. Stabilizing Agents

In order to stop aggregation, stabilizing substances including ligands, polymers, and surfactants cap the nanoparticles and regulate their size and structure. These compounds can affect the nucleation of particles, which makes them valuable for regulating size and form during the creation of nanoparticles. Research has been done on how well-suited certain capping agents are for a given nanoparticle size. These investigations have demonstrated that substances can alter a nanoparticle's size (Singh et al., 2009).

The nanoparticles' size is significantly reduced and their stability is enhanced by the confinement technique. Stearic hindrance, which enables the nanoparticles to stay stable for months, is one method that includes the creation of strong covalent connections between polymeric chains and the surfaces of the nanoparticles.

PHYSICAL PROPERTIES AFFECTED BY NANOPARTICLE SIZE

The form, size, and dispersion of nanoparticles and nanomaterials are enabling new or enhanced applications to emerge quickly. Biomedicine, healthcare, food and feed, medical gene transfer, machinery, optics, chemical industry, electronics, aerospace, energy science, catalysis, phosphorus, single electron transistors, nonlinear optical devices, and

photoelectrochemical applications are several of the areas in which nanoparticles find use. In a lot of ways, it works better. Metal nanoparticles show promise among the nanoparticles employed in various application areas.

The thermal characteristics of nanoparticles are significantly influenced by their size. The surface area/volume ratio rises as nanoparticle size decreases. Thus, greater surface area corresponds to smaller size. Higher surface area can result in more efficient heat transfer in materials like nanofluids that have scattered nanoparticles. Furthermore, microconvection brought on by the Brownian motion of NPs supports the thermal conductivity in NPs (Shima et al., 2009). Nevertheless, according to Syam et al. (2008), this phenomena only happens when solid NPs are distributed throughout a liquid, creating a nanofluid. Cu NPs, for instance, can raise ethylene glycol's thermal conductivity by as much as 40% (Eastman et al., 2001). The size, shape, and volume fraction of nanoparticles influence the temperature-dependent specific heat capacity of metal oxide nanofluids. This is the main focus of inquiry. According to research, the concentration, size, and shape of nanoparticles influence a nanofluid's specific heat capacity (Angayarkanni et al., 2015; Teng et al., 2010). In particular, it is known that the thermal conductivity of nanofluids diminishes with increasing particle size under constant temperature and particle mass fraction (Darvanjooghi et al., 2016; Teng et al., 2010; Chopkar et al., 2008; Chon et al., 2005). Certain research contain exceptions to this rule. Based on these investigations, it appears that the primary cause of the divergent findings about how different nanoparticle sizes affect a nanofluid's thermal conductivity is most likely the fluid's instability and potential for nanoparticle agglomeration (Warrier et al., 2011; Beck et al., 2009; Chen et al., 2008; Yu et al., 2007).

Energy conduction from photons and electrons (lattice vibration) and the concomitant scattering effects are the main sources of heat transmission in NPs (Savage and Rao, 2004). Increased heat energy quantum boundary scattering of phonons can lower thermal conductivity

in smaller nanoparticles. According to Dharmiah et al. (2016), Goyal (2024), and Cao et al. (2024), phonons are more likely to disperse on the surfaces and interfaces of smaller particles, disturbing their flow and lowering the total thermal conductivity. More interfaces produced by nanoparticles in a material may prevent heat transfer because of phonon scattering at these interfaces. Smaller grain size texturing and nanostructure are essential for scattering phonons and lowering the lattice heat conductivity (Wang et al., 2020). This is especially crucial for composite materials since they contain embedded nanoparticles in a matrix (Kumar et al., 2024).

A phenomenon known as the melting point falls with decreasing size in nanoparticles is seen. This is because, in comparison to atoms in the bulk material, surface atoms require less energy to shift to the liquid phase (Chernyshev et al., 2009; Koppes et al., 2012; Petters et al., 2020). The melting point drops as the size and radius of the nanoparticles decrease (Kibria et al., 2015). According to Gülseren et al. (1995), the primary cause of this phenomena is that the average liquid/vapor interface energy is typically lower than the solid/vapor interface energy. Because there is more free energy on the particle surface when the particle size reduces, the surface/volume ratio rises and the melting temperature falls (Shim et al., 2002). Very small nanoparticles can have a melting point that is significantly lower than the parent material's. For instance, according to Roduner (2006), the melting point of 3 nm Au NPs is 300 degrees lower than the melting point of bulk gold. Aluminum (Al) has been reported to melt at 660 °C, and 2 nm Al nanoparticles have a temperature of 140 °C (Lai et al., 2021). Because of the alloying effect, bimetallic alloy nanoparticles often exhibit greater thermal stability and melting temperatures than monometallic NPs (Cuenya, 2010).

The heat capacity of nanoparticles can be higher than that of their bulk counterparts. Because more of the nanoparticles' atoms are at or near the surface, where they have more degrees of freedom and raise the specific heat, this is the cause. According to experimental research, NPs' heat

capacity can be up to 10% higher than that of comparable bulk materials (Likhachev et al., 2006). This has an impact on how nanoparticles are used in thermal energy storage systems. The ability of nanoparticles to withstand high temperatures is correlated with their thermal stability. According to Ajroudi et al. (2014), metal oxide and ceramic nanoparticles in particular have remarkable thermal stability and retain their structural integrity at high temperatures. This characteristic is crucial for applications involving high temperatures and catalysts. Because of their small size and surface effects, nanoparticles' thermal expansion behavior can be separated from that of macroscopic materials. Nanoparticles can increase thermal resistance because of their enormous surface area. The application of nanoparticles in thermal barrier and insulation coatings is made possible by this property. According to Ho et al. (2009), ceramic nanoparticles in particular are renowned for having a high heat barrier capability.

In order to produce and employ nanoparticles in thermally essential applications including electronics, catalysis, thermal management systems, and nanocomposites, it is imperative to comprehend these consequences.

REFERENCES

- Abdulkareem, A. S., Hamzat, W. A., Tijani, J. O., Egbosiuba, T. C., Mustapha, S., Abubakre, O. K., ... & Babayemi, A. K. (2023). Isotherm, kinetics, thermodynamics and mechanism of metal ions adsorption from electroplating wastewater using treated and functionalized carbon nanotubes. *Journal of Environmental Chemical Engineering*, 11(1), 109180.
- Abubakar, H. L., Tijani, J. O., Abdulkareem, A. S., Egbosiuba, T. C., Abdullahi, M., Mustapha, S., & Ajiboye, E. A. (2023). Effective removal of malachite green from local dyeing wastewater using zinc-tungstate based materials. *Heliyon*, 9(9).
- Alqadi, M. K., Abo Noqtah, O. A., Alzoubi, F. Y., Alzoubi, J., & Aljarrah, K. (2014). pH effect on the aggregation of silver nanoparticles synthesized by chemical reduction. *Materials Science-Poland*, 32, 107-111.
- Ajrouti, L., Mliki, N., Bessais, L., Madigou, V., Villain, S., & Leroux, C. (2014). Magnetic, electric and thermal properties of cobalt ferrite nanoparticles. *Materials Research Bulletin*, 59, 49-58.
- Angayarkanni, S. A., Sunny, V., & Philip, J. (2015). Effect of nanoparticle size, morphology and concentration on specific heat capacity and thermal conductivity of nanofluids. *Journal of Nanofluids*, 4(3), 302-309.
- Arico, A. S., Bruce, P., Scrosati, B., Tarascon, J. M., & Van Schalkwijk, W. (2005). Nanostructured materials for advanced energy conversion and storage devices. *Nature materials*, 4(5), 366-377.
- Astruc, D. (2020). Introduction: nanoparticles in catalysis. *Chemical reviews*, 120(2), 461-463.
- Bala, N., Saha, S., Chakraborty, M., Maiti, M., Das, S., Basu, R., & Nandy, P. (2015). Green synthesis of zinc oxide nanoparticles using Hibiscus subdariffa leaf extract: effect of temperature on synthesis, anti-bacterial activity and anti-diabetic activity. *RSC Advances*, 5(7), 4993-5003.
- Beck, M. P., Yuan, Y., Warriar, P., & Teja, A. S. (2009). The effect of particle size on the thermal conductivity of alumina nanofluids. *Journal of Nanoparticle research*, 11, 1129-1136.

- Burschka, J., Pellet, N., Moon, S. J., Humphry-Baker, R., Gao, P., Nazeeruddin, M. K., & Grätzel, M. (2013). Sequential deposition as a route to high-performance perovskite-sensitized solar cells. *Nature*, 499(7458), 316-319.
- Cabrera, L. I., Somoza, Á., Marco, J. F., Serna, C. J., & Puerto Morales, M. (2012). Synthesis and surface modification of uniform MFe₂O₄ (M= Fe, Mn, and Co) nanoparticles with tunable sizes and functionalities. *Journal of Nanoparticle Research*, 14, 1-14.
- Cao, J., Wang, H., Ferrer-Argemi, L., Cao, P., & Lee, J. (2024). Highly tailorable thermomechanical properties of nanograined silicon: Importance of grain size and grain anisotropy. *Applied Physics Letters*, 124(8).
- Chen, G., Yu, W., Singh, D., Cookson, D., & Routbort, J. (2008). Application of SAXS to the study of particle-size-dependent thermal conductivity in silica nanofluids. *Journal of Nanoparticle research*, 10, 1109-1114.
- Chernyshev, A. P. (2009). Effect of nanoparticle size on the onset temperature of surface melting. *Materials Letters*, 63(17), 1525-1527.
- Chon, C. H., Kihm, K. D., Lee, S. P., & Choi, S. U. (2005). Empirical correlation finding the role of temperature and particle size for nanofluid (Al₂O₃) thermal conductivity enhancement. *Applied physics letters*, 87(15).
- Chopkar, M., Sudarshan, S., Das, P. K., & Manna, I. (2008). Effect of particle size on thermal conductivity of nanofluid. *Metallurgical and materials transactions A*, 39, 1535-1542.
- Cuenya, B. R. (2010). Synthesis and catalytic properties of metal nanoparticles: Size, shape, support, composition, and oxidation state effects. *Thin Solid Films*, 518(12), 3127-3150.
- Darvanjooghi, M. H. K., & Esfahany, M. N. (2016). Experimental investigation of the effect of nanoparticle size on thermal conductivity of in-situ prepared silica-ethanol nanofluid. *International Communications in Heat and Mass Transfer*, 77, 148-154.
- Dharmaiah, P., Kim, H. S., Lee, C. H., & Hong, S. J. (2016). Influence of powder size on thermoelectric properties of p-type 25% Bi₂Te₃75% Sb₂Te₃ alloys fabricated using gas-atomization and spark-plasma sintering. *Journal of Alloys and Compounds*, 686, 1-8.

- Ding, C., Zhu, A., & Tian, Y. (2014). Functional surface engineering of C-dots for fluorescent biosensing and in vivo bioimaging. *Accounts of chemical research*, 47(1), 20-30.
- Ealia, S. A. M., & Saravanakumar, M. P. (2017, November). A review on the classification, characterisation, synthesis of nanoparticles and their application. In *IOP conference series: materials science and engineering* (Vol. 263, No. 3, p. 032019). IOP Publishing.
- Egboasiuba, T. C., Abdulkareem, A. S., Kovo, A. S., Afolabi, E. A., Tijani, J. O., & Roos, W. D. (2020). Enhanced adsorption of As (V) and Mn (VII) from industrial wastewater using multi-walled carbon nanotubes and carboxylated multi-walled carbon nanotubes. *Chemosphere*, 254, 126780.
- Egboasiuba, T. C. Biochar and bio-oil fuel properties from nickel nanoparticles assisted pyrolysis of cassava peel, *Heliyon* 8 (2022), e10114.
- Eastman, J. A., Choi, S. U. S., Li, S., Yu, W., & Thompson, L. J. (2001). Anomalous increase in effective thermal conductivities of ethylene glycol-based nanofluids containing copper nanoparticles. *Applied physics letters*, 78(6), 718-720.
- Garcia-Gutierrez, D. I., Gutierrez-Wing, C. E., Giovanetti, L., Ramallo-López, J. M., Requejo, F. G., & Jose-Yacamán, M. (2005). Temperature effect on the synthesis of Au–Pt bimetallic nanoparticles. *The Journal of Physical Chemistry B*, 109(9), 3813-3821.
- Gülseren, O., Ercolessi, F., & Tosatti, E. (1995). Premelting of thin wires. *Physical Review B*, 51(11), 7377.
- Huang, J. H., Parab, H. J., Liu, R. S., Lai, T. C., Hsiao, M., Chen, C. H., ... & Hwu, Y. K. (2008). Investigation of the growth mechanism of iron oxide nanoparticles via a seed-mediated method and its cytotoxicity studies. *The Journal of Physical Chemistry C*, 112(40), 15684-15690.
- Huang, C. L., Qian, X., & Yang, R. G. (2017). Influence of nanoparticle size distribution on the thermal conductivity of particulate nanocomposites. *Europhysics Letters*, 117(2), 24001.
- Hufschmid, R., Arami, H., Ferguson, R. M., Gonzales, M., Teeman, E., Brush, L. N., ... & Krishnan, K. M. (2015). Synthesis of phase-pure and

- monodisperse iron oxide nanoparticles by thermal decomposition. *Nanoscale*, 7(25), 11142-11154.
- Ho, C. J., & Gao, J. Y. (2009). Preparation and thermophysical properties of nanoparticle-in-paraffin emulsion as phase change material. *International Communications in Heat and Mass Transfer*, 36(5), 467-470.
- Kazemi, M. S., & Sobhani, A. (2023). CuMn₂O₄/chitosan micro/nanocomposite: Green synthesis, methylene blue removal, and study of kinetic adsorption, adsorption isotherm experiments, mechanism and adsorbent capacity. *Arabian Journal of Chemistry*, 16(6), 104754.
- Khan, I., Saeed, K., & Khan, I. (2019). Nanoparticles: Properties, applications and toxicities. *Arabian journal of chemistry*, 12(7), 908-931.
- Kibria, M. A., Anisur, M. R., Mahfuz, M. H., Saidur, R., & Metselaar, I. H. S. C. (2015). A review on thermophysical properties of nanoparticle dispersed phase change materials. *Energy conversion and management*, 95, 69-89.
- Kim, G. H., García de Arquer, F. P., Yoon, Y. J., Lan, X., Liu, M., Voznyy, O., ... & Sargent, E. H. (2015). High-efficiency colloidal quantum dot photovoltaics via robust self-assembled monolayers. *Nano letters*, 15(11), 7691-7696.
- Klinkova, A., Choueiri, R. M., & Kumacheva, E. (2014). Self-assembled plasmonic nanostructures. *Chemical Society Reviews*, 43(11), 3976-3991.
- Konstantatos, G., & Sargent, E. H. (2009). Solution-processed quantum dot photodetectors. *Proceedings of the IEEE*, 97(10), 1666-1683.
- Kumar, V., Toffoli, G., & Rizzolio, F. (2013). Fluorescent carbon nanoparticles in medicine for cancer therapy. *ACS medicinal chemistry letters*, 4(11), 1012-1013.
- Kumar, A., Thoravat, S., Jin, H. J., Park, J., Jin, H., Rawat, P., & Rhyee, J. S. (2024). Hierarchical nano-/micro-architecture phonon scattering of p-type Bismuth telluride bulk composites with Ag-TiO₂ nano particles synthesized by fluidized bed spray coating method. *Journal of Alloys and Compounds*, 979, 173503.

- Koppes, J. P., Grossklaus, K. A., Muza, A. R., Revur, R. R., Sengupta, S., Rae, A., ... & Handwerker, C. A. (2012). Utilizing the thermodynamic nanoparticle size effects for low temperature Pb-free solder. *Materials Science and Engineering: B*, 177(2), 197-204.
- Lai, J. J., Wong, B. T., & Chai, J. Y. (2021). A Parametric Study of Coupled Photo-Electro-Thermal Responses of Thin Film a-Si: H Solar Cell with Embedded Nanoparticles. In *Materials Science Forum* (Vol. 1030, pp. 186-193). Trans Tech Publications Ltd.
- Li, Y., Liu, J., Wang, Y., & Wang, Z. L. (2001). Preparation of monodispersed Fe–Mo nanoparticles as the catalyst for CVD synthesis of carbon nanotubes. *Chemistry of Materials*, 13(3), 1008-1014.
- Likhachev, V. N., Vinogradov, G. A., & Alymov, M. I. (2006). Anomalous heat capacity of nanoparticles. *Physics Letters A*, 357(3), 236-239.
- López-Serrano, A., Olivas, R. M., Landaluz, J. S., & Cámara, C. (2014). Nanoparticles: a global vision. Characterization, separation, and quantification methods. Potential environmental and health impact. *Analytical Methods*, 6(1), 38-56.
- Mayer, K. M., & Hafner, J. H. (2011). Localized surface plasmon resonance sensors. *Chemical reviews*, 111(6), 3828-3857.
- Machado, S., Pacheco, J. G., Nouws, H. P. A., Albergaria, J. T., & Delerue-Matos, C. (2015). Characterization of green zero-valent iron nanoparticles produced with tree leaf extracts. *Science of the total environment*, 533, 76-81.
- Mbachu, C. A., Babayemi, A. K., Egboziuba, T. C., Ike, J. I., Ani, I. J., & Mustapha, S. (2023). Green synthesis of iron oxide nanoparticles by Taguchi design of experiment method for effective adsorption of methylene blue and methyl orange from textile wastewater. *Results in Engineering*, 19, 101198.
- Miguel-Sancho, N., Bomati-Miguel, O., Roca, A. G., Martinez, G., Arruebo, M., & Santamaria, J. (2012). Synthesis of magnetic nanocrystals by thermal decomposition in glycol media: effect of process variables and mechanistic study. *Industrial & engineering chemistry research*, 51(25), 8348-8357.

- Mubayi, A., Chatterji, S., K Rai, P., & Watal, G. (2012). Evidence based green synthesis of nanoparticles. *Advanced materials letters*, 3(6), 519-525.
- Neumann, O., Urban, A. S., Day, J., Lal, S., Nordlander, P., & Halas, N. J. (2013). Solar vapor generation enabled by nanoparticles. *ACS nano*, 7(1), 42-49.
- Nadaroglu, H., Güngör, A. A., & Ince, S. (2017). Synthesis of nanoparticles by green synthesis method. *International Journal of Innovative Research and Reviews*, 1(1), 6-9.
- Onu, D. C., Babayemi, A. K., Egbosiuba, T. C., Okafor, B. O., Ani, I. J., Mustapha, S., ... & Abdulkareem, A. S. (2023). Isotherm, kinetics, thermodynamics, recyclability and mechanism of ultrasonic assisted adsorption of methylene blue and lead (II) ions using green synthesized nickel oxide nanoparticles. *Environmental Nanotechnology, Monitoring & Management*, 20, 100818.
- Petters, M., & Kasparoglu, S. (2020). Predicting the influence of particle size on the glass transition temperature and viscosity of secondary organic material. *Scientific reports*, 10(1), 15170.
- Reinsch, H. (2016). "Green" synthesis of metal-organic frameworks. *European Journal of Inorganic Chemistry*, 2016(27), 4290-4299.
- Roduner, E. (2006). Size matters: why nanomaterials are different. *Chemical society reviews*, 35(7), 583-592.
- Roduner, E. (2006). Size matters: why nanomaterials are different. *Chemical society reviews*, 35(7), 583-592.
- Salem, S. S., & Fouda, A. (2021). Green synthesis of metallic nanoparticles and their prospective biotechnological applications: an overview. *Biological trace element research*, 199(1), 344-370
- Savage, T., & Rao, A. M. (2004). Thermal properties of nanomaterials and nanocomposites. In *Thermal Conductivity: Theory, Properties, and Applications* (pp. 261-284). Boston, MA: Springer US.
- Sedighi, A., & Montazer, M. (2016). Tunable shaped N-doped CuO nanoparticles on cotton fabric through processing conditions: synthesis, antibacterial behavior and mechanical properties. *Cellulose*, 23, 2229-2243.

- Shim, J. H., Lee, B. J., & Cho, Y. W. (2002). Thermal stability of unsupported gold nanoparticle: a molecular dynamics study. *Surface science*, 512(3), 262-268.
- Singh, A. K., Viswanath, V., & Janu, V. C. (2009). Synthesis, effect of capping agents, structural, optical and photoluminescence properties of ZnO nanoparticles. *Journal of Luminescence*, 129(8), 874-878.
- Shima, P. D., Philip, J., & Raj, B. (2009). Role of microconvection induced by Brownian motion of nanoparticles in the enhanced thermal conductivity of stable nanofluids. *Applied Physics Letters*, 94(22).
- Syam Sundar, L., & Sharma, K. V. (2008). Thermal conductivity enhancement of nanoparticles in distilled water. *International Journal of Nanoparticles*, 1(1), 66-77.
- Sobhani, A., & Alinavaz, S. (2023). ZnMn₂O₄ nanostructures: Synthesis via two different chemical methods, characterization, and photocatalytic applications for the degradation of new dyes. *Heliyon*, 9(11).
- Taifi, A., Alkadir, O. K. A., Oda, A. A., Aljeboree, A. M., Al Bayaa, A. L., Alkaim, A. F., & Abed, S. A. (2022, May). Biosorption by environmental, natural and acid-activated orange peels as low-cost adsorbent: optimization of disperse blue 183 as a model. In *IOP Conference Series: Earth and Environmental Science* (Vol. 1029, No. 1, p. 012009). IOP Publishing.
- Teng, T. P., Hung, Y. H., Teng, T. C., Mo, H. E., & Hsu, H. G. (2010). The effect of alumina/water nanofluid particle size on thermal conductivity. *Applied Thermal Engineering*, 30(14-15), 2213-2218.
- Vert, M., Doi, Y., Hellwich, K. H., Hess, M., Hodge, P., Kubisa, P., ... & Schué, F. (2012). Terminology for biorelated polymers and applications (IUPAC Recommendations 2012). *Pure and Applied Chemistry*, 84(2), 377-410.
- Wang, H., Luo, G., Tan, C., Xiong, C., Guo, Z., Yin, Y., ... & Jiang, J. (2020). Phonon engineering for thermoelectric enhancement of p-type bismuth telluride by a hot-pressing texture method. *ACS applied materials & interfaces*, 12(28), 31612-31618.
- Warrier, P., & Teja, A. (2011). Effect of particle size on the thermal conductivity of nanofluids containing metallic nanoparticles. *Nanoscale research letters*, 6, 1-6.

- Yang, J., & Caillat, T. (2006). Thermoelectric materials for space and automotive power generation. *MRS bulletin*, 31(3), 224-229. Yu, W., France, D. M., Choi, S. U., & Routbort, J. L. (2007). Review and assessment of nanofluid technology for transportation and other applications (No. ANL/ESD/07-9). Argonne National Lab.(ANL), Argonne, IL (United States).
- Zeng, H., Rice, P. M., Wang, S. X., & Sun, S. (2004). Shape-controlled synthesis and shape-induced texture of MnFe₂O₄ nanoparticles. *Journal of the American Chemical Society*, 126(37), 11458-11459.
- Wang, Z., Yang, Y., Zhao, Z., Zhang, P., Zhang, Y., Liu, J., ... & Zhang, Z. (2021). Green synthesis of olefin-linked covalent organic frameworks for hydrogen fuel cell applications. *Nature Communications*, 12(1), 1982.



Chapter 8

ON THE CONTINUITY WITH RESPECT TO DENOMINATOR OF RATIO NUMERICAL RADIUS AND RATIO CRAWFORD NUMBER FUNCTIONS

Ümmügülsün Çağlayan¹

Pembe İpek Al²

¹ Dr., Karadeniz Technical University, Faculty of Science, Department of Mathematics
Trabzon, Türkiye, ummugulsun.akbaba@gmail.com, ORCID ID: 0000-0002-5870-6802

² Asoc. Prof., Karadeniz Technical University, Faculty of Science, Department of Mathematics
Trabzon, Türkiye, ipekpembe@gmail.com, ORCID ID: 0000-0002-6111-1121

1. Introduction

Acquiring the supplied operator's spectrum set and numerical range set, and computing spectral radii, numerical radii, Crawford number, and subspectral radius are the primary problems in spectral theory of linear operators. Theoretically and practically, it is quite challenging to determine the set of spectra and the non-normal linear bounded operators' numerical range.

Let take a complex Hilbert space H with norm $\|\cdot\|$ and inner product (\cdot, \cdot) . Let $B(H)$ represent all bounded linear operators on H as an algebra. Also, $\|\cdot\|$ will represent the norm in $B(H)$.

The sole formula in the literature for determining the spectral radius $r(\Omega) = \sup\{\|\mu\| : \mu \in \sigma(\Omega)\}$ of linear bounded operators is the Gelfand formula. The Gelfand formula as follows:

$$r(\Omega) = \lim_{n \rightarrow \infty} \|\Omega^n\|^{1/n} \quad (1)$$

It should be noted that the relation $r(\Omega) = \|\Omega\|$ is true for a linear bounded normal operator Ω in Hilbert space H . It follows naturally that in the case where Ω and Γ are commutative operators, then

$$r(\Omega + \Gamma) \leq r(\Omega) + r(\Gamma) \quad (2)$$

The numerical radius of $\Omega \in B(H)$ is determined by

$$w(\Omega) = \sup_{\|v\|=1} \|(\Omega v, v)\| \quad (3)$$

It is said that

$$w(\Omega) = \sup_{v \in \mathbb{R}} \|Re(e^{iv}\Omega)\| = \sup_{v \in \mathbb{R}} \|Im(e^{iv}\Omega)\| \quad (4)$$

It is clear that the operator norm $\|\cdot\|$ is equal to the norm defined by the function $w(\cdot)$ on $B(H)$. For any $\Omega, \Gamma \in B(H)$, we have

$$\frac{\|\Omega\|}{2} \leq w(\Omega) \leq \|\Omega\| \quad (5)$$

Furthermore, the relation $r(\Omega) = w(\Omega) = \|\Omega\|$ is valid for normal operators $\Omega \in B(H)$. For each $\Omega, \Gamma \in B(H)$

$$w(\Omega + \Gamma) \leq w(\Omega) + w(\Gamma) \quad (6)$$

is true ([see 1]).

Additionally, keep in mind that for each $\Omega \in B(H)$, the spectral inclusion $\sigma(\Omega) \subset \overline{W(\Omega)}$ holds for the spectrum set $\sigma(\Omega)$ and numerical range $W(\Omega)$ (see [1,2]).

For $\Omega \in B(H)$, the Crawford number and subspectral radius of Ω are determined by

$$c(\Omega) = \inf\{|\mu|: \mu \in W(\Omega)\} \quad (7)$$

and

$$\tau(\Omega) = \inf\{|\mu|: \mu \in \sigma(\Omega)\} \quad (8)$$

where $(., .)$ is the inner product and $\|\cdot\|$ is its corresponding norm on H .

It is evident that for any $\Omega \in B(H)$, the inequality holds:

$$0 \leq c(\Omega) \leq \tau(\Omega) \leq r(\Omega) \leq w(\Omega) \leq \|\Omega\|. \quad (9)$$

Note that the basic information and results for spectrum and spectral radius in [1] and different types numerical ranges, numerical radius (and related inequalities) in [3] and references in it [1,2].

And also, about some investigates between the spectral norm, the numerical radius and the spectral radius have been showed in [4,5].

For $\Omega, \Gamma \in B(H)$, $\Gamma \neq 0$, define the ratio numerical range $W(\Omega/\Gamma)$ by

$$\begin{aligned} W(\Omega/\Gamma) &= \left\{ \frac{(\Omega v, v)}{(\Gamma v, v)} : v \in H, (\Gamma v, v) \neq 0 \right\} \\ &= \left\{ \frac{(\Omega v, v)}{(\Gamma v, v)} : v \in S, (\Gamma v, v) \neq 0 \right\}, \end{aligned} \quad (10)$$

where S stands for unit sphere of H . (The hypothesis $\Gamma \neq 0$ guarantees that $W(\Omega/\Gamma) \neq \emptyset$). Obviously, $W(\Omega) = W(\Omega/I)$ is the numerical range of the operator Ω .

In [6] the study focuses on the geometric features of the ratio numerical ranges of two Hilbert space operators. Connectivity of ratio numerical ranges and the cases where the ratio numerical ranges are enclosed in a circle or a line are characterized in terms of algebraic features of operators. Simple connectivity of ratio numerical ranges is demonstrated and their boundedness quality is defined under a weak sectoriality theory.

In this study, the continuity with respect to denominator of ratio numerical radius and ratio Crawford number functions via uniformly converges have been investigated.

2. Convergence of Ratio Numerical Radius and Ratio Crawford Number Sequences with Respect to Denominator of Ratio

Firstly, give of definition the uniformly convergent of operator sequences.

Definition 2.1. [7] Let H be any complex Hilbert space and (Ω_n) be an operator sequences in $B(H)$. The sequence (Ω_n) is said uniformly converges to the $\Omega \in B(H)$, if for any $\varepsilon > 0$, there is some $n_0 = n_0(\varepsilon) \in \mathbb{N}$, seen that for all $n > n_0$ is true $\|\Omega_n - \Omega\| < \varepsilon$.

Theorem 2.2. For any operators $\Omega, \Gamma, T \in B(H), \Gamma \neq 0, T \neq 0$ the following inequalities are true:

- i. $|w(\Omega/\Gamma) - w(\Omega/T)| \leq w(\Omega/\Gamma)w((\Gamma - T)/T)$
- ii. In addition, if for $v \in H, \|v\| = 1, |(\Gamma v, v)| \geq 1, |(Tv, v)| \geq 1$, then

$$|w(\Omega/\Gamma) - w(\Omega/T)| \leq w(\Omega)w((\Gamma - T)).$$

Proof.

- i. For $v \in H, \|v\| = 1, (\Gamma v, v) \neq 0$ and $(Tv, v) \neq 0$, we have

$$\begin{aligned} \left| \frac{(\Omega v, v)}{(\Gamma v, v)} \right| &\leq \left| \frac{(\Omega v, v)}{(\Gamma v, v)} - \frac{(\Omega v, v)}{(Tv, v)} \right| + \left| \frac{(\Omega v, v)}{(Tv, v)} \right| \\ &= \frac{|(\Omega v, v)| |(T - \Gamma)v, v|}{|(\Gamma v, v)| |(Tv, v)|} + \left| \frac{(\Omega v, v)}{(Tv, v)} \right|. \end{aligned}$$

Then it is obtained that

$$\begin{aligned} w(\Omega/\Gamma) &\leq w(\Omega/T) + \sup \frac{|(\Omega v, v)| |(T - \Gamma)v, v|}{|(\Gamma v, v)| |(Tv, v)|} \\ &= w(\Omega/\Gamma)w((T - \Gamma)/T) \end{aligned} \tag{11}$$

Similarly, for $v \in H, \|v\| = 1, (\Gamma v, v) \neq 0$ and $(Tv, v) \neq 0$, from following relation

$$\left| \frac{(\Omega v, v)}{(T v, v)} \right| \leq \left| \frac{(\Omega v, v)}{(\Gamma v, v)} \right| \left| \frac{((T - \Gamma)v, v)}{(T v, v)} \right| + \left| \frac{(\Omega v, v)}{(\Gamma v, v)} \right|$$

It is obtained that

$$w(\Omega/T) \leq w(\Omega/\Gamma) + w(\Omega/\Gamma)w((T - \Gamma)/T). \tag{12}$$

Consequently, from (11) and (12), it is established that;

$$|w(\Omega/\Gamma) - w(\Omega/T)| \leq w(\Omega/\Gamma)w((\Gamma - T)/T).$$

- ii. Indeed, if for each $v \in H$, $\|v\| = 1$, the conditions $|(\Gamma v, v)| \geq 1$, $|(T v, v)| \geq 1$ are satisfy, then

$$\left| \frac{(\Omega v, v)}{(\Gamma v, v)} \right| \left| \frac{((\Gamma - T)v, v)}{(T v, v)} \right| \leq |(\Omega v, v)| \left| \frac{((\Gamma - T)v, v)}{(T v, v)} \right|$$

From last inequality and claim (i) of this theorem, it is established that

$$|w(\Omega/\Gamma) - w(\Omega/T)| \leq w(\Omega)w((\Gamma - T)).$$

Theorem 2.3. Let $\Omega, \Gamma_n \in B(H)$, $n \geq 1$ and for $v \in H$, $\|v\| = 1$ is satisfied $|(\Gamma_n v, v)| \geq 1$, $n \geq 1$. If operator sequences $\Gamma_n \in B(H)$, $n \geq 1$ uniformly converges to the operator $\Gamma \in B(H)$, then

$$w(\Omega/\Gamma) = \lim_{n \rightarrow \infty} w(\Omega/\Gamma_n).$$

Proof. In this case of second claim of Theorem 2.2. it is clear

$$|w(\Omega/\Gamma_n) - w(\Omega/\Gamma)| \leq w(\Omega)w(\Gamma_n - \Gamma) \leq \|\Omega\| \|\Gamma_n - \Gamma\|, n \geq 1.$$

Hence, it implies the validity of proposition.

Theorem 2.4. For any operators $\Omega, \Gamma, T \in B(H), \Gamma \neq 0, T \neq 0$ are true:

- i. $|c(\Omega/\Gamma) - c(\Omega/T)| \leq w(\Omega/\Gamma)w((\Gamma - T)/T)$
- ii. In addition, if for $v \in H, \|v\| = 1, |(\Gamma v, v)| \geq 1, |(Tv, v)| \geq 1$, then

$$|c(\Omega/\Gamma) - c(\Omega/T)| \leq w(\Omega)w((\Gamma - T)).$$

Proof.

- i. For each $v \in H, \|v\| = 1, (\Gamma v, v) \neq 0$ and $(Tv, v) \neq 0$, we have

$$\begin{aligned} \left| \frac{(\Omega v, v)}{(\Gamma v, v)} \right| &= \left| \frac{(\Omega v, v)}{(Tv, v)} + \frac{((\Gamma - T)v, v)}{(Tv, v)(\Gamma v, v)} \right| \\ &\geq \left| \frac{(\Omega v, v)}{(Tv, v)} \right| - \left| \frac{(\Omega v, v)}{(\Gamma v, v)} \right| \left| \frac{((\Gamma - T)v, v)}{(Tv, v)} \right| \\ &\geq c(\Omega/T) - w(\Omega/\Gamma)w((\Gamma - T)/T). \end{aligned}$$

Then

$$-w(\Omega/\Gamma)w((\Gamma - T)/T) \leq c(\Omega/\Gamma) - c(\Omega/T). \tag{13}$$

Similarly, for $v \in H, \|v\| = 1, (\Gamma v, v) \neq 0$ and $(Tv, v) \neq 0$, from following inequality,

$$\begin{aligned} \left| \frac{(\Omega v, v)}{(Tv, v)} \right| &= \left| \frac{(\Omega v, v)}{(\Gamma v, v)} - \frac{((\Gamma - T)v, v)}{(Tv, v)(\Gamma v, v)} \right| \\ &\geq \left| \frac{(\Omega v, v)}{(\Gamma v, v)} \right| - \left| \frac{(\Omega v, v)}{(\Gamma v, v)} \right| \left| \frac{((\Gamma - T)v, v)}{(Tv, v)} \right| \\ &\geq c(\Omega/\Gamma) - w(\Omega/\Gamma)w((\Gamma - T)/T). \end{aligned}$$

It implies that $c(\Omega/\Gamma) - w(\Omega/\Gamma)w((\Gamma - T)/T)$. Then,

$$c(\Omega/\Gamma) - c(\Omega/T) \leq w(\Omega/\Gamma)w((\Gamma - T)/T) \quad (14)$$

Consequently, from relations (13) and (14), it is established that

$$\begin{aligned} c(\Omega/\Gamma) - c(\Omega/T) &\leq w(\Omega/\Gamma)w((\Gamma - T)/T) \\ |c(\Omega/\Gamma) - c(\Omega/T)| &\leq w(\Omega/\Gamma)w((\Gamma - T)/T) \end{aligned} \quad (15)$$

- ii. Indeed, if for each $v \in H$, $\|v\| = 1$, the conditions $|\langle \Gamma v, v \rangle| \geq 1$, $|\langle T v, v \rangle| \geq 1$ are satisfy, then

$$\left| \frac{\langle \Omega v, v \rangle}{\langle \Gamma v, v \rangle} \right| \leq |\langle \Omega v, v \rangle| \text{ and } \left| \frac{\langle (\Gamma - T)v, v \rangle}{\langle T v, v \rangle} \right| \leq |\langle (\Gamma - T)v, v \rangle|$$

From last equation, it is established that

$$w(\Omega/\Gamma) \leq w(\Omega) \text{ and } w((\Gamma - T)/T) \leq w(\Gamma - T).$$

In this case from last relation and first claim of this theorem, it is established that

$$|c(\Omega/\Gamma) - c(\Omega/T)| \leq w(\Omega)w(\Gamma - T). \quad (16)$$

Theorem 2.5. Assume that $\Omega, \Gamma_n \in B(H)$, $n \geq 1$ and for each $v \in H$, $\|v\| = 1$, $|\langle \Gamma_n v, v \rangle| \geq 1$, $n \geq 1$ is satisfied. If operator sequences $\Gamma_n \in B(H)$, $n \geq 1$ uniformly converges to $\Gamma \in B(H)$, then

$$c(\Omega/\Gamma) = \lim_{n \rightarrow \infty} c(\Omega/\Gamma_n).$$

Proof. From the second claim of Theorem 2.4., we have

$$|c(\Omega/\Gamma_n) - c(\Omega/\Gamma)| \leq W(\Omega)W(\Gamma_n - \Gamma) \leq \|\Omega\| \|\Gamma_n - \Gamma\|, n \geq 1.$$

By using this and from uniformly convergence of operator sequences (Γ_n) in $B(H)$ to the $\Gamma_n \in B(H)$, the validity of this proposition is established.

Example 1. Assume that $H = l_2(\mathbb{R})$, $a_m \geq 1, m \geq 1, \sup_{m \geq 1} a_m < \infty$,

$$\Gamma_n v = \left(\left(a_m + \frac{1}{n} \right) v_m \right), v = (v_m) \in l_2(\mathbb{R}), \Gamma_n: l_2(\mathbb{R}) \rightarrow l_2(\mathbb{R}), n \geq 1,$$

$$\Omega v = (a_m v_m), v = (v_m) \in l_2(\mathbb{R}), \Omega: l_2(\mathbb{R}) \rightarrow l_2(\mathbb{R}).$$

In this case, it is clear that $\Omega, \Gamma_n \in B(l_2(\mathbb{R})), n \geq 1$ and also

$$\|(\Gamma_n - \Omega)v\| = \left\| \left(\frac{1}{n} v_m \right) \right\| = \frac{1}{n} \|v\|, n \geq 1.$$

Then

$$\|\Gamma_n - \Omega\| = \frac{1}{n} \rightarrow 0, n \rightarrow \infty.$$

Hence the operator sequences (Γ_n) uniformly converges to the operator Ω in $l_2(\mathbb{R})$. Consequently, by Theorem 2.3 and 2.5 implies that

$$\lim_{n \rightarrow \infty} w(\Omega/\Gamma_n) = w(\Omega/\Omega) = 1 \text{ and } \lim_{n \rightarrow \infty} c(\Omega/\Gamma_n) = c(\Omega/\Omega) = 1.$$

Example 2. Let $H = L^2(0,1), \varphi_n, \varphi \in C[0,1], |\varphi_n| \geq 1, n \geq 1, \varphi_n \xrightarrow{[0,1]} \varphi$,

$$\Gamma_n f(v) = \varphi_n(v) f(v), f \in L^2(0,1), \Gamma_n: L^2(0,1) \rightarrow L^2(0,1),$$

$$\Omega f(v) = \varphi(v) f(v), f \in L^2(0,1), \Omega: L^2(0,1) \rightarrow L^2(0,1).$$

It is clear that $\Gamma_n, \Omega \in B(L^2(0,1))$, $n \geq 1$ and operator sequences (Γ_n) uniformly converges to the Ω in $L^2(0,1)$. Hence, by Theorem 2.3 and 2.5, we have

$$\lim_{n \rightarrow \infty} w(\Omega/\Gamma_n) = w(\Omega/\Omega) = 1 \text{ and } \lim_{n \rightarrow \infty} c(\Omega/\Gamma_n) = c(\Omega/\Omega) = 1.$$

Remark. For recent development research in this area, it can be found in [8-19].

References

1. Gustafson K. E., and Rao, D. K. M. (1997). *Numerical Range: The Field of Values of Linear Operators and Matrices*, New York: Springer.
2. Halmos, P. R. (1982). *A Hilbert space problem book*. Springer -Verlag, New York.
3. Bhunia, P., Dragomir, S. S., Moslehian, M. S., & Paul, K. (2022). *Lectures on numerical radius inequalities* (pp. XII+-209). Cham, Switzerland: Springer.
4. Al-Hawari, M. (2013). The ratios between the numerical radius and spectral radius of a matrix and the square root of the spectral norm of the square of this matrix. *International Journal of Pure and Applied Mathematics*, 82(1), 125-131.
5. Du, K. (2010). The ratios between the spectral norm, the numerical radius and the spectral radius. *Int. J. Comput. Math. Sci.*, 4(8), 388-391.
6. Rodman, L., & Spitkovsky, I. M. (2011). Ratio numerical ranges of operators. *Integral Equations and Operator Theory*, 71, 245-257.
7. Bachman, G. and Narici, L. (1966). *Functional Analysis*. Academic Press. New York.
8. İsmailov, Z., Mert, R. (2022). Gaps between some spectral characteristics of direct sum of Hilbert space operators. *Operators and Matrices*, 16(1).
9. Otkun Çevik, E., İsmailov, Z. I. (2022). Some Gap Relations Between Operator Norm with Spectral and Numerical Radii of Direct Sum Hilbert Space Operators. *Lobachevskii Journal of Mathematics*, 43(2), 366-375.
10. İsmailov, Z. I., İpek Al, P., (2022). Some Spectral Characteristic Numbers of Direct Sum of Operators. *Turkish Journal of Analysis and Number Theory*, 10(1),21-26.
11. İpek Al, P., İsmailov, Z. I. (2021). On the spectral radius of antidiagonal block operator matrices. *Journal of Mathematical Chemistry*, 59(10), 2206-2217.
12. Otkun Çevik, E., &İsmailov, Z. I. (2021). Radius and Operator Norm of Infinite Upper Triangular Double Band Block Operator Matrices *Journal of Analysis & Number Theory*, 9(2), 19-22.
13. İpek Al, P., İsmailov, Z. I. (2021). Gaps Between Operator Norm and Spectral and Numerical Radii of the Tensor Product of Operators. *Turkish Journal of Analysis and Number Theory*, 9(2), 22-24.

14. Otkun Çevik, E., Ismailov, Z. I. (2021). Spectral Radius and Operator Norm of Infinite Upper Triangular Double Band Block Operator Matrices. *Journal of Analysis & Number Theory*, 9(2), 19-22.
15. Ismailov Z. I. and Otkun Çevik E., (2022). On the one spectral relation for analytic function of operator, *Journal of Nonlinear Science and Applications*, 15, 301-307.
16. Çağlayan Ü., Ismailov Z.I., (2024), On The Convergence Properties Of p-Numerical Radii And p-Crawford Numbers Sequences, O. Talaz, A. Demirçalı. içinde, *Current Studies in Science and Mathematics* (s. 5-18), Ankara: Platanus Publishing.
17. Çağlayan Ü., Ismailov Z.I., (2024), On The Continuity Properties of Davis-Wielandt Radius and Crawford Number Functions, E. Otkun Çevik içinde, *Matematik Alanında Analizler* (s. 16-24), Afyonkarahisar: Yaz Yayınları.
18. Otkun Çevik E., Ismailov Z.I., (2024), On The Continuity of Ratio Numerical Radius and Ratio Crawford Number Functions, E. Otkun Çevik içinde, *Matematik Alanında Analizler* (s. 25-34), Afyonkarahisar: Yaz Yayınları.
19. Bhunia, P., Ipek Al, P., Ismailov, Z. I. (2024). On the convergence of some spectral characteristics of the converging operator sequences. *Proceedings-Mathematical Sciences*, 134(1), 1-15.